CR26H "Iced Cappogee" Final Design Report

Competing Project 12

CU InSpace

Team Lead: Sophia Verma
Chief Engineer: Jack Hartman
Carleton University, Ottawa, Ontario, K1S 5B6, Canada

LAUNCH CANADA CHALLENGE 2026

Revision History

REVISION	DESCRIPTION	DATE
R0	Initial Release	2026-07-10

Acknowledgements

CU InSpace is thankful for the support we have received from our many sponsors and supporting organizations including:

Carleton University Faculty of Engineering and Design
Carleton University Department of Mechanical and Aerospace Engineering
Carleton Student Engineering Society
Metal Pros Ottawa
Dassault Systèmes SOLIDWORKS Corp.
Protocase
Ansys
Altium
Carleton Undergraduate Engineering Student Equipment Fund
Carleton University Students Association
Seco Seals Inc.
Swagelok Ottawa
AVSS
Dominion Dynamics
Apache NuttX
MHI RJ Aviation
Leonardo DRS
Kostiuk Engineering Fund Collective
Titan Building Products
Morrison's Quarry

Authors

The following team members of CU InSpace have all taken part as authors of this report for Project 12:

- Anuj Snider
- Atharva Vaishampayan
- Callie Song
- Cian Fensky
- Jack Hartman
- Jia Lin
- Mahdeen Wahed
- Massimo Capotorto
- Nasu Caplan
- Nathan Huber
- Renton Hutt
- Roland Neill
- Sebastien Thibodeau
- Sophia Verma
- Tom Birnie-Wortley
- William Kruse

Abstract

CU InSpace, Carleton University's rocketry design team, is participating in the advanced launch with a NOS/paraffin blowdown hybrid for the Launch Canada 2026 launch challenge. This project is divided into 5 subteams with focuses broadly aligned to aerostructures, avionics, propulsion, and recovery respectively. The project started development on the 1st of September in 2025, and will culminate with the launch of the hybrid vehicle in August 2026. Since the submission of the IDP, the team has made many strides towards the completion of the vehicle. In particular, the team has completed engine testing, with moderate success; recovery's bulkhead has been redesigned to accommodate SRAD black powder ejection and to share a bulkhead with the avionics stack; aerostructures have completed the air frame using new manufacturing methods. Major programmatic and technical risks affecting the success of the project include receiving minimal funding as it relates to the purchasing of consumables for engine testing, as well as not meeting timelines due to continuous unfavourable testing outcomes. The team will maintain an adaptive and strategic nature to ensure viable test outcomes are obtained via minimum funding.

Contents

1 Introduction **13**
- 1.1 Updates and Lessons Learned . . . 13
- 1.2 Team Organization . . . 15
  - 1.2.1 Team Development and Succession Planning . . . 15
- 1.3 Outreach . . . 15

2 Conops **18**

3 Requirements **21**
- 3.1 Mission Requirements . . . 21
- 3.2 Mission Requirements . . . 22
- 3.3 System Requirements . . . 22
- 3.4 Subsystem Requirements . . . 24

4 Systems Architecture **31**
- 4.1 Architecture Overview and Layout . . . 31
- 4.2 Mass Budget . . . 33

5 Performance Analysis **36**
- 5.1 Flight/Demo Performance . . . 36
- 5.2 Recovery Dispersion Analysis . . . 36
  - 5.2.1 Maximum Expected Wind Conditions . . . 37
  - 5.2.2 Typical Wind Levels . . . 37

6 Aerostructures **39**
- 6.1 Aerostructures Overview . . . 39
- 6.2 Nose Cone . . . 39
  - 6.2.1 Detailed Design . . . 39
  - 6.2.2 Manufacturing Process . . . 39
  - 6.2.3 Analysis . . . 40
  - 6.2.4 Testing and Validation . . . 41
- 6.3 Airframe . . . 42
  - 6.3.1 Detailed Design . . . 42
  - 6.3.2 Manufacturing Process . . . 42
  - 6.3.3 Analysis . . . 43
  - 6.3.4 Testing and Validation . . . 43
- 6.4 Aluminum Structural Parts . . . 43
  - 6.4.1 Recovery Bulkhead and Support Ring . . . 44
  - 6.4.2 Metal Separation Coupler . . . 47
  - 6.4.3 Aft Tube Attachment Ring . . . 47
  - 6.4.4 Fin System Retention Ring . . . 48
  - 6.4.5 Manufacturing Process . . . 48
- 6.5 Couplers . . . 48
  - 6.5.1 Detailed Design . . . 48
  - 6.5.2 Manufacturing Process . . . 49
  - 6.5.3 Analysis . . . 49
  - 6.5.4 Testing and Validation . . . 49
- 6.6 Fins . . . 50

6.6.1 Detailed Design . . . 50
6.6.2 Manufacturing Process . . . 52
6.6.3 Analysis . . . 52
6.6.4 Testing and Validation . . . 54
6.7 Tank(s) . . . 55
6.7.1 Detailed Design . . . 55
6.7.2 Manufacturing Process . . . 55
6.7.3 Analysis . . . 56
6.7.4 Testing and Validation . . . 57

7 Propulsion **59**
7.1 Motor Performance . . . 59
7.2 Oxidizer Systems . . . 60
7.2.1 Fill System . . . 60
7.2.2 Main Valve . . . 63
7.2.3 Passive Umbilical System . . . 65
7.2.4 Vent System . . . 65
7.3 Combustion Chamber . . . 65
7.3.1 Structures . . . 65
7.3.2 Injector Design . . . 67
7.3.3 Bulkhead . . . 67
7.3.4 Retaining Ring . . . 68
7.3.5 Injector . . . 69
7.3.6 Thermal Protection . . . 70
7.3.7 Nozzle . . . 72
7.3.8 Fuel . . . 73
7.3.9 Mixing Plate . . . 74
7.3.10 Ignitor . . . 74
7.4 Propulsion Testing . . . 75
7.4.1 Hydrostatic Tests . . . 75
7.4.2 Cold Flows . . . 76
7.4.3 Valve Actuation . . . 76
7.4.4 Igniter Tests . . . 77
7.4.5 Static Fires . . . 77
7.4.6 Procedures . . . 77

8 Recovery **78**
8.1 Overview of Recovery . . . 78
8.2 SRAD Wireless Reefing System . . . 78
8.3 Deployment . . . 82
8.4 Parachute Design . . . 83
8.5 Rigging . . . 86

9 Avionics **87**
9.1 SRAD Telemetry . . . 88
9.1.1 SRAD Telemetry . . . 88
9.1.2 Power . . . 88
9.1.3 Telemetry Software . . . 89
9.1.4 Ground Station . . . 90
9.2 COTS Tracking . . . 90

9.3 Power . . . 91
9.4 Enclosure Design . . . 91
9.5 Arming . . . 91

10 GSE **93**
10.1 Launch Tower . . . 93
10.1.1 Tower . . . 93
10.1.2 Base . . . 94
10.1.3 Loads . . . 96
10.2 Hybrid Engine Control . . . 96
10.2.1 Mission Control Center . . . 97
10.2.2 Pad Control Center . . . 99
10.3 Networking . . . 104

11 Range Safety **107**
11.1 Hazard Analysis . . . 107
11.2 Hybrid Development Hazard Matrix and Risk Assessment . . . 108

12 Risks and Mitigation Strategies **109**

13 Technical Risks **111**

A Payload **115**
A.1 Overview of Payload . . . 115
A.2 Rat Cortex Neurons . . . 115
A.3 Life Support System . . . 115
A.4 Micro Electrode Array . . . 115
A.5 Fluorescent Microscopy . . . 115

B Detailed Design Trade Studies and Calculations **118**

C Thrust Chamber Structural Calculations **118**
C.1 Safety Factors . . . 118
C.2 Calculation Inputs . . . 118
C.3 Recessed Bolt Head Calculations . . . 120
C.3.1 Bolt Shear . . . 120
C.3.2 Casing Bearing Stress and Bolt Tear-Out . . . 120
C.3.3 Bulkhead Bearing Stress . . . 120

List of Figures

1 2025-2026 Executive Role Flowchart . . . 15
2 CU InSpace Educating Members About Rocketry . . . 16
3 InSpace Flight School at URRG . . . 16
4 L1 Certification Launch . . . 16
5 Participants at Small Rocket 2025 . . . 17
6 Mission Concept of Operations Flowchart . . . 18
7 Mission Concept of Operations Diagram . . . 18
8 Main Airframe Components and Sections Breakdown, CR26H, Launch Canada 2026 . . . 31
9 CR26H Mass Budget Page 1 . . . 33
10 CR26H Mass Budget Page 2 . . . 34
11 CR26H Mass Budget Page 3 . . . 35
12 Dispersion UI and Parameters . . . 36
13 Dispersion Results Under Maximum Expected Wind Conditions . . . 37
14 Dispersion Under Typical Wind Conditions . . . 38
15 Nosecone Manufacturing . . . 40
16 Nosecone CFD Results . . . 41
17 Airframe Overview . . . 42
18 CR26H Bending Loads . . . 43
19 Metal Part Overview . . . 44
20 Recovery Bulkhead Exploded View . . . 45
21 Topology Optimization Results . . . 45
22 Topology Optimization Results . . . 46
23 Cut Section of Assembly Stress Result . . . 46
24 Support Ring and Bolt Stress Results . . . 46
25 Metal Coupler . . . 47
26 Aft Tube Attachment Ring . . . 48
27 Fin System Retention Ring . . . 48
28 Coupler Manufacturing . . . 49
29 Bending Test . . . 50
30 Cut-out Carbon Fiber Fin Plate . . . 51
31 Fin Tip CFD Results . . . 52
32 CR26H Pitching Frequency over Time. . . . 53
33 CR26H Damping Ratio under Worst Case 20km/hr Winds. . . . 54
34 Ras Aero Angle of Attack under Worst Case 20km/hr Winds. . . . 54
35 Cross-section of the run tank assembly. . . . 55
36 Run tank assembly. . . . 56
37 Run tank hydrostatic-test setup. . . . 58
38 SB-3 in Flight Configuration (Note: Image Missing Stringers) . . . 59
39 SB-3 During Static Fire . . . 59
40 Combined Static Fire and Simulated Thrust Curve . . . 60
41 Fill and Run System P&ID . . . 61
42 Fill System for SB-3 . . . 63
43 Main Valve for SB-3 . . . 63
44 Main Valve Normal Position . . . 64
45 Main Valve Pressurized Position . . . 64
46 Tear Away Testing . . . 65
47 Thrust Chamber Casing . . . 66

48 Injector Bolt Circle . . . 66
49 Nozzle Bolt Circle . . . 66
50 Top of Injector Bulkhead . . . 67
51 Injector Bulkhead Vent Line Port . . . 68
52 Injector Bulkhead . . . 68
53 Retaining Ring . . . 69
54 94 Hole Injector Plate . . . 70
55 Injector Spray During Cold Flow . . . 70
56 Combustion Chamber Fuel Liner Cross Section . . . 70
57 Post Combustion Chamber Spacers . . . 71
58 Recovered Retaining Ring . . . 71
59 Recovered Graphite Nozzle . . . 71
60 Nozzle Assembly Cross-Section . . . 72
61 Phenolic Carrier . . . 72
62 Graphite Nozzle . . . 73
63 Nozzle Assembly Cross-Section . . . 73
64 Mixing Plate w/ Ceramic Coating . . . 74
65 Ignitor Puck . . . 75
66 Hydrostatic Test Setup . . . 76
67 CR26H Recovery Diagram . . . 78
68 Receiving Box CAD Assembly . . . 79
69 Recovery Section Full Assembly . . . 80
70 Receiving box line cutter test . . . 80
71 TGD 3D CAD Assembly . . . 81
72 Recovery reefing electronics assembly . . . 81
73 Recovery Wireless Reefing Logic . . . 82
74 BP Charge Visualization . . . 83
75 Toroidal Parachute Visualization . . . 85
76 Toroidal chute inflated side profile . . . 85
77 Assembled Avionics Stack Flown at Launch Canada 2025 . . . 87
78 Avionics Stack Wiring Diagram . . . 87
79 Flight Computer Software Architecture . . . 90
80 Ground Station Frontend . . . 90
81 Exemplar Screw Switch . . . 92
82 Aluminium U-channel (left), and Aluminium Extrusion (Right) . . . 93
83 Side View of Tower Section . . . 94
84 PE 36 helical Ground Anchors . . . 95
85 Tower Base . . . 95
86 Tower Raising Process . . . 96
87 The Valve Control Console (VCC) Switch Box Alongside User Portable Electronic Devices (PEDs) Running the Telemetry Monitoring User Interface (UI) . . . 97
88 The Hybrid Engine User Interface when Idle . . . 98
89 The Hybrid Engine UI P&ID Display . . . 99
90 The Pad Control Box with its Lid Open During Testing. . . . 100
91 igniter Control Circuitry . . . 103
92 Network Topology of the Electrical Control Systems . . . 105
93 SRAD Fluorescent Microscope Block Diagram . . . 117

List of Tables

1 Summary of Design Updates and Lessons Learned . . . 14
2 Mission Requirments . . . 21
3 Mission Performance Requirments . . . 22
4 System Requirements . . . 22
5 Subsystem Requirements . . . 24
6 Airframe Breakdown by Section . . . 31
7 Key CR26H Airframe + Hybrid Motor Dimensions . . . 32
8 CR26H Flight Performance - No Wind . . . 36
9 Major Fin Dimensions . . . 51
10 Run Tank Design Summary . . . 55
11 Bulkhead Bearing Failure . . . 56
12 Casing Pressure Stress . . . 57
13 Casing Bearing Failure with M6 Bolts . . . 57
14 Casing Tensile Failure . . . 57
15 Casing Bolt Tear-Out . . . 57
16 M6 Bolt Shear . . . 57
17 Motor Performance Data Summary . . . 60
18 Oxidizer System Component Summary . . . 62
19 Oxidizer System Component Working Pressure and Orifice Summary . . . 62
20 Injector Bolt Circle Factors of Safety . . . 69
21 Fuel Grain Material Summary . . . 73
22 Parachute Parameters . . . 84
23 Parachute Characteristics . . . 84
24 Parachute Geometric Dimensions . . . 85
25 Recovery System Parameters . . . 86
26 Student Researched and Designed (SRAD) Flight Computer Sensors . . . 88
27 Josh Flight Computer Power Budget . . . 89
28 Josh Flight Computer Battery Calculations . . . 89
29 SRAD and Commercial Off The Shelf (COTS) Battery Pack Specifications . . . 91
30 Potential Hazards . . . 107
30 Potential Hazards . . . 108
31 Potential Hybrid Development Hazards . . . 108
31 Potential Hybrid Development Hazards . . . 109
32 CR25H Programmatic Risk Matrix . . . 110
33 CR25H Technical Risk Matrix . . . 111
34 Chamber Casing Factors of Safety . . . 118
35 Injector Bolt Circle Factors of Safety . . . 118
36 Nozzle Bolt Circle Factors of Safety . . . 118
37 Aluminum 6061-T6 Material Properties . . . 119
38 M4 Fastener Mechanical Properties . . . 119
39 Chamber Casing Geometry . . . 119
40 Injector Bolt Circle Geometry . . . 119
41 Nozzle Bolt Circle Geometry . . . 119

Nomenclature

AC Advisory Circular.
ADC Analog to Digital Converter.
AP Access Point.
AWG American Wire Gauge.

COTS Commercial Off The Shelf.

DAQ Data Acquisition.
DHCP Dynamic Host Configuration Protocol.
DTEG Design, Test, and Evaluation Guide.

EEPROM Electrically Erasable Programmable Read-Only Memory.

FAA Federal Aviation Administration.

GPS Global Positioning System.

HRAP Hybrid Rocket Analysis Program.

LAN Local Area Network.
Li-Po Lithium Polymer.
Li-on Lithium Ion.
LoRa Long Range radio.

MCC Mission Control Center.
MCU Microcontroller Unit.
MEOP Maximum Expected Operating Pressure.
MMPDS Metallic Materials Properties Development and Standardization.
MOSFET Metal-Oxide-Semiconductor Field-Effect Transistor.

P&ID Process & Instrumentation Diagram.
PCC Pad Control Center.
PED Portable Electronic Device.
POE Power Over Ethernet.

RTOS Real Time Operating System.
RTV Room Temperature Vulcanizing.

SRAD Student Researched and Designed.

TCC Telemetry Control Center.
TCP Transport Control Protocol.

UART Universal Asynchronous Reciever/Transmitter.
UDP User Datagram Protocol.
UI User Interface.
uORB Micro-Object Request Broker.
UPS Uninteruptable Power Supply.

VCB Valve Control Board.
VCC Valve Control Console.

Wi-Fi Wireless Fidelity.

1. Introduction

Carleton University has a long-standing relationship with aerospace engineering, opening its first aerospace program in 1988, making it the first university in Canada to offer such a program. It now offers four different aerospace specializations; Aerodynamics and Vehicle Performance, Lightweight Structures, Avionics, and Space Systems Design. Carleton has always had a proud history of hands-on learning experiences as well, being the first Canadian university to develop a capstone project in the student's final year of study to showcase the skills learned during their time at Carleton. Additionally, Carleton has always endeavoured to excel in its extracurricular clubs, from FSAE cars to UAV Blackbird. Carleton has always provided support and financial assistance to students looking to further their education with hands-on experience. CU InSpace is one of those teams, bringing dozens of undergraduate students from various engineering disciplines together to design, develop, and test high-performance sounding rocket systems.

CU InSpace is a dynamic engineering competition team that specializes in the production of high-powered rockets. The team is comprised of undergraduate students that have a passion for rockets and design. Founded in 2014, CU InSpace works to compete in the annual International Rocket Engineering Competition and Launch Canada challenges, launching to 30,000ft above the surface of the Earth.

This year, CU InSpace is competing in the Advanced Launch (Hybrid) competition of the Launch Canada Competition with our rocket Iced Cappogee, also referred to as CR26H. CR26H is expected to be a 11.50 ft (3.51 m) tall high-power sounding rocket designed to reach an expected apogee of 44,562 ft [13,582 m] . The vehicle weighs 100.5 lb [45.6 kg] when fully loaded and is propelled by a paraffin wax and nitrous oxide hybrid rocket motor (70% O-Class). Once the vehicle reaches its expected apogee, the student-developed reefed-main parachute is ejected from the rocket using two black powder charges. The timing of the deployment and the relaying of telemetry is facilitated by the vehicle's avionics system, consisting of custom software with several redundant COTS systems. The student-developed main parachute will disreef at an altitude of 1500 ft (457.2 m) and fully inflate.

1.1 Updates and Lessons Learned

Since the Initial Design Proposal, the design of and overarching philosphy of the CR26H project has undergone several changes, focused primarily on optimization of weight and space of the overall rocket. The table below summarizes major changes, reasons behind decisions, and important learnings throughout the design cycle.

Table 1 Summary of Design Updates and Lessons Learned

Initial Approach	Design Change Driver	Design Update	Lessons Learned
Implementation of a biological 3U payload into CR26H	Selected for the CAN-SBX challenge, which occurs during LC2026	Payload was removed from CR26H, and allocation for 3U payload removed	For more information on the CR26H payload, see appendix A.
SRAD parachute deployment utilizing Guanidine Nitrate (GN) deployment charges	The complex chemical requirements to successfully ignite GN charges, along with system estimations showing only marginal benefits over more traditional BP charges.	GN charges were replaced with SRAD BP charge cannons, which are more weight efficient than the previous Raptor-CO_2 charges.	Cost-benefit trade-offs, and alternative proven designs should be more carefully considered when deciding which SRAD engineering projects to pursue.
Running a vent port out of the chamber in the form of a burn away nylon line to facilitate coming up to temperature and not impede performance.	Testing revealed that it would break earlier then expected, and could snuff out the igniter.	Changed to a static vent out the side of the rocket. Still using a nylon line to allow coming up to pressure. Nylon line will tear away upon launch.	Chamber vent lines require better insulation from the igniter as well as more testing.
Creation of a new primary SRAD flight computer	Other more pressing initiatives existed for the Avionics subteam; resources needed to be allocated to the hybrid engine control system and tracking antenna project	New flight computer design deemed not mature enough for flight. 2025 legacy design selected to fly in place of new design.	Resources and manpower are limited on a volunteer team. A more thorough investigation of capability vs. workload must take place early in design cycle.
Fin can designed to utilize a tip-to-tip carbon fiber layup over 3D-printed AeroASA core	Non-structural mass of 3D printed core, difficulty of layup, risk of leading edge delamination, all contributed to re-evaluation of fin system design	Design updated to use carbon fiber plates surface mounted to tail cone. Tip-to-tip carbon layup added after surface mounting.	Minimizing non-structural mass is crucial to efficient airframe design. Overall specific strength and stiffness greatly improved by excluding the use of a 3D printed core.

1.2 Team Organization

CU InSpace has a total of 27 executive roles, ranging from the two presidents who provide high level oversight and leadership, to the subteam leads who manage individual projects and delegate tasks, to the vice presidents who work behind the scenes to ensure the team runs smoothly day to day. A flowchart of the executive roles can be found in Fig. 1 below.

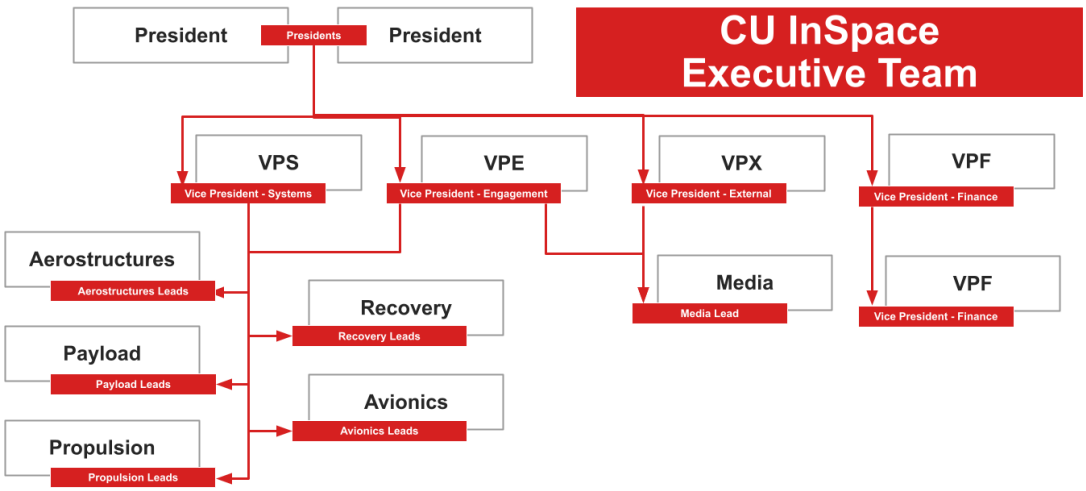

Figure 1 2025-2026 Executive Role Flowchart

1.2.1 Team Development and Succession Planning

Shortly after the winter reading week, positions for the next year's executive and admin positions become available. Students must interview for each position they wish to hold in front of a panel of current and outgoing executives, including the executive who's role they intend to take on. After interviews have concluded, the panel reconvenes to discuss the candidates, with a decision being made in the form of a blind vote. The successful candidate is then notified, and can begin learning from the current executive/admin over the summer semester before they assume their duties in the fall. Currently, CU InSpace has 18 subteam leads and 9 admin positions.

1.3 Outreach

Over the course of the 2025-2026 year, CU InSpace has continued to expand its presence in STEM youth engagement and academic outreach. The team regularly participates in school events such as open houses and STEM fairs, displaying rockets to prospective students and answering questions about Carleton University's aerospace stream and other engineering programs. CU InSpace has also maintained a strong relationship with Virtual Ventures, a Faculty of Engineering and Design organization that facilitates technology and engineering programs for youth. Team representatives have engaged with Ottawa youth through multiple events, reaching a broad audience from elementary to high school students. Additionally, members have presented at local high schools, inspiring students to explore aerospace and rocketry. These outreach efforts aim to not only educate young minds but also build a pipeline of future engineers passionate about space exploration and rocketry.

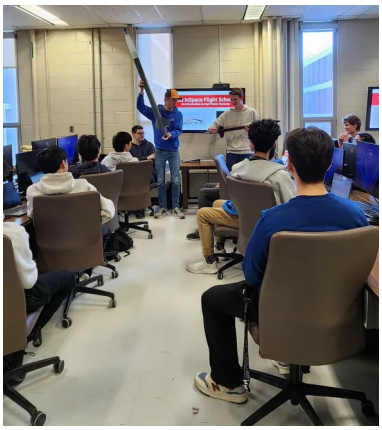

Figure 2 CU InSpace Educating Members About Rocketry

This year, CU InSpace's largest outreach initiative was the creation of *InSpace Flight School*, which aims to provide Carleton undergraduate students exposure to the amateur rocketry hobby, and the resources to participate. More specifically, the objective of InSpace Flight School is to guide students through the entire process of designing, building, and flying L1 certification rockets. Through bi-weekly lessons on all aspects of high power rocketry, rocket assembly workshops, and an excursion to the Upstate Research Rocketry Group (URRG) launch site, a total of 10 L1 certifications were achieved, with one student obtaining their L2 certification the day after their L1 flight. Notably, out of 10 rockets launched, 10 received a certification. In addition to these certifications, the team facilitated the construction of 6-10 rockets which did not fly and still await a launch.



Figure 3 InSpace Flight School at URRG



Figure 4 L1 Certification Launch

The InSpace Flight School initiative has been seen as a resounding success. This hands-on experience provide team members with invaluable practical skills in design, fabrication, and launch operations, further preparing them for careers in the aerospace industry, or just allowing them to go further into the amateur rocketry hobby. This initiative builds on the success of several team members who earned their first L1 certifications at Launch Canada 2024. As part of this effort, experienced members are mentoring new

participants, guiding them through the certification process and ensuring they understand best practices for safe and successful rocketry operations.

CU InSpace also continues to host its annual hands-on events designed to engage new members and spark excitement for rocketry from the start of the year. The annual Small Rocket event was once again held this fall, bringing together over 75 participants who were divided into 18 teams. Each team designed and built a model rocket with a strong emphasis on safety, stability, and successful recovery. These rockets, powered by A and B class motors, provided participants with valuable hands-on experience in rocketry fundamentals. This event served as an introduction for new members, allowing them to familiarize themselves with key rocket components and the principles behind a successful launch, setting the stage for deeper involvement in the team's projects throughout the year.



Figure 5 Participants at Small Rocket 2025

In the academic community, CU InSpace members have attended multiple conferences, including the Space Canada Horizons Conference and the SEDS Canadian Space Conference. In addition to this, members of CU InSpace's executive team presented research conducted by CU InSpace at the 2022 International Astronautical Congress in Paris, France. These opportunities allow team members to showcase their research, gain valuable insights from industry professionals, and build connections within the aerospace and rocketry community. Avionics team members have also given presentations to computer science students, highlighting how their involvement in CU InSpace has helped them develop key skills and secure employment opportunities. This event also served to introduce computer science students to the open-source development community by emphasizing CU InSpace's relationship with the Apache NuttX project. By engaging with students from diverse academic backgrounds, the team fosters interdisciplinary collaboration and knowledge-sharing.

2. Conops

The mission concept of operations (CONOPS) for this rocket is made up of nine stages, ranging from pre-flight activities to post-flight recovery. A flowchart of the progression of these stages may be seen in Fig. 6. An illustration of each portion of flight is also provided in Fig. 7.

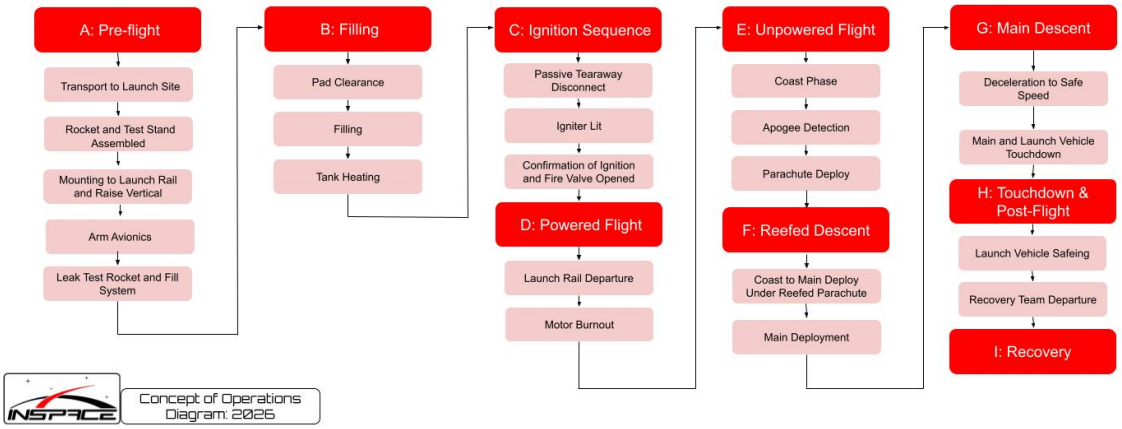

Figure 6 Mission Concept of Operations Flowchart

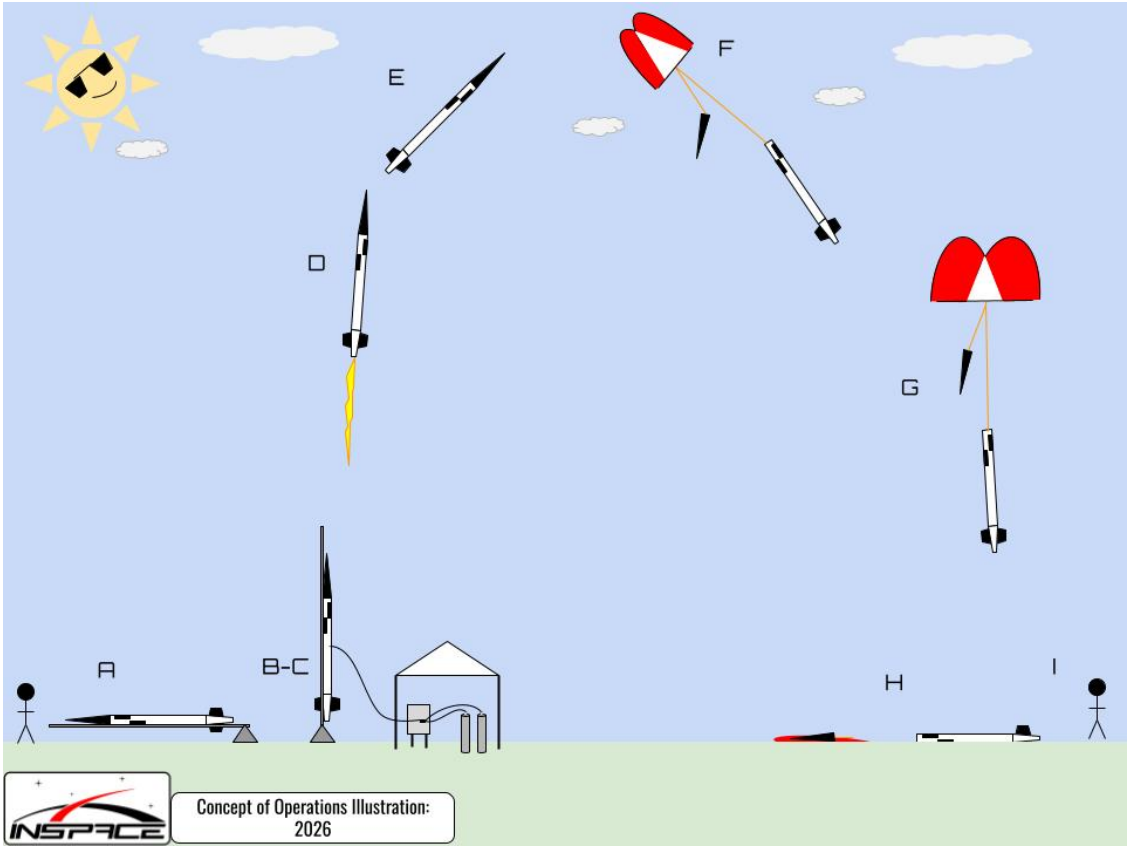

Figure 7 Mission Concept of Operations Diagram

A. Pre Flight (Duration: 2-3 hours)

Start: Rocket is transported to launch site and arrives on advanced pads.
End: The launch vehicle is assembled and integrated vertically on the launch rail. Leak testing of the fill system has been completed, and tanks have been opened. avionics, recovery and igniter have been armed.
Once the pad fill system and launch rail have been set up, the launch vehicle can be the transported to the launch site for integration. At the pad, the launch rail is taken horizontal, and the fill system is leak tested, while the recovery system is integrated into the forward tube. Once initial leak testing has been completed successfully, the rocket is carefully loaded onto the horizontal launch rail through its rail attachment buttons. The nylon lines are then connected to the rocket, and the avionics are armed. An additional high pressure leak test is performed once the rocket is horizontal on the rail, as a final check before the rocket is raised to the vertical position. After approval from RSO's, the rocket is raised and the recovery system is armed. Finally, the fill tanks are opened, igniter is armed, and all pad personnel return to the viewing/control area.

B. Filling (Duration: 20-25 minutes)
Start: Pad personnel clear the pad and return to the mission control centre.
End: The vehicle's oxidizer tank is full and at temperature.
Pad personnel depart the pad and return to the mission control centre, inserting the key to arm the control client. Filling of the rocket begins with a 5 minute high pressure leak test and nitrogen pre-pressurization. Then a 15 minute filling and temperature hold take place. Once the temperature hold is complete the rocket is ready to launch at any moment.
Off Nominal Procedures: In the case of the following off nominal scenarios abort procedures will be referenced from the flight procedures as linked in section 7.4.6 and summarized below.
Ignitor failure to ignite: Pulse ignitor power, abort launch and depressurize
Ignitor fails to light motor: Approach pad and safe the test stand
Communication lost with pad server: Attempt to reconnect, if unsuccessful wait for auto abort, if unsuccessful pull manual abort rope.

C. Ignition Sequence (Duration: 1 minute)
Start: The control client is armed for flight
End: The main fire valve has been opened.
When permission is acquired from LC staff, the rocket is armed for flight. After a 5 second count down the ignitor switch is flipped. Visual indication through cameras or a spotting scope is used to determine when smoke leaves the end of the chamber. Once smoke is seen another five second count down is given and the main fire valve opened.

D. Powered Flight (Duration: 11.5 seconds)
Start: Main fire valve is opened via the control client, and acceleration is detected by the flight avionics.
End: The avionics detect motor burnout at nominal burn duration.
When the fire valve switch, XV-5, is actuated, the nitrous from the oxidizer tank enters the combustion chamber, signifying the beginning of powered flight. As the rocket accelerates up the launch rail, the avionics bay begins to log sensor and telemetry data to the local SD card. The structures of the vehicle transmit the thrust from the engine casing to the surrounding airframe to lift the entire vehicle. Once the launch rail has been cleared, the fins maintain stability of the vehicle through the entire powered and unpowered upwards flight. The vehicle remains in powered flight until the avionics detect the acceleration and altitude is consistent with the coast period. Once this threshold is crossed, the motor has burned out and unpowered flight begins.

E. Unpowered Flight (Coast) (Duration: 36.4 seconds)
Start: Avionics accelerometer data indicate the motor has burned out and the rocket is coasting upwards.
End: Apogee is detected by the recovery deployment avionics, and the recovery deployment charges

deploy.
As the motor burns out, the launch vehicle decelerates as it coasts to an expected apogee of 44,562 ft [13,582 m] . The avionics and payload continue to collect data, the avionics continually check the altitude to determine when apogee has been detected. The recovery system is activated for deployment once apogee is detected.

F. Reefed Descent (Duration: 11 minutes 10 seconds)
Start: The recovery system deploys the reefed parachute, and the avionics detect a nominal drogue descent rate.
End: The rocket has descended to an altitude of 457 m (1500 ft) above the surface as the main parachute deployment begins.
Once apogee is detected, the avionics bay sends the signal for the recovery system to activate. An E-Match ignites the primary black powder charge cannon with an additional E-Match igniting a second later as a backup. This pressurizes the internals of the rocket and provides sufficient force to shear the shear pins, ejecting the parachute. The parachute then inflates to it's reefed diameter and configuration. The descent rate is slowed to a constant speed of approximately 25.6 m/s. At an altitude of 457m (1500 ft) AGL, the Transmitting Wireless Pico PCB sends a signal to the receiving box PCB, located on the skirt of the parachute. A Mako Line Cutter, also located in the receiving box, then cuts the reefing line, triggering dis-reefing of the parachute. A redundant receiving box on the opposite side of the parachute skirt containing a COTS Easy-Mini Altimeter also cuts the reefing line using a Mako Line Cutter. This occurs at an altitude of 1400 ft, acting as a redundant main deployment method.

G. Main Descent (Duration: 1 minute)
Start: The rocket has descended to an altitude of 457m (1500 ft) AGL, the parachute has been successfully dis-reefed. Avionics tracking detects a nominal main parachute descent rate.
End: The launch vehicle touches down on the surface.
Once the reefing line is cut and the main parachute deploys, the launch vehicle descends at approximately 7.8 m/s until touchdown. The avionics continues to log data throughout this, and future stages.

H. Touchdown & Vehicle Post Flight (Duration: Depends on time of launch / salvo. If recovering same-day, approximately 1 hour.)
Start: The launch vehicle contacts the ground.
End: Recovery team departs to the last transmitted coordinates of the launch vehicle.
Once the launch vehicle detects touchdown, the avionics trackers transmit the location of the rocket to the team's ground station and the recovery team begins planning the trip to recover the vehicle. Once launch vehicle location is known, routes are planned, and clearance is attained, the recovery team departs to the expected location of the launch vehicle.

I. Ground Recovery (Duration: 2-4 hours, depending on landing location of launch vehicle)
Start: The recovery team has been cleared to depart for the recovery of the launch vehicle.
End: The recovery team returns the launch vehicle to the mission control centre for inspection.
Once obtaining permission to depart for the landing zones, the recovery team proceeds towards the last known location of the vehicle. Once at the landing zone, the vehicle is safely recovered. This includes disconnecting potential un-ignited recovery deployment energetics for which protective equipment must be worn. The rocket is then transported back to the control centre for inspection of damage to the vehicle and any hazards to the team. The rocket is then returned for post-flight evaluation.

3. Requirements

3.1 Mission Requirements

Table 2 Mission Requirements

ID	Title	Requirement	Source	Comment/Explanation
INS-FUN-001	System Compliance	The rocket and related systems shall be fully functional and compliant to the Launch Canada DTEG.	DTEG	
INS-FUN-002	On-Board Camera	The rocket shall incorporate a fully functional on-board camera.	Self-Imposed	
INS-FUN-003	Official Altitude Logging	The rocket shall have a COTS barometric altimeter with on-board storage.	Rules and Requirements 3.3 and 3.2	The COTS altimeter will provide the official altitude log for scoring.
INS-FUN-004	COTS Tracking	The rocket shall incorporate redundant COTS GPS tracking methods.	Rules and Requirements 3.2	
INS-FUN-005	ID Markings	The Team ID especially, shall be prominently displayed (preferably visible on all four quadrants of the vehicle, as well as fore and aft), assisting competition officials to positively identify the project hardware with its respective team throughout the LC Challenge.	DTEG R8.8.14	
INS-FUN-006	CG/CP Markings	The CG and CP location of the fully-loaded vehicle shall be clearly marked on the rocket. For liquid/hybrid rockets, the fully-fueled CG can be a calculated value.	DTEG R8.8.15	
INS-FUN-007	Avionics	The rocket shall have a fully functional SRAD telemetry system compliant to the Launch Canada DTEG.	DTEG	
INS-FUN-008	Propulsion	The rocket shall have a fully functional SRAD engine compliant to the Launch Canada DTEG.	DTEG	
INS-FUN-009	Recovery	The rocket shall have a fully functional SRAD recovery system compliant to the Launch Canada DTEG.	DTEG	
INS-FUN-010	Payload	The rocket shall have a fully functional SRAD payload system compliant to the Launch Canada DTEG.	DTEG	
INS-FUN-011	Aerostructures	The rocket shall have a fully functional SRAD airframe compliant to the Launch Canada DTEG.	DTEG	
INS-FUN-012	Ground Systems	The rocket launch operations shall be supported by SRAD ground systems, of which all elements are compliant to the Launch Canada DTEG.	DTEG	
INS-FUN-013	Weight Limit	The rocket should have a maximum loaded weight of 45kg, with a minimum payload mass of 2kg.	Self-imposed	

3.2 Mission Requirements

Table 3 Mission Performance Requirements

ID	Title	Requirement	Source	Comment/Explanation
INS-PER-001	Apogee	The rocket shall achieve an apogee of at least 32,000 ft (9750 m).	Self-imposed	
INS-PER-002	Off-The-Rail Velocity	The rocket shall depart the launch rail with a velocity of at least 100 ft/s (31 m/s).	DTEG R10.2.1	In lieu of detailed analysis, a rail departure velocity of at least 100 ft/s (30.5 m/s) is generally acceptable.
INS-PER-003	Impulse Limit	The propulsion system shall not produce more than 40,000 Ns of impulse.	Rules and Requirements 3.1	
INS-PER-004	Thrust-to-Weight	The rocket shall have a TWR of at least 6:1	DTEG R.10.2.1	
INS-PER-005	Static Stability	The rocket shall have a minimum static stability margin of 1.5 to 2 calipers with a maximum of 6 calipers during ascent.	DTEG R10.3.1 and R10.4.1	Under 1.5 calipers will be considered under-stable and over 6 calipers will be considered over-stable.
INS-PER-006	Dynamic Stability	The rocket shall have a nominal parabolic trajectory until the initial deployment event at apogee.	Rules and Requirements	

3.3 System Requirements

Table 4 System Requirements

ID	Title	Requirement	Source	Comment/Explanation
SYS-AER-001	SRAD Composite Airframe	The rocket shall comprise of a fully SRAD composite airframe that shall be built to withstand conditions encountered during handling, transportation and during flight and be fully compliant of the SRAD airframe DTEG requirements.	INS-FUN-012	
SYS-AER-002	Camera	The rocket shall have an outside-view camera pointed downward toward the fins.	INS-FUN-002	
SYS-AER-003	Rocket Diameter	The rocket shall have a maximum outer diameter of 153mm and a minimum inner diameter of 143mm	INS-FUN-014	
SYS-AER-004	Static Stability	The rocket shall have a minimum static stability of 1.5 body calipers	INS-PER-005	
SYS-AER-005	Dynamic Stability	The rocket shall be dynamically stable	INS-PER-006	
SYS-AER-006	Off the Rail Velocity	The rocket shall leave the rail at no less than 100 ft/s (30.5m/s)	INS-PER-002	
SYS-AER-007	CG/CP Markings	The CG and CP positions shall be easily identifiable on the rocket exterior as per their simulated positions.	INS-FUN-007	
SYS-AVI-001	SRAD Avionics	The rocket shall incorporate an SRAD telemetry system which shall be capable of recording and transmitting the rocket's current 3D position and attitude through all stages of the flight. This system shall meet all DTEG requirements for SRAD GPS tracking solutions.	INS-FUN-007	
SYS-AVI-002	COTS GPS Tracking	The rocket shall incorporate a COTS GPS tracker which shall meet all relevant DTEG requirements.	INS-FUN-004	

SYS-PRP-001	SRAD Oxidizer Systems	The rocket shall have fully functioning, SRAD oxidizer systems. This system shall include a main fire valve, fill and dump system, vent system, and source tank system. This system shall comply with all Launch Canada DTEG requirements.	INS-FUN-008	
SYS-PRP-002	SRAD Flight Tank	The rocket shall have a SRAD flight oxidizer tank. The tank shall be capable of holding the nessary oxidizer required to reach specified height requirement. The tank shall follow all Launch Canada DTEG requirements.	INS-FUN-008	
SYS-PRP-003	Hydrostatic Testing	All SRAD pressure Vessel shall be hydrostatic tested in accordance and must pass all Launch Canada DTEG specifications prior to being used on rocket systems.	INS-FUN-008	
SYS-PRP-004	Cold Flow Testing	The oxidizer system shall be tested in a "Cold Flow" with an inert gas before use for an oxidizer applications. In accordance with all Launch Canada DTEG requirements.	INS-FUN-008	
SYS-PRP-005	Static Fire Testing	A minimum of 1 static fire will be performed before competiton. This test shall be performed in accordance with all Launch Canada DTEG requirements.	INS-FUN-008	
SYS-PRP-006	On Rocket Systems Height	All on rocket propulsion systems shall be designed such that the overall height of the hybrid motor is minimized.	INS-FUN-008	
SYS-GDS-001	SRAD Source Tank Inverters	There shall be the needed number of cylinder inverters to ensure the maximum amount of liquid flowing into the fill system.	INS-FUN-012	
SYS-GDS-002	SRAD Launch Rail	The team shall have a fully SRAD launch rail that can be transported to and from competition and meats all DTEG and RSO safety requirements.	INS-FUN-012	
SYS-REC-001	COTS Avionics	The rocket avionics stack shall communicate apogee and main disengaging altitude of 1500ft with a barometric altimeter.	INS-FUN-003	
SYS-REC-002	Deployment	The rocket shall deploy 'main' parachute at apogee in reefed configuration.	INS-FUN-009	
SYS-REC-003	Reefing	The rocket's parachute shall disreef at 1500ft.	INS-FUN-009	
SYS-REC-004	Drogue (reefed) descent rate	The rocket shall descend under drogue (reefed) at a rate no more than 30 m/s, and no less than 23 m/s.	INS-FUN-009	
SYS-REC-005	Main (disreefed) descent rate	The rocket shall descend under main (disreefed) at a rate no more than 9 m/s.	INS-FUN-009	

3.4 Subsystem Requirements

Table 5 Subsystem Requirements

ID	Title	Requirement	Source	Means of Compliance
AER-STR-001	Rocket Diameter	Body tubes shall be made using the existing mandrel from the 2024-25 year	SYS-AER-005 The mandrel is designed with a 147mm OD which as per SYS-AER-005 shall be the ID of the rocket.	Design/Manufacturing
AER-STR-002	SRAD Body Tubes	All body tubes used on the final airframe shall be fully SRAD. • These body tubes shall be 147mm ID as defined by SYS-AER-005 • The body tubes shall be 3K plain weave Carbon Fibre • The layup shall use a 0/90 weave pattern • The body tubes shall be roll wrapped • The body tubes shall be 8 plies thick	SYS-AER-001	Manufacturing
AER-STR-003	SRAD Body Nosecone	The nosecone used on the final airframe shall be fully SRAD. • This nosecone shall be made of fibreglass sleeve • The nosecone shall be 8 layers thick • The nosecone tip shall be machined aluminium	SYS-AER-001	Manufacturing
AER-STR-004	SRAD Couplers	All copuplers used on the final airframe shall be fully SRAD. • These couplers shall be 147mm OD • The couplers shall be 3K plain weave Carbon Fibre • The layup shall have a 0/90 weave pattern • The couplers shall be roll wrapped • The couplers shall be 8 plies thick • The couplers shall be tested thoughroughly in bending prior to final use	SYS-AER-001	Manufactring/Testing
AER-STR-005	SRAD Fincan	The fincan used on the final airframe shall be fully SRAD. • The fincan should be made of either 3K plain weave carbon fibre or fiberglass composite • The layup shall be in alternating layers ""I"" and ""v"" (0/90 and -45/45) weave patterns • The fincan may taper to the Nozzle eliminating the previously used metal boattail	SYS-AER-001	Design/Manufacturing
AER-DES-001	Ease of Integration	The design of the airframe and internal structures shall be constructed with ease of integration being a predominant factor. SYS-AER-001	Design	
AER-DES-002	Camera Integration	The camera shall be placed opposite to the rail lugs to minimally impead the aerodynamic capabilities of the rocket.	SYS-AER-002 SYS-AER-005	Design
AER-DES-003	Length to Diameter Ratio	The L/D of the rocket shall not exceed 26.	SYS-AER-005	Design
AER-DES-004	Maximum Height	The maximum height of the rocket shall be 13ft	SYS-AER-005	Deisgn

AER-DES-005	RELOCATION OF COMPONENTS	The rocket shall relocate components to better its CG and pitching frequency. • Avionics may be placed further into the nosecone. • Payload may be placed on top of the Ox-Tank	SYS-AER-004 SYS-AER-005	Design
AER-DES-006	Nosecone	The nosecone shall be a 5:1 Von Karman profile with a coupling shoulder extruding 150mm below flat surface	SYS-AER-001	Design
AER-SIM-001	FinFlutter	The flutter velocity of the fins shall be simulated using finsim. • A test specimen may then be tested to verify the simulation	SYS-AER-005	Simulation/Testing
AER-SIM-002	Topology Optimization	The bulkheads and corresponding shelves shall be topology optimized to endure the max shock force experienced during separation plus a safety factor	SYS-AER-001	Simulation/Testing
AVI-DAT-001	Attitude	The telemetry system shall report the rocket's pitch, roll and yaw	SYS-AVI-001	Testing/Analysis/Design
AVI-DAT-002	Acceleration	The telemetry system shall report the rocket's acceleration in the X, Y and Z axes • This requirement may be accomplished by two accelerometers, one high G range and one lower G range for higher precision at low accelerations. • The acceleration shall be recorded at a minimum of 500 Hz • The acceleration shall be able to be recorded to at least 32g acceleration	SYS-AVI-001	Testing/Analysis/Design
AVI-DAT-003	Angular Velocity	The telemetry system shall report the rocket's angular velocity • The angular velocity shall be able to be recorded to at least 200 deg/s rotation. • The angular velocity shall be recorded at a minimum of 250 Hz	SYS-AVI-001	Testing/Analysis/Design
AVI-DAT-004	Altitude	The telemetry system shall report the rocket's altitude • The altitude shall be accurate to at least 50 m at 10 km altitude AGL • The altitude shall be capable of being reported to at least 30 km altitude. • The altitude calculation should be accurate when it breaks Mach (If possible) • This shall be recorded at a minimum of 50 Hz	SYS-AVI-001	Testing/Analysis/Design
AVI-DAT-005	Pressure	The telemetry system shall record the barometric pressure of the rocket. • This shall be recorded to an accuracy of 2.5 mBar. • This shall be recorded at a minimum of 50 Hz.	SYS-AVI-001	Testing/Analysis/Design
AVI-DAT-006	Remaining Battery Life	The telemetry system shall report the remaining battery life of the system • This shall be recorded at a minimum of 1 Hz"	SYS-AVI-001	Testing/Analysis/Design
AVI-DAT-007	GPS Location	The telemetry system shall report the rocket's GPS position (latitude, longitude, altitude) • The GPS position shall be recorded at a minimum of 10 Hz • The GPS position shall be able to be reported up to a minimum of 30 km altitude • The GPS position shall be available through as much of the flight as practically possible	SYS-AVI-001	Testing/Analysis/Design

AVI-DAT-008	Timestamps	The telemetry system shall report all recorded measurements with a timestamp indicating the measurement time • The time stamp shall be accurate to at least 1 ms	SYS-AVI-001	Testing/Analysis/Design
AVI-DAT-009	Max Radio Update Rate	The telemetry system shall report packets to the ground station no more than 30 times a second	SYS-AVI-001	Testing/Analysis/Design
AVI-DAT-010	Prefered Radio Update Rate	The system should report packets to the ground station at least 10 times a second during flight mode.	SYS-AVI-001	Testing/Analysis/Design
AVI-DAT-011	Min Radio Update Rate	The telemetry system shall report packets to the ground station no less than 2 times a second.	SYS-AVI-001	Testing/Analysis/Design
AVI-DAT-012	Variable Radio Rate	The telemetry system may have a variable reporting rate depending on the flight state.	SYS-AVI-001	Not Required
AVI-DAT-013	Data Recording	The telemetry system shall record all telemetry data to non-volatile memory for post-flight recovery • This memory shall have space to store at least 30 minutes of flight data after 6 hours of pad time, and will not lose any flight data if the system is not recovered until the battery life has been exhausted. • This may be accomplished through not recording data while in the pad or landed states.	SYS-AVI-001	Anaysis/Testing
AVI-DAT-014	Data Recording Testing	The telemetry data recording should be tested and verified before flight	SYS-AVI-001	Testing
AVI-PYS-001	Volume Reduction	The telemetry system shall have a 25 % decrease in volume from CR_25	SYS-AVI-001	Analysis
AVI-PYS-002	Enclosure	The telemetry system shall have an enclosure which can resist flight stresses and protect the system through all expected flight loads. • The enclosure shall be designed to withstand the forces exerted by a landing under drogue.	SYS-AVI-001	Analysis
AVI-PYS-003	Single Board	The telemetry system may integrate the flight computer and radio transmitter onto a singular one board system.	SYS-AVI-001	Not Required
AVI-PYS-004	Rocket Integration	The telemetry system may be integrated with both competition launch vehicles	SYS-AVI-001	Not Required
AVI-MIS-001	Battery Life	The telemetry system shall have at least thirty hours of battery life • This may be accomplished through the use of a lower power pad/landed mode.	SYS-AVI-001	Alaysis/Testing
AVI-MIS-002	Power Failures	The telemetry system shall be robust to power failures	SYS-AVI-001	Analysis
AVI-MIS-003	Range	The telemetry system radio transmitter shall have a minimum range of 15km	SYS-AVI-001	Testing
AVI-MIS-004	NuttX	The telemetry system shall operate using the NuttX RTOS	SYS-AVI-001	Design
AVI-MIS-005	Indicating LEDs	The telemetry system shall have sufficient LEDs to implement the NuttX LED specification: https://nuttx.apache.org/docs/latest/reference/os/led.html	SYS-AVI-001	Design
AVI-MIS-006	Audible Arming Indicator	The telemetry system shall have an audible way to indicate successful arming	SYS-AVI-001	Design
AVI-MIS-007	Visual Arming Indicator	The telemetry system shall have an visual indicator for arming	SYS-AVI-001	Design

AVI-MIS-008	Flight State Detection	The telemetry system shall incorporate flight state detection.	SYS-AVI-001	Design
AVI-MIS-009	Recharable Batteries	The system shall be powered by rechargeable batteries • The system shall be capable of recharging these batteries while in the rocket. • The system should achieve this with no holes required in the airframe	SYS-AVI-001	Design
AVI-MIS-010	Arming	The system shall be capable of being armed and disarmed with no holes required in the aircraft • One possible way to achieve this would be through the use a a magnetic jumper which when shorted disarms the system • The arming/disarming solution should use low enough current that it may be left in the disarmed configuration for 2 weeks with no more then a 10% reduction in system battery life	SYS-AVI-001	Design
AVI-MIS-011	Vibration Resistance	The telemetry system shall be resistant to vibrations expected to be experienced during flight • This system should be tested for functionality under expected vibrations during flight.	SYS-AVI-001	Analysis/Testing
AVI-MIS-012	Wow factor	The telemetry system hardware should be visually appealing and have a "wow" factor (make non-technical individuals say "wow")	SYS-AVI-001	Statement
AVI-MIS-013	POSIX Standard	The telemetry system software shall use the POSIX standard	SYS-AVI-001	Design
AVI-MIS-014	Software Modularity	The telemetry system software shall be modular in nature	SYS-AVI-001	Design
AVI-MIS-015	Software approachablity	The telemetry system software shall be easily approachable for incoming members • The telemetry system software shall be comprehensively documented	SYS-AVI-001	Statement
AVI-MIS-016	NuttX Standards	The telemetry system software utilizing kernel space shall comply with the NuttX standards so that it may be contributed to the NuttX kernel	SYS-AVI-001	Design
AVI-MIS-017	Packet Latency	The telemetry system shall transmit packets with more than 500 ms latency	SYS-AVI-001	Testing
AVI-MIS-018	Ease of Assembly	The telemetry system shall be designed with ease of assembly in mind	SYS-AVI-001	Analysis/Integration Testing
AVI-MIS-019	System Portability	The telemetry system shall be portable across multiple rockets with minimal effort	SYS-AVI-001	Analysis/Design
AVI-MIS-020	Peripheral Failures	The telemetry system shall be robust to peripheral failures	SYS-AVI-001	Analysis
PRP-OXS-001	Oxidizer Compatible Components	Any materials in a fluid system or component that would not normally be directly exposed to a given fluid but could be exposed during a credible failure or by migrating downstream shall similarly be compatible with that fluid.	SYS-PRP-001 DTEG R2.2.3 DTEG R2.2.4	Design
PRP-OXS-002	Oxdizer Safe Design and Assembly	All fluid systems shall incorporate provisions in design, assembly and operation to prevent any contamination or foreign object debris (FOD) that would impede the operation and safety of the system.	SYS-PRP-001 DTEG R2.2.5	Design

PRP-OXS-003	Capped Openings	Caps, plugs or other protective covers shall be used on all ports and openings in fluid systems to prevent contamination when not in use.	SYS-PRP-001 DTEG R2.2.6	Design and Procedures
PRP-OXS-004	Oxidizer Safe Cleaning	All components which will or may come in contact with nitrous oxide during operation or testing shall be properly oxidizer cleaned and stored. No hydrocarbons must be left on surfaces which contact the nitrous and they must be stored in a verifiable oxidizer safe way.	SYS-PRP-001 DTEG R2.2.7 DTEG R2.2.8 DTEG R2.2.9 DTEG R2.2.10 DTEG R2.2.11 DTEG R2.2.12	Procedures and Cleaning
PRP-OXS-005	Remote Tank Filling	Any experimental pressure vessel, system or component thereof with a burst pressure less than 4.0 times the maximum expected operating pressure (i.e., factor of safety of 4.0) shall only be pressurized and de-pressurized remotely.	SYS-PRP-001 DTEG R2.2.30	Design and Procedures
PRP-OXS-006	Pressure Relief Valves Requirements	Pressure relief devices or features shall be incorporated on all systems having a pressure source which can exceed the maximum allowable pressure of the system, or where the malfunction / failure of any component can cause the maximum allowable pressure to be exceeded.	SYS-PRP-001 DTEG R2.2.35	Design
PRP-OXS-007	Pressure Relief Valve Sizing and Setting	All pressure relief valves shall be sized such that in the worst credible failure situation that there is sufficient flow rate to stop the pressure from rising to a hazardous level. Relief valves shall be sized and set such that the pressure does not exceed a point that would cause general yielding of the system, and provide full flow at the that pressure.	SYS-PRP-001 DTEG R2.2.37 DTEG R2.2.38 DTEG R2.2.39	Design
PRP-OXS-008	On Rocket Pressure Relief	When a relief device is installed on a flight vehicle the output of the relief device shall be plumbed to the outside of the airframe	SYS-PRP-001 DTEG R2.2.42	Design
PRP-OXS-009	Flight Tank Filling	Propellant tanks shall be filled and drained from the bottom of the tank, near the top of the main propellant valves.	SYS-PRP-001 DTEG R2.2.43	Design
PRP-OXS-010	Flight Tank Dumping	The flight tank shall have the ability to be remotly filled and dumped.	SYS-PRP-001 DTEG R2.2.44 DTEG R2.2.50	Design
PRP-OXS-011	Vent Line Routing	Vents shall be routed to minimize the hazard they pose to personnel	SYS-PRP-001 DTEG R2.2.45	Design
PRP-OXS-012	Power Fail Dump	Pressurized systems shall be designed to ensure that there is no credible failure case that would cause the loss of the ability to remotely depressurize the system. This requirement applies to all high-pressure sources on a vehicle or static test stand: propellant tanks, pressurant tanks, etc.	SYS-PRP-001 DTEG R2.2.48	Design
PRP-OXS-013	Flight Tank Vent	A rocket or engine test stand shall implement an emergency vent capability to relieve pressure to a safe level (less than 689 kPa (150 psig)) for all the pressurant and propellant tanks that is independent of the nominal control system	SYS-PRP-001 DTEG R2.2.49	Design
PRP-OXS-014	Fire Valve Fail	The main fire valve shall fail closed when pressure or power is lost.	SYS-PRP-001 DTEG R2.2.51	Design
PRP-OXS-015	Check Valves	Under no scenario shall a team ever use two check valves in a row	SYS-PRP-001 DTEG R2.2.51	Design
PRP-OXS-016	Check Valves on Fill Systems	Any check valve used shall be able to be manually opened from the outside of a vehicle.	SYS-PRP-001 DTEG R2.2.51	Design

PRP-OXS-017	Pilot Valves	Piloted valves shall open to abort in the depressurized state and their piloting valve shall depressurize the pilot line in the depressurized state.	SYS-PRP-001 DTEG R2.2.55	Design
PRP-OXS-018	FIll/Dump Valve Duty Cycle	Dump and Vent Valves shall have a duty cycle 3 times the abort time or operational time whichever is more. Fill valves shall have a duty cycle 2 times the fill time or operational time whichever is more.	SYS-PRP-001 DTEG R2.2.56	Design and Testing
PRP-OXS-019	SRAD Valve Reliability	SRAD valves shall be tested for reliability. Demonstrating a less than 5% probability of failure at MEOP with a maximum margin of error of 25%.	SYS-PRP-001 DTEG R2.2.57	Testing
PRP-OXS-020	Nitrous Line Filters	A nitrous line filters are not to be used in line with any nitrous flow pathway between the supply bottle and the engine.	SYS-PRP-001 DTEG R2.2.58	Design
PRP-OXS-021	Main Fire Valve Flow Rate	The main fire valve shall have a miniimium flow rate through the valve equivalent to that of a 0.8 inch inner diameter straight tube. Though 0.87 inch equivalent flow is preferred.	SYS-PRP-001	Design and Testing
PRP-OXS-022	Main Fire Valve Size	The main fire valve shall be designed such that it's height is minimized and it's diameter is less than the inner diameter of the tube.	SYS-PRP-001 SYS-PRP-006	Design
PRP-OXS-023	Main Fire Valve Normal State	The main fire valve shall be normally closed when there is no power delivered to the pilot valve as well when there is either pressure or no pressure in the system.	SYS-PRP-001	Design
PRP-OXS-024	Flight Tank Vent	The hybrid motor shall incorporate an active vent system capable of remote actuation.	SYS-PRP-001	Design
PRP-OXS-025	Flight Tank Vent Valve	The vent valve shall be placed on the ground systems to minimize on rocket valves and excess motor height.	SYS-PRP-001 SYS-PRP-006	Design
PRP-OXS-026	Fill and Dump System	The flight tank shall have a fill and dump system with a minimum flow rate through a 3/8 inch tube.	SYS-PRP-001	Design
PRP-OXS-027	Quick Disconnect System	The quick disconnect system shall be designed to minimize complexity and on rocket hardware	SYS-PRP-001	Design
PRP-OXT-001	Burst Safety Factor	The flight oxidizer tank shall not have a burst pressure less than 1.5 times the maximum expected operating pressure.	SYS-PRP-002 DTEG R2.2.13	Design
PRP-OXT-002	Yield Safety Factor	The flight oxidizer tank shall have the ability to be hydrostatic tested to 1.5 times maximum expected operating pressure without yielding.	SYS-PRP-002	Design and Testing
PRP-OXT-002	Less than 2 Burst Safety Factor	If a propellant tank is designed with a burst pressure of less than 2.0 times the maximum expected operating pressure, hydrostatic burst testing shall be performed to demonstrate that the design and manufacturing process actually achieved or exceeded the design burst pressure.	SYS-PRP-002 DTEG R2.2.14	Testing
PRP-OXT-003	Personal Proximity at Pressure	Experimental pressure vessels shall never be approached by personnel while pressurized to more than 25% of its burst pressure	SYS-PRP-002 DTEG R2.2.31	Testing and Procedures
PRP-OXT-004	Remote Pressure Sensing	"Experimental pressure vessels shall incorporate electronic pressure measurement and telemetry to allow tank pressures to be monitored remotely"	SYS-PRP-002 DTEG R2.2.34	Design

PRP-HST-001	Hydrostatic Testing Safety	Hydrostatic tests shall be only performed with faculty permission in designated locations with appropriate safety precautions and PPE for members during the test. For safety reasons, all hydrostatic tests shall be performed with water.	SYS-PRP-003 DTEG R2.2.22 DTEG R2.2.27	Testing
PRP-HST-002	Pressure Worthiness	All SRAD components intended to be used on a pressurized system must pass either a proof test and/or a burst test.	SYS-PRP-003 R2.2.23	Testing
PRP-HST-003	Proof Test Pressures	Each component shall have a proof test selected so that the pressure does not exceed 95 % of yield strength of material and does not exceed 75% of ultimate strength of material	SYS-PRP-003 DTEG R2.2.24	
GDS-LTR-001	Launch Angle	The launch tower shall be able to launch at angles between 0 and 9 degrees off vertical.	SYS-GDS-002 DTEG R11.2.2 DTEG R10.1.1	Design
GDS-LTR-002	Launch Tower Stability	The tower will be a stable structure with minimal deflection under predicted wind loads.	SYS-GDS-002	Design
GDS-CIV-001	Cylinder Inverter Anchoring	All source tank inverters shall be fully anchored to the ground to avoid tipping and ensure stability on site.	SYS-GDS-001	Procedures
GDS-CIV-002	Cylinder Inverter Securement	All source tanks shall be immobilized with respect to the inverter in both the upright and inverted positions.	SYS-GDS-001	Design/Procedures
GDS-CIV-003	Full Inversion of Source Tanks	The source tanks will be in the fully inverted position when filling allowing the maximum amount of liquid to exit the port.	SYS-GDS-001	Design
REC-DEP-001	Deployment Redundancy	The deployment system shall have redundant energetics and electronics.	DTEG R4.8.2	Design
REC-DEP-002	Ejection Testing	The full recovery system must have a minimum of two full ground ejection tests.		Testing
REC-DEP-003	COTS Deployment	The SRAD deployment system shall have a redundant COTS system	DTEG R4.8.2	Design
REC-DEP-004	Rigging	The shock cords will be sized such that the rocket sections will not interact with eachother.		Design
REC-PAR-001	Parachute	The parachute volume shall respect the recovery section of the aerostructure body tube.		Design and Testing
REC-PAR-002	Reefing line	The reefing line shall be sized such that in the reefed configuration, the rocket falls between 23-30 m/s.		Design
REC-ELEC-001	Arming Buzzer	The SRAD deployment system shall have a method to signal the arming state of electronics.		Design
REC-ELEC-002	SRAD Reefing Electronics	The SRAD reefing electronics shall be ground tested to ensure: 1) A proper connection can be maintained for rigging distances		Testing
REC-ELEC-003	SRAD Reefing Electronics Deployment	The SRAD reefing electronics shall not be influenced by the order of arming electronics while on the pad.		Design and Testing
REC-ELEC-004	Reefing altimeters	The SRAD reefing electronics system shall have a redundant and independent COTS Easymini altimeter reefing system.	DTEG R4.8.3	Design

4. Systems Architecture

4.1 Architecture Overview and Layout

The primary target of the CR26H airframe development is to implement the team's second SRAD hybrid motor into a dynamically sound flight vehicle. As this is the team's second time flying a hybrid motor, many lessons learned can be applied to various design considerations, in particular looking at the intertank section of the engine, length of the forward airframe and design of sub systems within, and the design of the fins and how that impacts dynamic stability. The airframe is organized into four main sections.

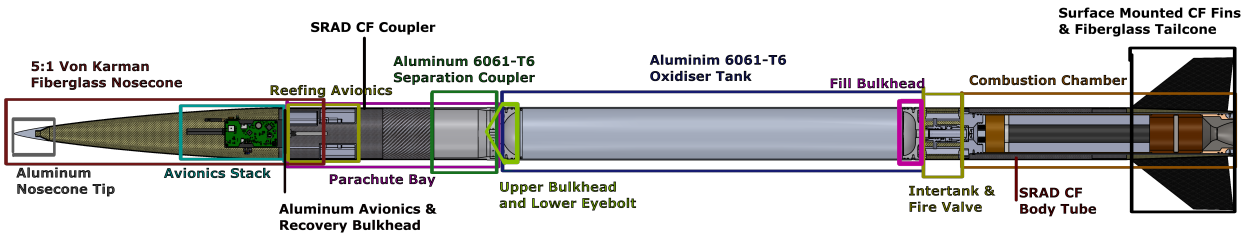

Figure 8 Main Airframe Components and Sections Breakdown, CR26H, Launch Canada 2026

The airframe is composed of SRAD roll-wrapped carbon fiber body tubes mated using COTS carbon fiber couplers, an SRAD fiberglass and aluminum nose cone, tip-to-tip carbon fiber layup over surface mounted carbon fiber plates, and a hybrid motor. A preliminary breakdown of the airframe based on the diagram in Fig. 8 are presented in Table 6. Furthermore, key dimensions of the airframe are provided in Table 7.

Table 6 Airframe Breakdown by Section

Section	Structural Components	Manufacturing
Forward (Black)	Nose Cone Tip	CU Machine Shop - 6061-T6 Aluminum Alloy
	Fiberglass Nose Cone	SRAD Fibreglass Layup Nosecone
	Carbon Fiber Coupler	SRAD Carbon Fiber Coupler Layup
	Carbon Fiber Body Tube	SRAD Carbon Fiber Roll-Wrapped Body Tube
	Avionics and Recovery Bulkhead and Support Ring	CU Machine Shop - 6061-T6 Aluminum Alloy
	Metal Coupler	CU Machine Shop - 6061-T6 Aluminum Alloy
Ox-Tank (Green)	Oxidizer Tank	CU Machine Shop - 6061-T6 Aluminum Alloy
	Carbon Fiber Body Tube	SRAD Carbon Fiber Roll-Wrapped Body Tube
Intertank (Red)	Fire Valve	CU Machine Shop - 6061-T6 Aluminum Alloy
	Stringers	CU Machine Shop - 6061-T6 Aluminum
Aft (Blue)	Aft Tube Mounting Ring	CU Machine Shop - 6061-T6 Aluminum Alloy
	Combustion Chamber	CU Machine Shop - 6061-T6 Aluminum Alloy
	Carbon Fiber Body Tube	SRAD Carbon Fiber Roll-Wrapped Body Tube
	Fiberglass Tailcone	SRAD Fiberglass Tailcone
	Carbon Fiber Fins	SRAD Carbon Fiber Fin
	Retention Ring	CU Machine Shop - 6061-T6 Aluminum Alloy

Table 7 Key CR26H Airframe + Hybrid Motor Dimensions

Components	Dimension [Imperial]	Units
Tip-to-Tail length	3.51 [138"]	m
Fin Semi-Span	0.1397 [5.5"]	m
Airframe OD	0.1515 [5.965"]	m
Oxidizer Tank Diam.	152.4 [6"]	mm
Oxidizer Tank Len.	1225.6 [48.25"]	mm
Combustion Chamber Diam.	121 [4.75"]	mm
Combustion Chamber Len.	745 [29.315"]	mm

4.2 Mass Budget

SUBSYSTEM	ASSEMBLY (OR GROUP)	COMPONENT	QTY	MASS PER ITEM (kg)	TOTAL MASS (kg)	CONFIDENCE IN MASS	ADDED MASS MARGIN (%)	CORRECTED MASS (kg)	WET MASS FRACTION (%)
AEROSTRUCTURES	**FORWARD SECTION**								
		Nosecone	1	1.1350	1.1350	MEASURED	*0%*	1.135	2.40%
		Nosecone Tip	1	0.1000	0.1000	MEASURED	*0%*	0.100	0.21%
		Forward Coupler	1	0.3770	0.3770	MEASURED	*0%*	0.377	0.80%
		Avionics/Recovery Support Ring	1	0.0330	0.0330	MEASURED	*0%*	0.033	0.07%
		Avionics/Recovery Bulkhead	1	0.2410	0.2410	MEASURED	*0%*	0.241	0.51%
		Assembly Total			***1.8860***			1.886	3.98%
	CENTER SECTION								
		Body Tube	1	0.6080	0.6080	MEASURED	*0%*	0.608	1.28%
		Metal Coupler	1	0.8790	0.8790	MEASURED	*0%*	0.879	1.86%
		Eye Bolt	2	0.0680	0.1360	MEASURED	*0%*	0.136	0.29%
		Eye Bolt Nut	2	0.0078	0.0155	MEASURED	*0%*	0.016	0.03%
		Assembly Total			***1.6385***			1.639	3.46%
	AFT SECTION								
		Inter-Tank Panels	1	0.1660	0.1660	MEASURED	*0%*	0.166	0.35%
		Runtime Camera (Control Board & Camera)	1	0.0102	0.0102	HIGH CONF.	*5%*	0.011	0.02%
		18650 Batteries	2	0.0400	0.0800	MED CONF.	*10%*	0.088	0.19%
		Camera Mount	1	0.1300	0.1300	LOW CONF.	*20%*	0.156	0.33%
		Aft Tube Attachment Ring	1	0.1000	0.1000	MEASURED	*0%*	0.100	0.21%
		Aft Body Tube	1	0.6230	0.6230	MEASURED	*0%*	0.623	1.31%
		Fincan Attachment Ring	1	0.0830	0.0830	MEASURED	*0%*	0.083	0.18%
		Fincan Coupler	1	0.1250	0.1250	MEASURED	*0%*	0.125	0.26%
		Tailcone	1	0.6000	0.6000	MEASURED	*0%*	0.600	1.27%
		Fins	1	0.5370	0.5370	MEASURED	*0%*	0.537	1.13%
		Fincan (use this value for final mass budget)	1	0.5000	0.5000	LOW CONF.	*20%*	0.600	1.27%
		Assembly Total			***1.9172***			1.952	4.12%
	Airframe Fasteners								
		Fasteners	35	0.0021	0.0752	HIGH CONF.	*5%*	0.079	0.17%
		Shear Pins	6	0.0011	0.0064	HIGH CONF.	*5%*	0.007	0.01%
		Airframe Fasteners Total			***0.0752***			0.086	0.18%
	Other Components								
		Paint	1	1.2500	1.2500	LOW CONF.	*20%*	1.500	3.17%
		Other Total			***1.2500***			1.500	3.17%
	Aerostructures Subsystem Total				**6.7669**			7.062	14.90%
PROPULSION	**Oxidizer Assembly**								
		Oxidizer	1.000	15.000	15.000	Medium	10.00%	16.500	34.82%
		Casing	1.000	4.485	4.485	Very High	2.50%	4.597	9.70%
		Vent Bulkhead	1.000	1.936	1.936	Measured	0.00%	1.936	4.09%
		Fill Bulkhead	1.000	1.510	1.510	High	5.00%	1.586	3.35%
		Pressure Port Plug	1.000	0.007	0.007	Very High	2.50%	0.007	0.02%
		Tank Bolts	40.00(	0.005	0.200	High	5.00%	0.210	0.44%
		Assembly Total			***23.138***			23.138	48.83%
	InterTank							0.000	0.00%
		Upper Housing	1.000	0.264	0.264	Measured	0	0.264	0.56%
		Main Housing	1.000	0.277	0.277	Measured	0	0.277	0.58%

Figure 9 CR26H Mass Budget Page 1

SUBSYSTEM	ASSEMBLY (OR GROUP)	COMPONENT	QTY	MASS PER ITEM (kg)	TOTAL MASS (kg)	CONFIDENCE IN MASS	ADDED MASS MARGIN (%)	CORRECTED MASS (kg)	WET MASS FRACTION (%)
		Poppet	1.000	0.137	0.137	Measured	0	0.137	0.29%
		Valve Bolts + Spring	1.000	0.116	0.116	Measured	0	0.116	0.24%
		QD Fittings	2.000	0.038	0.076	Low	25.00%	0.095	0.20%
		Vent fittings and lines	1.000	0.034	0.034	Low	25.00%	0.043	0.09%
		Pressure Port Plugs	2.000	0.006	0.012	High	5.00%	0.013	0.03%
		Stringers	3.000	0.073	0.219	High	5.00%	0.230	0.49%
		Stringer Bolts	12.00(	0.005	0.060	Medium	10.00%	0.066	0.14%
		Assembly Total			**1.195**			1.195	2.52%
	Combustion Chamber Assembly	**There is about a kilo of discrepancy in the openrocket file**						0.000	0.00%
		Casing	1.000	2.401	2.401	High	5.00%	2.521	5.32%
		Nozzle	1.000	0.682	0.682	High	5.00%	0.716	1.51%
		Injector Bulkhead + Injector Plate	1.000	1.544	1.544	Measured	0	1.544	3.26%
		Nozzle Retainer	1.000	0.274	0.274	High	5.00%	0.288	0.61%
		Mixing Plate	1.000	0.683	0.683	High	5.00%	0.717	1.51%
		Solid Fuel Mass	1.000	2.000	2.000	Low	25.00%	2.500	5.28%
		Fuel Liner	1.000	0.706	0.706	High	5.00%	0.741	1.56%
		Post and Pre Phenolics	1.000	0.590	0.590	High	5.00%	0.620	1.31%
		O-Rings	4	0.0040	0.016	MEASURED	*0%*	0.016	0.03%
		Assembly Total			***8.8800***			9.663	
	Propulsion Fastener Section :)								
		Radial Injector Bulkhead Fasteners	16	0.0015	**0.0240**	MEASURED	*0%*	0.024	0.05%
		Injector Fasteners	6	0.0020	**0.0120**	MEASURED	*0%*	0.012	0.03%
		Nozzle Carrier Fasteners	12	0.0015	**0.0180**	MEASURED	*0%*	0.018	0.04%
	Propulsion Subsystem Total Wet		1	32.7818	**32.7818**				
	Propulsion Subsystem Total Dry		1	15.7818	**15.7818**				
AVIONICS	**Nosecone Avionics**								
		Avionics from Baja (will probs increase slightly due to recovery easy minis)	1	1.3000	1.3000	MEASURED	*0%*	1.300	2.74%
		Assembly Total			***1.3000***				
	Avionics Subsystem Total				**1.3000**				
RECOVERY	**BP Ejection System**								
		~~RAPTOR + CO2 Canister~~	0		0.0000	MEASURED	*0%*	0.000	0.00%
		BP + Assembly	2	0.0828	0.1656	LOW CONF.	*20%*	0.199	0.42%
		E-MATCH	4	0.0020	0.0080	LOW CONF.	*20%*	0.010	0.02%
		Assembly Total			***0.1736***				
	Parachute Assembly								
		Transmitter Box 3D Print	1	0.0760	0.0760	MEASURED	*0%*	0.076	0.16%
		Transmitter Box Nuts & Bolts	1	0.0090	0.0090	MEASURED	*0%*	0.009	0.02%
		Transmitter Box PCB	1	0.0130	0.0130	MEASURED	*0%*	0.013	0.03%
		Transmitter Box Screw Switch	1	0.0030	0.0030	MEASURED	*0%*	0.003	0.01%
		Transmitter Box Wires	1	0.0040	0.0040	MEASURED	*0%*	0.004	0.01%
		Transmitter Box Battery INR14500 1500mAh	1	0.0220	0.0220	MEASURED	*0%*	0.022	0.05%
		Receiver Box Black Powder	2	0.0060	0.0120	MEASURED	*0%*	0.012	0.03%
		Receiver Box Wires	2	0.0060	0.0120	HIGH CONF.	*5%*	0.013	0.03%
		Shock Cord (Rocket to Swivel)	1	0.3000	0.3000	HIGH CONF.	*5%*	0.315	0.66%

Figure 10 CR26H Mass Budget Page 2

SUBSYSTEM	ASSEMBLY (OR GROUP)	COMPONENT	QTY	MASS PER ITEM (kg)	TOTAL MASS (kg)	CONFIDENCE IN MASS	ADDED MASS MARGIN (%)	CORRECTED MASS (kg)	WET MASS FRACTION (%)
		Shock Cord (Swivel To Chute)	1	0.4150	0.4150	HIGH CONF.	*5%*	0.436	0.92%
		Swivel	2	0.1350	0.2700	MEASURED	*0%*	0.270	0.57%
		Main Chute (chute+suspension lines+receiving boxes	1	1.6000	1.6000	MEASURED	*0%*	1.600	3.38%
		M4 Rods	4	0.1100	0.4400	MEASURED	*0%*	0.440	0.93%
		Shock Cord (Swivel To Nosecone)	1	0.0500	0.0500	MEASURED	*0%*	0.050	0.11%
		Pilot Chute	1	0.1910	0.1910	MED CONF.	*10%*	0.210	0.44%
		Assembly Total			***3.4170***				
	Recovery Subsystem Total				**3.5906**				
PAYLOAD	**Payload Assembly**								
		Payload	1	0.0000	0.0000	MEASURED	*0%*	0.000	0.00%
		Assembly Total			***0.0000***				
	Payload Subsystem Total				**0.0000**				
	Total Rocket Dry			**No Propellant**	*27.439*		**No Propellant**	***28.382***	***59.90%***
	Total Rocket Wet				*44.439*	Added Margin:	6.62%	***47.382***	
				Dry No Margin (lb)	60.493		Dry (lb)	62.572	
				Wet No Margin (lb)	97.972		Wet (lb)	104.460	

CR26H Mass Budget

CU InSpace 2026 Launch Canada Competition Rocket

Document Revision Number	*REV3*
Document Revision Date	*2026-06-26*
Solidworks CSM Version	*7.1*
OpenRocket Version	*5-2*
RasAero II Version	5-2

Revision History

Revision	Date	Editor	Changes
REV0	*2025-09-27*	Atharva Vaishampayan	Document Creation
REV1	*2025-10-31*	Atharva Vaishampayan	Updated Preliminary Values
REV2	*2026-03-13*	Thomas Birnie-Wortley	Updated Preliminary Values
REV3	*2026-06-26*	Sophia	Updated aerostructure values with measured values
REV4	*2026-7-4*	Sophia	Updated recovery values
REV5			
REV6			

Figure 11 CR26H Mass Budget Page 3

5. Performance Analysis

5.1 Flight/Demo Performance

The rocket's predicted flight performance was tabulated into Table 8.

Table 8 CR26H Flight Performance - No Wind

Performance Specification	Value
Max Velocity	655 m/s [Mach 2.01]
Off the Rail Velocity	31.1 m/s [102 ft/s]
Apogee	13 582.5 m [44 562 ft]
Max Acceleration	99.3 m/s^2 [325.8 ft/s^2]
Thrust to Weight Ratio	8.87
Stability Margin	17.5% [4.03 cal]

For in-depth discussion of dynamic stability analysis, see Section 6.

5.2 Recovery Dispersion Analysis

Dispersion is done using RocketPY, a 6 degrees of freedom module for python that includes capabilities for Hybrid engines. A Monte Carlo simulation was created for our specific engine. This allows the variation of every parameter imaginable. Using RocketPy's built in weather model capability old weather conditions can be used to simulated the conditions of launch. Each possible flight option was given 2000 iterations to ensure accurate result, this totals to 12000 total simulations run. The resulting maximum impact range from launch site for each condition is noted. For main at apogee the maximum impact range is 61468 ft, for drogue only it is 35443 ft, and for a ballistic impact it is 39981 ft. A user interface was designed to allow for easy repeatability of the simulations, as well as ease of transition for new leads learning dispersion. Fig. 12 is a screenshot of the user interface including all flight parameters used for the dispersion results in the sections below. Some assumptions are made to simplify the simulations. The rocket is assumed to be a straight tube after the nose cone, neglecting the tail cone, as well as it is simulated as a single surface finish. For ease of notice the highways are highlighted yellow in the figures below.

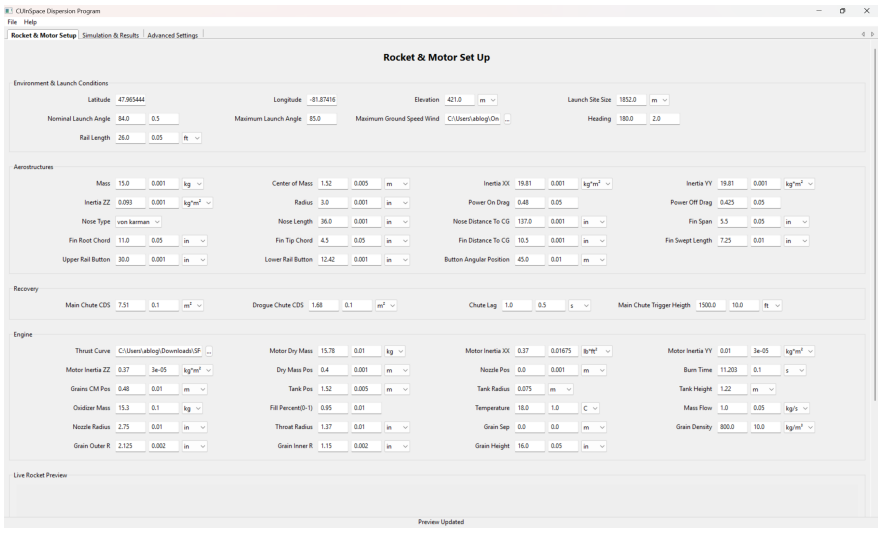

Figure 12 Dispersion UI and Parameters

5.2.1 Maximum Expected Wind Conditions

The first weather model that is used simulates the maximum winds that our team is comfortable launching in. A .nc weather file from July 2024 is used as the ground speed wind in the Timmins area was 20 mph. This file will give expected drift distance under those wind speeds. Figure 13 below shows the 1 and 2 sigma ellipses for flight under ballistic, main at apogee, and drogue only flights. The ground winds on this day are southern winds so the normal launch heading was 180 degrees.

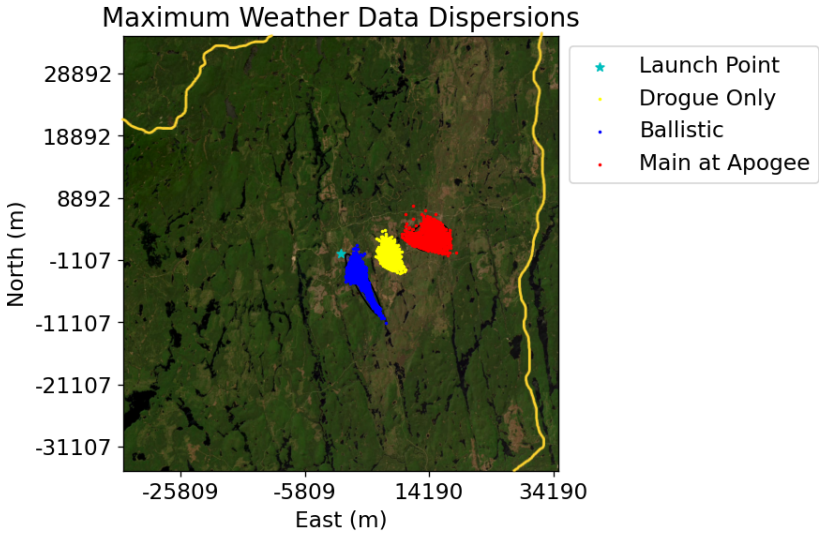

Figure 13 Dispersion Results Under Maximum Expected Wind Conditions

5.2.2 Typical Wind Levels

The second set of weather conditions used are meant to demonstrate the typical wind levels for mid August is the Timmins area. Another .nc file was downloaded from our teams launch day at competition last year. The results of the dispersion under these conditions is given in Fig. 14 below. The heading was selected the same as last years at competition, as 302 degrees.

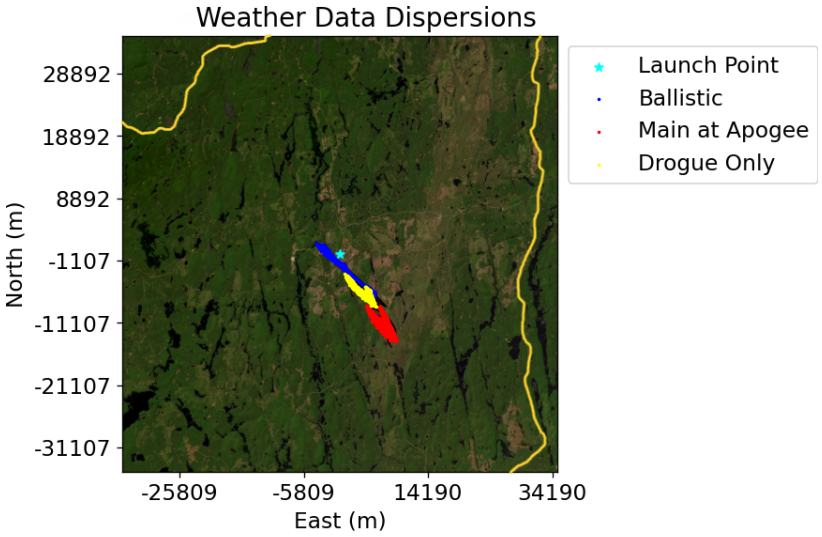

Figure 14 Dispersion Under Typical Wind Conditions

6. Aerostructures

6.1 Aerostructures Overview

The aerostructures sub-team is responsible for the design and manufacturing of the vehicle's airframe and its integration components. CR26H looks to expand on the lessons learned at Launch Canada 2025 with CR25H, in addition to taking on the challenge of creating the team's second complete SRAD airframe featuring surface-mounted fins and corresponding integration components. These components consisted of the nosecone, fin can, body tubes, couplers, aluminum bulkheads and accompanying support rings, oxidizer tank, and intertank fairing. Learning from CR25H, this year, aerostructures looks to reduce the overall vehicle height to reduce its slenderness ratio. Additionally, the team is increasing its investigation into dynamic stability by looking at the vehicle's maximum pitching coefficient, reducing the probability of a similar failure.

6.2 Nose Cone

6.2.1 Detailed Design

The nosecone of CR26H is a 5:1 Von Karman fiberglass nosecone with an aluminum tip. CU InSpace has used 5:1 Von Karman nosecones for several years with great success, as they provide the lowest drag force for supersonic flight between Ma 1 and Ma 2, where the rocket is spending a significant portion of time in ascent. The nosecone is made of fiberglass to allow for radio transparency as the avionics stack in charge of telemetry is located within the nosecone. The use of the metal tip allows the team to achieve a much sharper point than would be possible with composites only, greatly reducing pressure-induced drag from a bow shock forming on the nosecone. The transition from the metal tip to the main body of the nosecone is carefully controlled to ensure a smooth joint, further eliminating shockwave-induced drag. The nosecone includes a 1 caliber (5.96 in [151.5 mm]) shoulder section to interface with the SRAD carbon fiber coupler that joins the nosecone to the main body tube. The nosecone is affixed to the coupler during flight by 4 radially mounted counterbored M4 bolts, which are located approximately 1 inch from the top of the coupling section. The bolts pass through the fiberglass nosecone, carbon fiber coupler, the aluminum support ring and finally thread into the avionics and recovery bulkhead. Previous years' design saw the nosecone coupler bonded to the nosecone and bolted to the body tube; however, the subject design change allows the avionics to be mounted higher up in the nosecone, reducing the required space in the body tube and decreasing overall rocket length, one of the main goals of this year. Future iterations of this design will attempt to make further use of the space inside the nosecone, as the use of that space would serve to greatly reduce rocket length beyond what was achieved this year.

6.2.2 Manufacturing Process

The nosecone is made with 5 layers of medium 6-inch diameter fiberglass sock overlayed on top of a 3D printed mold and bonded with aeroepoxy PT2712. This mold is then removed, leaving a fiberglass shell. The tip of the shell is specifically designed to interface as seamlessly as possible with the aluminum 6061-T6 nosecone tip and is bonded to the nosecone with PT2712 epoxy.



Figure 15 Nosecone Manufacturing

6.2.3 Analysis

As a part of aerostructures' goal to reduce the overall height of the rocket, several sensors were pushed further into or closer to the nosecone. The team was concerned that these sensors would be affected by shockwaves on the nosecone, so a CFD simulation was performed using Ansys Fluent to estimate the shockwave locations on the nosecone. A 2D domain of 2x the length of the nosecone and 9x the nosecone shoulder diameter in width. The nosecone shoulder was also extended to double the length of the actual nosecone shoulder to account for computational errors arising from using a pressure outlet as a boundary condition. A mesh convergence study was tested from 10 mm to 2 mm using 1 mm intervals and had minimal variation in static pressure and drag counts, which was sufficient to deem the simulation convergent, but the 2 mm solution was utilised as it has the least amount of residuals near the side boundaries. The simulation utilised a velocity inlet at Mach 2, a pressure outlet behind the nosecone, and far-field pressure boundaries on the side boundaries of the simulation.Figures 16a to 16c show the pressure contour, velocity contour, and the mass residual contours from the simulation, which was then used to estimate the shock location on the nosecone and to evaluate the accuracy of the simulation based on meshed mass residuals.

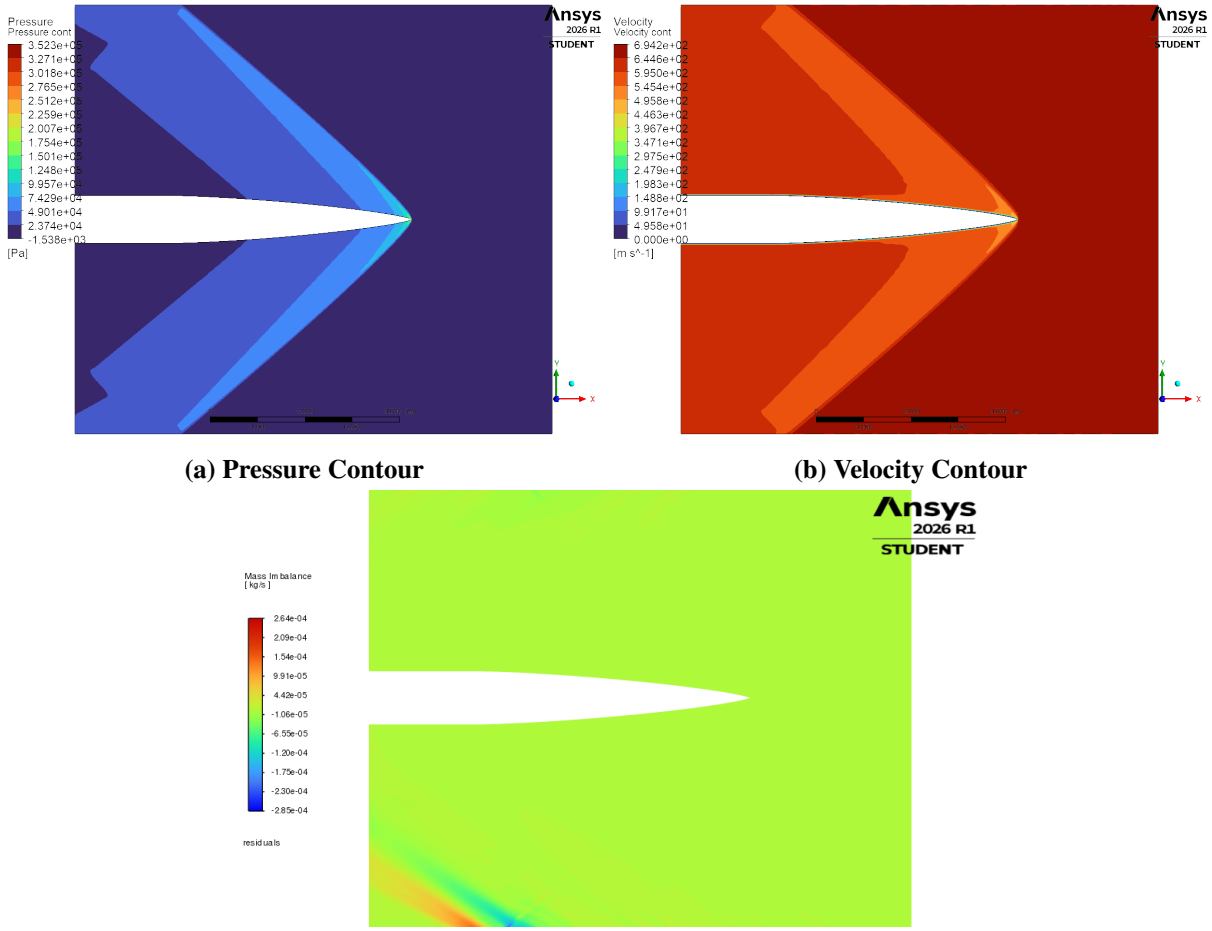

(a) Pressure Contour **(b) Velocity Contour**

(c) Residuals Contour

Figure 16 Nosecone CFD Results

Based on this CFD result, it was determined that adding the vent holes for the avionics would not be affected by the shockwave, as the shockwave occurred significantly further forward on the nosecone. The results show that a bow shock would occur at the tip of the nosecone, and a normal shock would occur at around 60% of the total length of the nosecone when measured from the tip, whereas the vent holes are located at 86% of the total length of the nosecone from the same reference. This was deemed acceptable as CR26H is unlikely to greatly exceed Ma 2, and the normal shock will not progress closer to the vent holes at speeds less than Ma 2. One section of the CFD simulation had several residuals likely caused by a few lower-quality mesh cells, as can be seen in Fig. 16c. This section did not seem to influence the results and was far enough afield of the simulation to deem it to have no overall effect on the location of the shockwave.

6.2.4 Testing and Validation

This nosecone design has extensive flight heritage, having survived 6 rocketry flights to date and reached a max speed of Ma 2.1 on CR26. The nosecone undergoes several visual and auditory (tap) tests upon completion to ensure no internal defects or cracks are present in the composite. It has also sustained 100 N radial loads as part of a comparison test with a carbon fiber body tube.

6.3 Airframe

6.3.1 Detailed Design

The main body of CR26H consists of two carbon fiber tubes, colloquially termed the "forward tube" and the "aft tube," the aluminum flight tank, a non-structural fiberglass fairing, and the fin system, which is made of both fiberglass and carbon fiber. The fin system and the flight tank are discussed in later sections. Figure 17

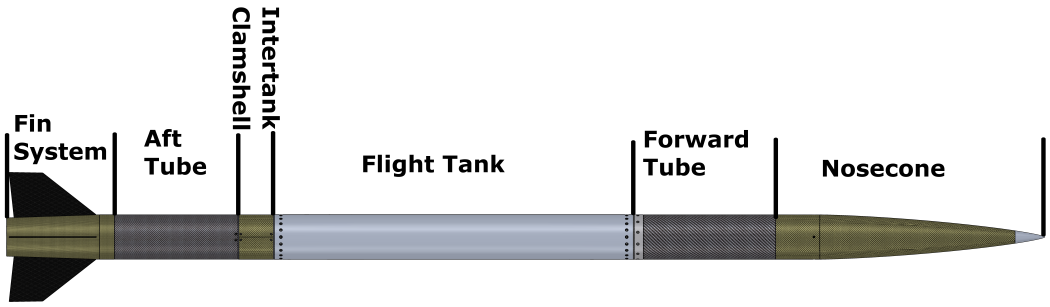

Figure 17 Airframe Overview

The forward and aft tubes are 151 mm nominal OD, 147 mm nominal ID, and made of 8 layers of 3k carbon fiber. These tubes are 450 mm and 420 mm long respectively. The forward tube contains the parachute and all of the recovery hardware required for the reefed parachute system. It is also the main structural body for the upper portion of the rocket, sustaining aerodynamic loading from the nosecone, ejection charge forces, and any gust loads during flight. The aft tube functions as a load path for the aerodynamic forces acting on the fin system, and as a secondary load path in the event of a failure at the upper combustion chamber bulkhead. The fiberglass fairing covers the intertank region and is meant for easy access to the fire valve and the plumbing for fill and vent processes. This part is 117 mm in length and permits the rocket surface to remain continuous, reducing drag that would otherwise occur at that location.

6.3.2 Manufacturing Process

The body tubes are made of 3k plain-carbon weave, roll-wrapped onto a metal mandrel. They consist of 8 layers of carbon bonded with aero epoxy PT2712. The tubes are then cut to length using a Dremel metal cutting wheel, sanded with progressively smaller sandpaper grits to a 220-grit finish, painted, and clear-coated. Extra skim coats of epoxy are applied to the tubes if required. The fiberglass fairing is made of 5 layers of 6” fiberglass sock overlayed onto a 3D printed mandrel, where each layer of fiberglass sock is liberally coated in aeroepoxy. The fairing is then cut to length using the Dremel metal cutting wheels, and then cut into 3 pieces to align with the 3 stringers, dividing the intertank section into even thirds. The fairing is sanded smooth to 220 grit, painted, and clear-coated before flight.

6.3.3 Analysis

The body tubes are expected to experience a maximum load of 900 N m. This number was determined by calculating the force experienced by the airframe at a conservative angle of attack at maximum velocity. Shear and bending moment diagrams were generated, as seen in Fig. 18 below.

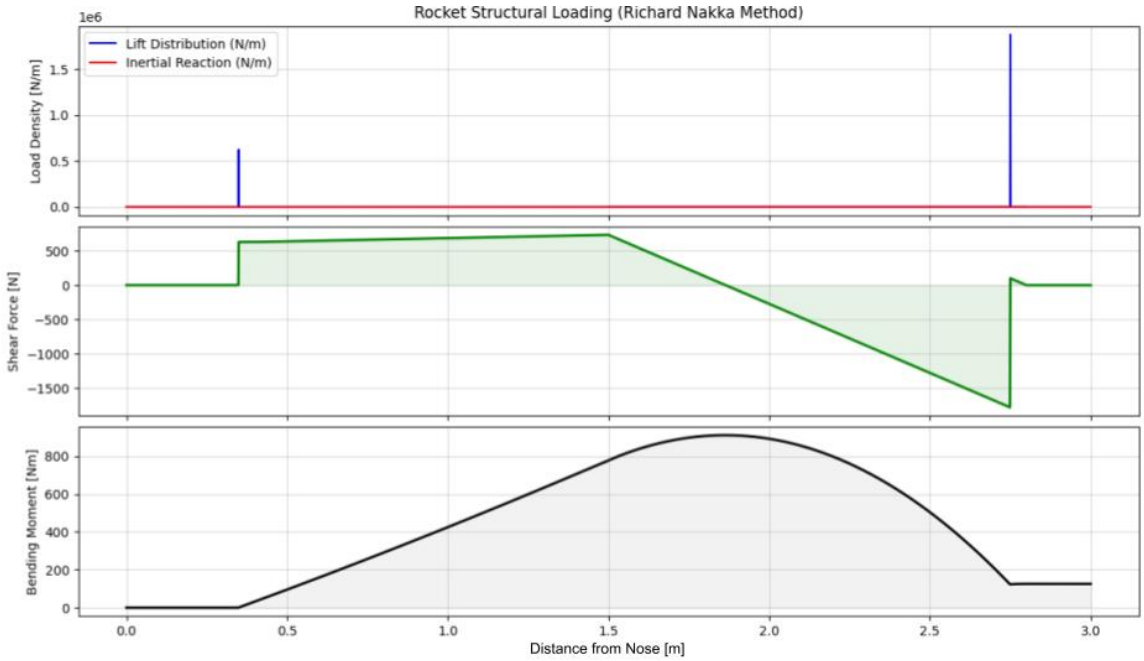

Figure 18 CR26H Bending Loads

6.3.4 Testing and Validation

The aerostructures team has successfully manufactured carbon fiber body tubes that have survived flight two of InSpace's vehicles at the Launch Canada Challenge, with no unexpected damage, and once at IREC, where the aft body tube survived landing with a tangled parachute. The body tube recovered from CR25H had minimal damage despite the airframe failing in bending and applying bending loads that greatly exceeded the expected bending loads on the body tube. Newly manufactured body tubes were tested to 30 kN during a crush test in 2025, where they reached the limit of the testing machine.

6.4 Aluminum Structural Parts

CR26H has 5 structural aluminum 6061-T6 parts that integrate components between the other subteams. These 5 components are marked in Fig. 19. They consist of the avionics & recovery bulkhead and support ring, the metal separation coupler, an aft tube attachment ring, and a fin system attachment ring.

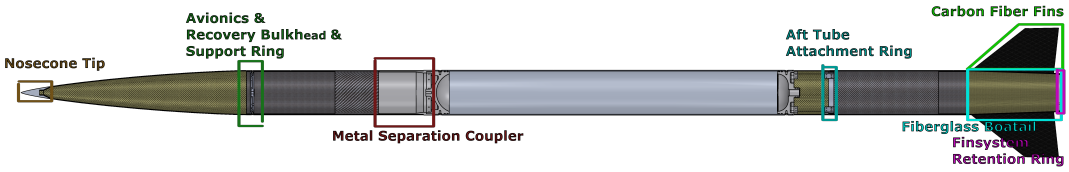

Figure 19 Metal Part Overview

6.4.1 Recovery Bulkhead and Support Ring

The avionics & recovery bulkhead and support ring work together to redirect the inertial loads during acceleration of the avionics systems and the shock loading during parachute deployment. They redirect the load into the nosecone and the nosecone coupler and through the rest of the rocket body. The bulkhead functions as both a mounting plate for recovery hardware and the avionics stack and as a pressure seal for the ejection charges. The support ring is epoxied into the nosecone coupler, and the bulkhead is held in place with 4 M4 bolts that bolt through the nosecone, nosecone coupler, support ring, and into the bulkhead. With this configuration, the bolt heads must shear, or rip through the epoxy attaching the support ring to the coupler, and the bolt shanks attached to the bulkhead, for this system to reach catastrophic failure. This year's design uses a 'Shoulder-and-Ring' system, where the bulkhead possesses an overhanging shoulder that catches against the support ring to ensure alignment. The bulkhead is then spun and aligned using the bolt holes.



Figure 20 Recovery Bulkhead Exploded View

In order to obtain the design for this bulkhead, the team leveraged the topology optimization method, using the Ansys Mechanical suite. By simulating the loads that the bulkhead will experience during flight, the software can remove all non-load-bearing material which the team can serve as a base that can be used for design. Once the bulkhead design is made, it is then re-simulated using the same loads and scrutinized for points deflecting beyond limits or stresses beyond yield. When simulating results, multiple mesh convergences were performed to account for any solver-based errors, which may provide incorrect results. For the optimization settings, the bulkhead was optimized to maximize stiffness while minimizing weight, achieving 60% weight reduction, compared to a blank plate. Figure 21 results demonstrated how the topology optimizer attempted to keep the primary load paths from the bolts to the center of the bulkhead, where the highest load acting through the eye-bolt was observed.

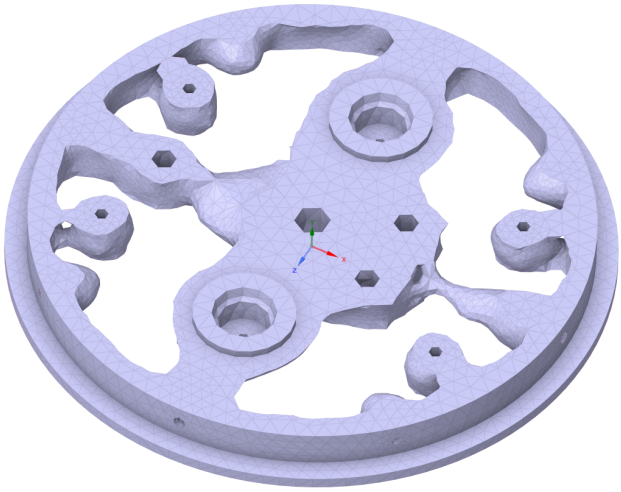

Figure 21 Topology Optimization Results

Once the design was obtained from the optimized geometry, it could then be simulated against the real loading and its stress/deformation scrutinized. Load paths were maintained towards the bolts, notably with

two stringers extending from the bolts towards the center of the bulkhead, increasing stiffness. The outcome provided supporting results, with the bulkhead operating well below the reported yield strength for 6061-T6 aluminum, operating at a safety factor of 1.5. See Fig. 22

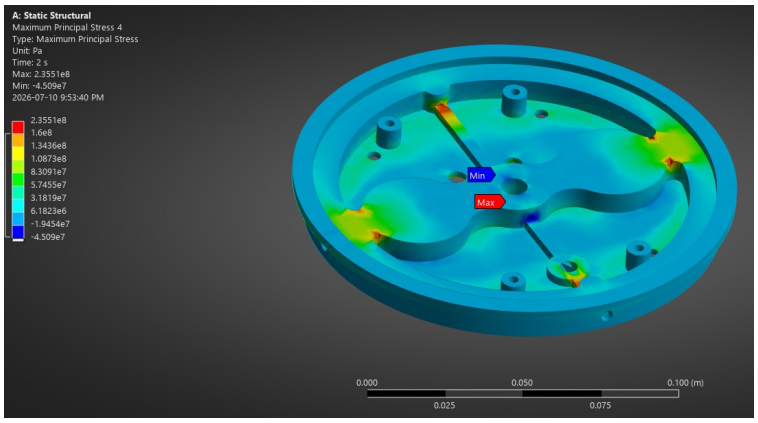

Figure 22 Topology Optimization Results

Additionally, the support ring and M4 bolts held in shear were also observed to be performing well below the ultimate limit of aluminum and black-oxide steel, respectively. The support ring demonstrated to be operating at a safety factor of 2.4 (See Fig. 24b). The black oxide M4 bolts used to retain the components have a minimum safety factor of 3.3 or 210 MPa applied in shear during shock loading at the bulkhead, as determined by $\sigma = \frac{F}{\pi D^2}$ where the load is distributed by 4 bolts. The calculations agreed with the results of the simulation within a tolerance of 1 MPa demonstrated in Fig. 24a. None of the other bolts are expected to experience a greater magnitude of loading.

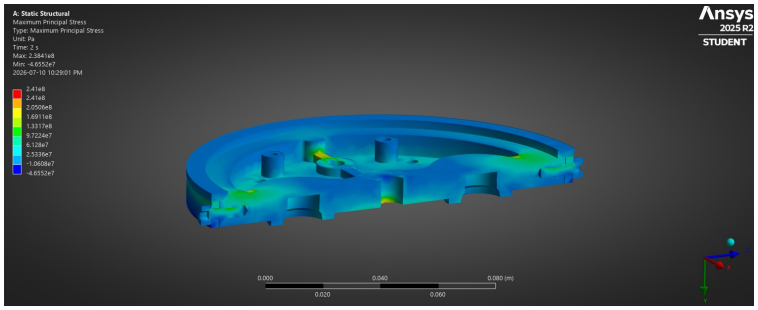

Figure 23 Cut Section of Assembly Stress Result

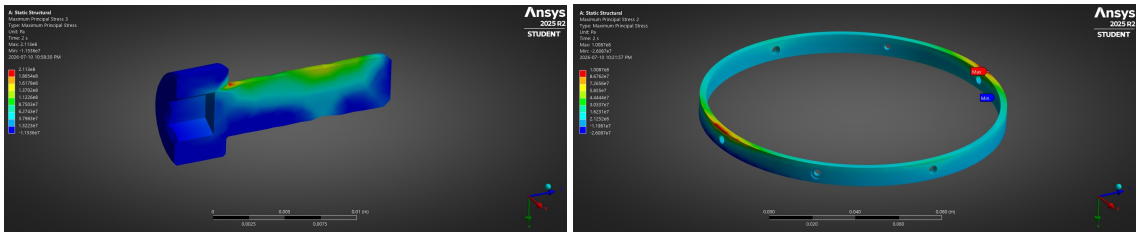

(a) M4 Bolt Stress Result **(b) Support Ring Stress Result**

Figure 24 Support Ring and Bolt Stress Results

6.4.2 Metal Separation Coupler

The metal separation coupler is the connection between the upper airframe and the upper tank bulkhead. It is designed to withstand the bending loads that are applied to the airframe due to any roll-yaw coupling in the rocket, which is believed to have caused the failure of CR25H. It is attached to the upper tank bulkhead with 12 M4 screws.

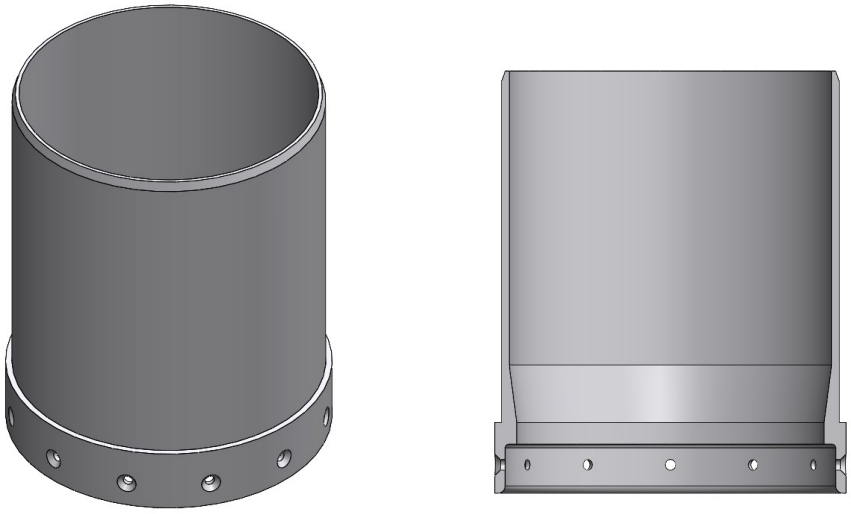

(a) Metal Coupler Isometric View **(b) Cut Section**

Figure 25 Metal Coupler

The aluminum coupler is expected to experience a maximum load of 900 N m. This number was determined by calculating the force experienced by the airframe at a conservative angle of attack at maximum velocity using the same process as the body tubes as seen in Fig. 18. Using ANSYS Mechanical and SolidWorks Static Structural, it was determined that none of the components would experience deformation from the expected flight loads.

6.4.3 Aft Tube Attachment Ring

The aft tube attachment ring is designed to be an interface between the structural load path of the intertank stringers and the aerodynamic components of the aft tube and intertank clamshell. It attaches directly to the upper chamber bulkhead through 6 M4 bolts that bolt through the aft body tube. The clamshell also bolts to the aft tube attachment ring. The aft tube attachment ring can be seen below Figure 26

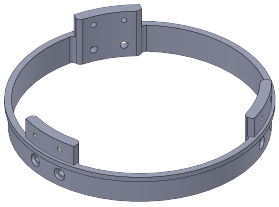

Figure 26 Aft Tube Attachment Ring

6.4.4 Fin System Retention Ring

The fin system retention ring bolts longitudinally into the bottom of the chamber using 4 M4 countersunk bolts and is epoxied to the fiberglass boattail. In an ideal case, its only function is to center and secure the lower part of the boattail as the aerodynamic loading on the aft tube and the fins should be directed through the aft tube into the chamber bulkhead, but in the event the chamber separates from the upper chamber bulkhead, it would function as part of the secondary load path through the aft body tube back to the bulkhead. The fin system retention ring is shown in Figure 27

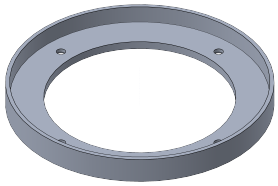

Figure 27 Fin System Retention Ring

6.4.5 Manufacturing Process

All aluminum parts are machined in-house by Carleton University machinists from aluminum 6061-T6 stock purchased from Metal Pros. All 5 components were machined from 6" round bar stock.

6.5 Couplers

6.5.1 Detailed Design

There are three couplers present on CR26H, including the nosecone and aft couplers, which are made of carbon fiber, and the break coupler, which is made of aluminum. The nosecone coupler serves to connect the nosecone to the forward body tube and provides a location to mount the avionics and recovery bulkhead, and

support ring assembly. Furthermore, the nosecone coupler distributes the bending loads caused by aerodynamic forces on the nosecone to the rest of the rocket.

6.5.2 Manufacturing Process

The nosecone and aft couplers on CR26H are made using 8 layers of 3k carbon plain weave, roll-wrapped in a 0-90 configuration, mirrored about the center of the composite. The couplers have a density of $1.36\,\mathrm{kg/mm^3}$, and an inner diameter of 143 mm and outer diameter of 147 mm. The nosecone coupler was cut to a length of 302 mm, allowing for 1 body caliper of length on either side of the nosecone and forward tube. The aft coupler in CR26H is a non-structural joint, serving simply as a connection between the fin can and the aft tube. CR26H's forward coupler is machined from 6061 T6 aluminum, with a length of 183 mm, inner diameter of 143 mm and outer diameter of 147 mm. This coupler is bolted to the ox-tank through 12 4 mm screws.



Figure 28 Coupler Manufacturing

6.5.3 Analysis

To determine if the carbon fiber coupler could withstand the bending loads, the aerodynamic loads were calculated for CR26 Baja Blaster, which flew in early June at the International Rocket Engineering Competition. The maximum expected loading occurred near the midpoint of the airframe, near the location where the rocket would split to deploy the parachute. This value yielded an expected bending moment of 900 N m. Given that the aerodynamic loads are expected to be lower in magnitude at the nosecone and given that the coupler used in CR26H was produced in the same manner as the one used on CR26, the design is proven by comparison.

6.5.4 Testing and Validation

The couplers were tested to the maximum bending load expected on CR26 of 900 N m. This was chosen to be suitable for the hybrid as the hybrid has an expected maximum velocity significantly slower than that of the solid; the aerodynamic loading on the nosecone and fins will be significantly less. The coupler was tested

using a cantilevered bending test as shown below (Fig. 29), where a hanging scale was used to measure the load applied at a distance of 1.1m from the midpoint of the coupler.

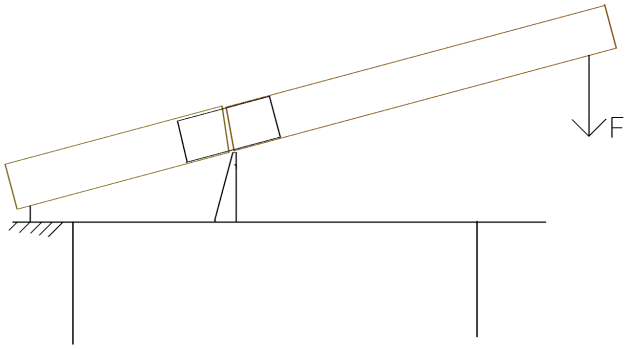

Figure 29 Bending Test

The loading was applied quasi-statically in increments of 150N until the desired maximum was reached. At each increment, the coupler was inspected for delamination and cracks. Once the coupler was tested to the design load, it was tested to failure, which occurred at approximately 900 Nm. While this results in a 1.125 factor of safety, there were several flaws in the experimental setup that likely caused premature failure of the carbon fiber composite. First and most importantly, the coupler hinged about a 2x4 at the midpoint of the apparatus. While this provided enough height off of the table to allow for deformation of the cantilevered moment arm, the coupler experienced a singular reaction load from the surface of the 2x4 that was tangent to the tube. While not explicitly tested, this likely produced a stress concentration that caused premature failure of the composite. Secondly, the lack of side support at the hinge point allowed the coupler to deform into an oval shape, unevenly distributing hoop stresses along the circumference of the tube and creating an environment where localized buckling along the flatter bottom side of the oval was possible.

6.6 Fins

6.6.1 Detailed Design

The fins were machined from 3K plain weave carbon fiber plates, which were then surface-mounted to a fiberglass tail cone and finished with a tip-to-tip carbon fiber layup. The major dimensions of the fins and a picture of the cut-out carbon fiber plates can be seen below in Table 9 and Fig. 30. The tip-to-tip layup is formed from 4 layers of sequentially smaller pieces of 3K plain weave carbon fiber, subject to a vacuum bag to ensure the even distribution of epoxy through the layup. The largest layer is inset 1 inch from the edge of the fins to allow for the leading and trailing edges to be beveled, with each successive layer being inset 0.5 inches.

Table 9 Major Fin Dimensions

Feature	Dimension [Imperial]	Units
Semi-Span	1397 [5.5"]	mm
Root Chord	2794 [11"]	mm
Tip Chord	1143 [4.5"]	mm
Sweep Distance	1842 [7.25"]	mm
Thickness	4.3 [0.169"]	mm



Figure 30 Cut-out Carbon Fiber Fin Plate

This design has two advantages, the first being that the successive layers form a flattened diamond wedge cross-section, decreasing the drag as compared to a blunt flat profile. The second advantage is that the carbon plate allows a vacuum bag to be used, which will produce a much more consistent product with a more consistent profile than what has been manufactured with previous processes.
One of the reasons for changing the manufacturing process of the fin system on CR26H was to allow for the implementation of fins with a double-wedge diamond cross-section, which is expected to reduce the wave drag on the fins. Qualitative CFD was performed on the fins in ANSYS Fluent to determine the significance of the change.

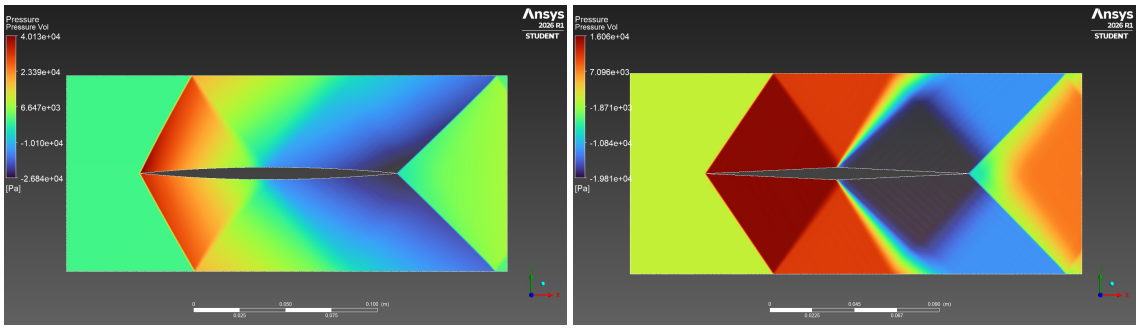

(a) Biconvex Fin Tip **(b) Double-Wedged Diamond Fin Tip**

Figure 31 Fin Tip CFD Results

6.6.2 Manufacturing Process

The team is trying a new manufacturing method for the fins on CR26H in order to reduce the overall drag of the fins and the overall complexity of the fin system layup. The fin system on CR26H is assembled using 3 components: a fiberglass tailcone, COTS carbon plates, and 3K carbon fiber sheets. The fiberglass tailcone is made from 5 layers of 6” medium fiberglass sock layered over a 3D printed mold, similar to the nosecone manufacturing process, and bonded with aeroepoxy PT2712. The carbon plates are made of 3k plain weave carbon and are layered into 3 mm thick plates. The plates are cut to the shape of the fins using a band saw and surface-mounted to the fiberglass tailcone using cyanoacrylate glue with a 3D printed alignment jig. 1” Epoxy fillets are then created using PT2712 epoxy with West Systems 406 colloidal silica adhesive filler to permanently bond the fins. Once cured, 3k plain weave carbon fiber sheets are then cut to a trapezoidal shape to allow the sheet to be overlaid onto the top of the surface-mounted fins with more PT2712 epoxy.

6.6.3 Analysis

To expand on the analysis of fins, it is important to consider the failure that the design stands on. The CR25H failure was attributed to having a large longitudinal moment of inertia and small fins that did not provide enough damping and restorative forces to counteract the large MoI quickly enough. To avoid this mistake on CR26H, the easiest answer is to simply increase the size of the fins. A more detailed response is inclusive of reducing the moment of inertia via weight and length, as well as properly sizing fins such that the rocket has the desired dynamic response during flight.

To determine the fin shape and size as a function of desired response, the longitudinal moment of inertia, damping ratio, restorative moment, and natural pitching frequency were considered. The longitudinal moment of inertia indicates how fast the rocket will respond to disturbances from its original flight path. While having a high MoI makes a rocket harder to disturb, it takes longer for the rocket to return to a zero angle of attack. A lower MoI results in the rocket’s oscillations happening more easily and faster, but it will return to a zero angle of attack quicker than the alternative. CR26H had a simulated longitudinal MoI of approximately 30 kgm^2, slightly greater than that of our traditional solid 30k ft altitude rockets, but 2x less than CR25H. This, along with the distribution of weight due to the engine, begins to indicate that CR26H may require "moderately" sized fins to adequately damp its motion in a timely fashion [1].

The corrective and damping moment coefficients are then considered. These terms describe how quickly and with how much force the rocket will react to disturbances, how far the rocket will be deflected, and how quickly the oscillations will dampen respectively. Primary drivers of the corrective moment coefficient (CMC) are speed and distance between CG and CP. Thus, bigger fins lead to a bigger CMC, indicating a quicker response to disturbances, which is beneficial to our case [2]. The damping moment coefficient

(DMC) is driven primarily by aerodynamic damping as a function of the normal force coefficient of each rocket component and its distance from the CG. A small portion of the DMC is driven by jet damping. This indicates bigger fins will have a bigger damping effect [3].
An important term that dictates the shape and size of the fins is the pitching frequency as a function of the restorative moment over AoA and longitudinal moment of inertia. CR25H barely passed a pitching frequency of 2 Hz at 7 seconds into flight before violently ripping in half. This indicates that the fins were not big enough to adequately increase the pitching frequency during flight, and thus, when the rocket started rolling after exiting the rail, it quickly locked into the pitching frequency [4]. Lower MoIs and bigger fins both contribute to increasing a rocket's pitching frequency. Due to the MoI largely being constrained, the fins were designed to have a large root chord to increase the overall fin surface area. This increased the pitching frequency to around a peak of approximately 3 Hz as seen in Fig. 32. While this value is not incredibly high relative to the 30k solid rockets the team has flown with pitching frequencies in the range of 4.5 hz, it is thought that, based on the CR25H roll rate data of approximately 2-3 hz, CR26H should either stay below the pitching frequency or surpass it. The reason for such ambiguity is due to the uncertainty that surrounds manufacturing. While CR26H is lighter and has bigger fins than CR25H which suggests a faster roll, the imperceptible manufacturing flaws and variability of the fins and the tip-to-tip layup play a big role in how fast a rocket might roll and are virtually impossible to control outside of good engineering practises and attention to detail.

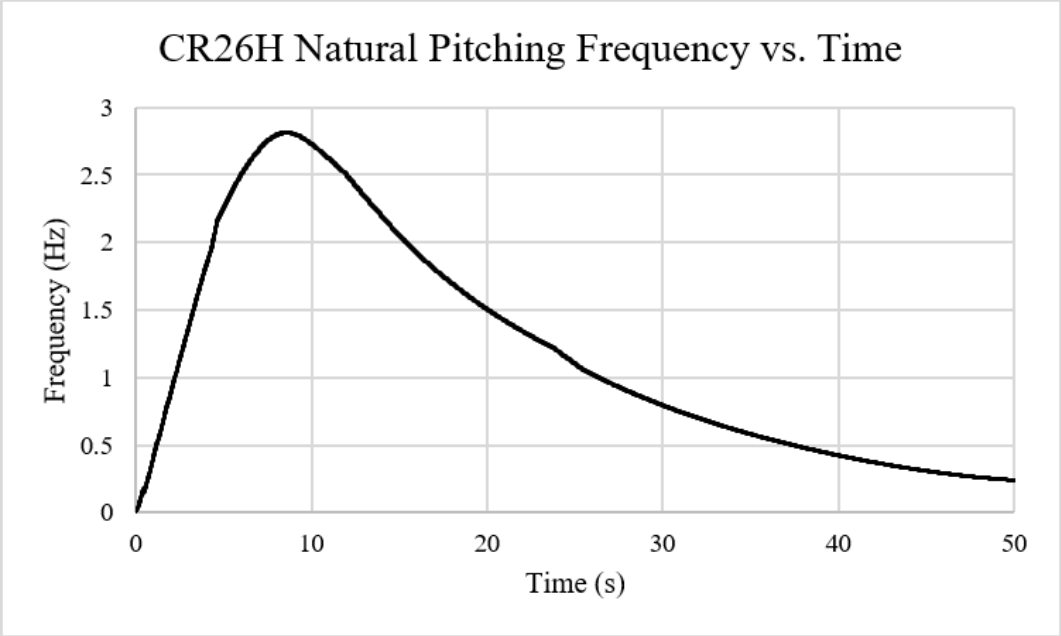

Figure 32 CR26H Pitching Frequency over Time.

Lastly, the damping ratio of the rocket was considered. Following both FAR-OUTs stability tutorial [5] and Apogee Rockets newsletter 197 in which the tutorial was based, leads to the damping ratio as seen in Figure 33. While both the tutorial and newsletter cite 0.05 to 0.3 as an adequate range, this is *not* comprehensive of supersonic high powered vehicles [6]. More realistically, the damping ratio of a similar vehicle to CR26H will likely be within a range of 0.3 to 0.6 due to being a function of DMC, CMC, and MoI. More explicitly, the numerator of the equation for the damping ratio is the DMC, which is a function of how big a rocket is. Thus, it would be unreasonable to expect a supersonic, 11ft, 6in dia. rocket to have a damping ratio of 0.05.

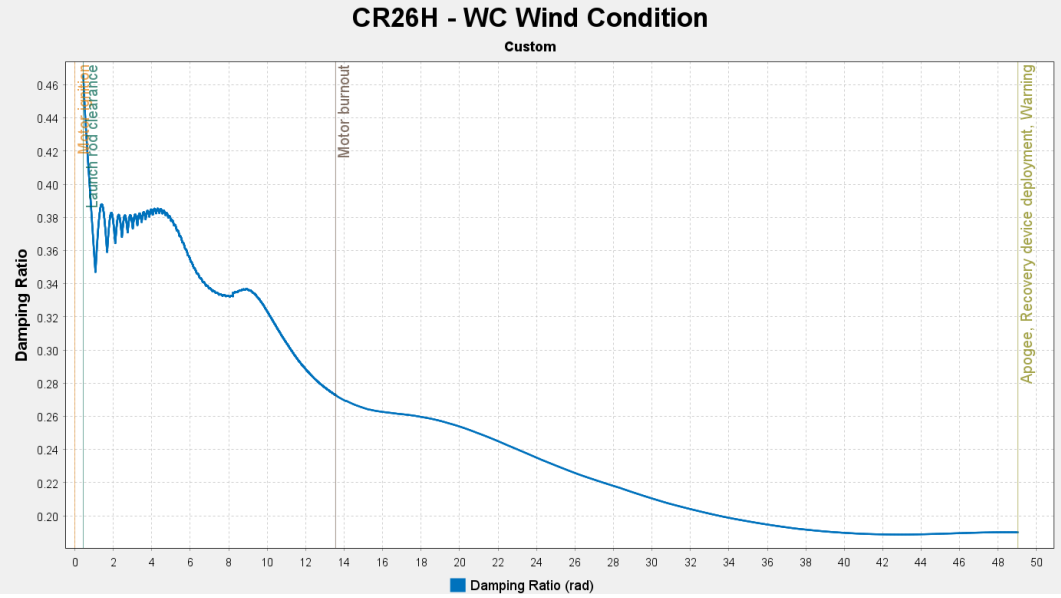

Figure 33 CR26H Damping Ratio under Worst Case 20km/hr Winds.

This analysis leads to the determination that the fins should have a size and shape that provides a higher CMC, DMC, damping ratio, and pitching frequency through large surface area and slightly further aft CP placement. However, it is critical to understand that "higher" is relative, and a good database is lacking in order to draw important conclusions on exactly what range these values should fall within. While these values can be compared to values derived from the 7 seconds of flight data from CR25H and the various 30k ft solid vehicles the team has flown, these flights are not representative of what CR26H could expect to see in flight, largely due to the mass distribution of a hybrid rocket. This leads to the desired response in flight being a rocket with the capability to adequately dampen any oscillations (roll-pitch coupling, wind, or other) and return to a zero AoA within three seconds. This results in fins with a "large" surface area and a rocket on the more stable side.

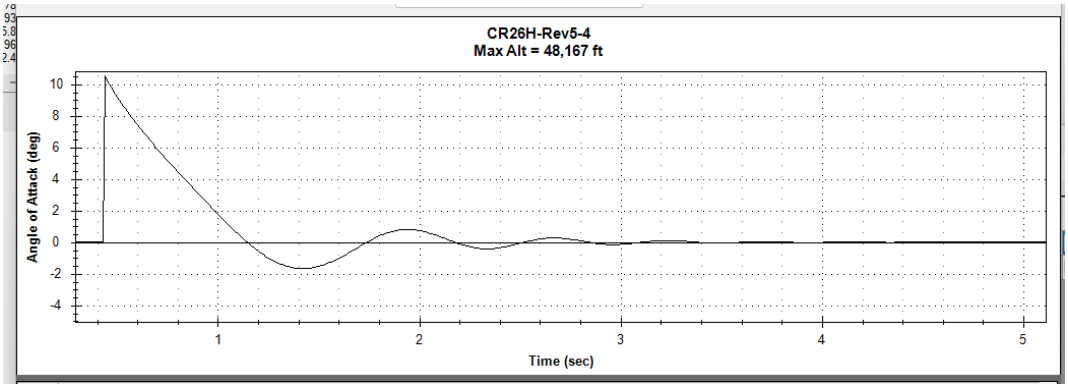

Figure 34 Ras Aero Angle of Attack under Worst Case 20km/hr Winds.

6.6.4 Testing and Validation

The fins are deemed to be sufficiently stiff by a physical squeeze test, where the fincan is placed on the ground and a point load of 175lbs applied to the center of the cone. In previous years, this test would validate

the strength of the tip to tip and "I" shaped gore fincan construction, however, given the novel design this year, the test validates the strength of the large 1" fillet joining the fin to the tailcone, as well as the strength of the tip to tip connecting each adjacent fin to each other, greatly increasing the bending strength of the design.

6.7 Tank(s)

6.7.1 Detailed Design

The run tank is a student-researched and student-developed (SRAD) pressure vessel used on the rocket. The bulkheads are retained using radial bolts. The casing is 48 in long, with an inner diameter of 5.75 in and an outer diameter of 6.00 in. The designed maximum expected operating pressure (MEOP) is 900 psi. structure. The vent line exits from the bottom of the run tank. To permit a nominal 95% fill level, a siphon tube is installed inside the tank. From the bottom bulkhead, the vent passes through a elbow to a push-to-connect fitting with an inline vent orifice and out a nylon line to normally open solenoid valve. More information on the vent system is in **??**. Tank fill indication is provided by liquid expulsion through the solenoid valve, observed either directly or through live camera monitoring. A pressure tap is present on the top of the tank but will be plugged during flight. The bottom bulkhead of the flight tank is built directly into the top of the fire valve.

Table 10 Run Tank Design Summary

Parameter	Value	Units
Material	Aluminum 6061-T6	–
Casing length	48.00	in
Casing inner diameter	5.75	in
Casing outer diameter	6.00	in
Bulkhead retention	20 M6 bolts per bulkhead	–
Bolt grade	12.9	–
O-ring seals	2 -254 O-rings per bulkhead	–
MEOP	900	psi
Proof pressure	1350	psi

6.7.2 Manufacturing Process

Except for the bolts, the run tank assembly is manufactured from aluminum 6061-T6. The vent bulkhead is retained to the casing using 20 Grade 12.9 M6 bolts, and the fill bulkhead is retained using another 20 Grade 12.9 M6 bolts. Each bulkhead is sealed with two 1/8 in -254 O-rings.



Figure 35 Cross-section of the run tank assembly.

The run tank is filled through the three-way fill-fire valve using a 3/8 in Nylon line. The bottom bulkhead includes an SRAD connection point for filling and firing through the valve; this connection has an inner

diameter of 0.87 in. The bottom bulkhead also includes a 1/4 in ORB fitting connected to the vent line. An identical 1/4 in ORB fitting is installed on the inside of the bottom bulkhead, allowing the siphon tube to extend to 95% of the tank volume.



Figure 36 Run tank assembly.

6.7.3 Analysis

The oxidizer tank structural calculations follow the team's pressure-vessel analysis method and use aluminum 6061-T6 material properties with the selected radial fastener properties. The reported factors of safety are calculated by comparing the applicable material strength to the corresponding stress:

$$\mathrm{FOS}_y = \frac{S_y}{\sigma}, \qquad \mathrm{FOS}_u = \frac{S_u}{\sigma} \tag{1}$$

where FOS_y is the factor of safety against yielding, FOS_u is the factor of safety against ultimate failure, S_y is the yield strength, S_u is the ultimate strength, and σ is the calculated stress for the failure mode.

Table 11 Bulkhead Bearing Failure

Parameter	Value	Units
Bearing stress	10674.49	psi
Safety factor, yield	5.06	–
Safety factor, burst	6.00	–

Table 12 Casing Pressure Stress

Parameter	Value	Units
Hoop stress	21600.00	psi
Axial stress	17799.15	psi
Safety factor, yield	1.85	–
Safety factor, burst	2.08	–

Table 13 Casing Bearing Failure with M6 Bolts

Parameter	Value	Units
Bearing stress	168.73	MPa
Safety factor, yield	2.29	–
Safety factor, burst	2.61	–

Table 14 Casing Tensile Failure

Parameter	Value	Units
Maximum tensile stress	122.72	MPa
Safety factor, yield	2.25	–
Safety factor, burst	2.53	–

Table 15 Casing Bolt Tear-Out

Parameter	Value	Units
Tear-out stress	44.09	MPa
Safety factor	4.69	–

Table 16 M6 Bolt Shear

Parameter	Value	Units
Force on each bolt	5197.87	N
Bolt shear stress	74.38	MPa
Safety factor	2.22	–

6.7.4 Testing and Validation

The SRAD run tank has been hydrostatically tested to 1350 psi for a duration of one hour. The tank has also completed numerous fill-and-dump cycles and has been used in previous cold-flow and static fire testing. The gap between the bulkhead and casing was measured before the hydrostatic test and again after one hour at 1350 psi, with negligible measured change. The most recent hydrostatic-test setup is referenced in Figure 37.

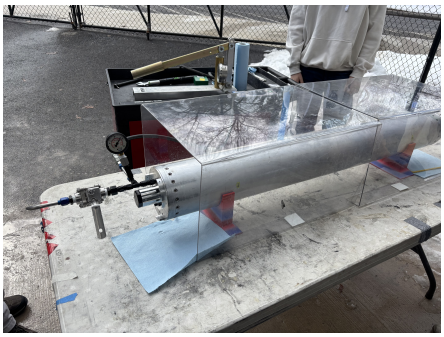

Figure 37 Run tank hydrostatic-test setup.

7. Propulsion

Iced Cappogee is propelled by CU InSpace's "SB-3" SRAD Nitrous-parrafin hybrid motor. SB-3 is the third revision of the hybrid engine that CU InSpace has developed; SB-1 was only ever static fired while SB-2 flew at Launch Canada 2025 on Quarter Pounder. The engine in flight configuration is shown below in Fig. 38 and firing during static fire in Fig. 39.

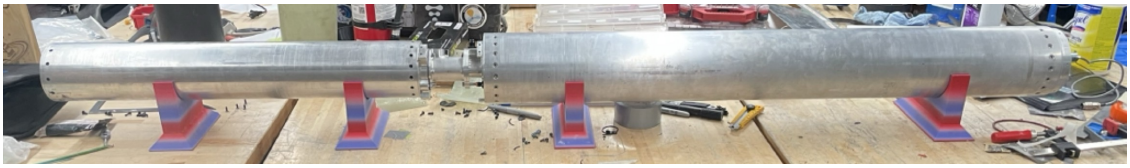

Figure 38 SB-3 in Flight Configuration (Note: Image Missing Stringers)



Figure 39 SB-3 During Static Fire

7.1 Motor Performance

SB-3 was successfully static fired on July 5th. While no anomalies occurred on the engine, the data collection system failed 1.5 seconds into the burn. To fill in the missing data a simulation was run, matching the simulated data with all known data points, and appended to the end of the 1.5 second of data to create a full thrust curve. The combined thrust curve is shown below in Fig. 40; the simulated data begins 1.5 seconds in when the noise stops. Table 17 below provides a summary of the key performance stats of the engine and where they came from.

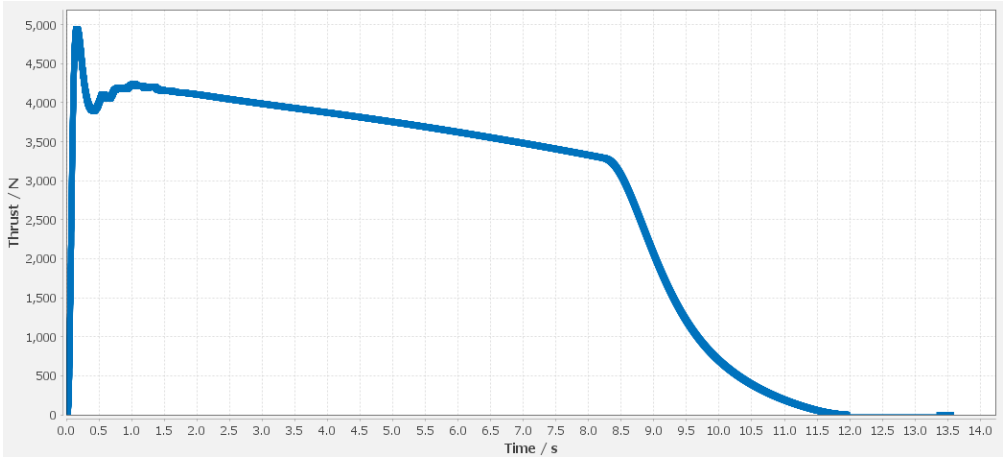

Figure 40 Combined Static Fire and Simulated Thrust Curve

Table 17 Motor Performance Data Summary

Parameter	Value	Unit	Data Source
Average Thrust	3245	N	Static fire + simulated data
Peak Thrust	5000	N	Static fire
Average Thrust On Rail	4123	N	Static fire
Impulse	35154	Ns	Static fire + simulated data
Liquid Burn Time	8.26	s	Static fire (Video)
Total Burn Length	11.3	s	Static fire (Video)
ISP	204.7	s	Static fire + simulated data
Peak Chamber Pressure	450	PSI	Static fire
Oxidizer Consumed	15.3	Kg	Static fire
Fuel Consumed	1.546	Kg	Static fire

7.2 Oxidizer Systems

The oxidizer system consists of the fill system, main fill and fire valve, the passive umbilical system, and vent system. The system allows for remote filling and venting of the run tank on the rocket. The system was designed such that there is no way in which the rocket can be pressurized with no way to dump the tank. The oxidizer system as well as the run tank were designed for a MEOP (Maximum Expected Operating Pressure) of 900 PSI with a 700 PSI working pressure corresponding to the pressure of Nitrous at 20°C

7.2.1 Fill System

The fill system enables the filling of the run tank with both Nitrogen and Nitrous Oxide. It also consists of pressure relief valves in every isolated volume as well as hand valves for emergency dumping. The fill system used for SB-3 in Iced Cappogee is closely related to the fill system used for our hybrid rocket at Launch Canada 2025, Quarter Pounder. This fill system has also been tested at 6 static fire attempts and more than 15 cold flows/operations rehearsals. A P&ID of the fill system and run system is shown below in Fig. 41.

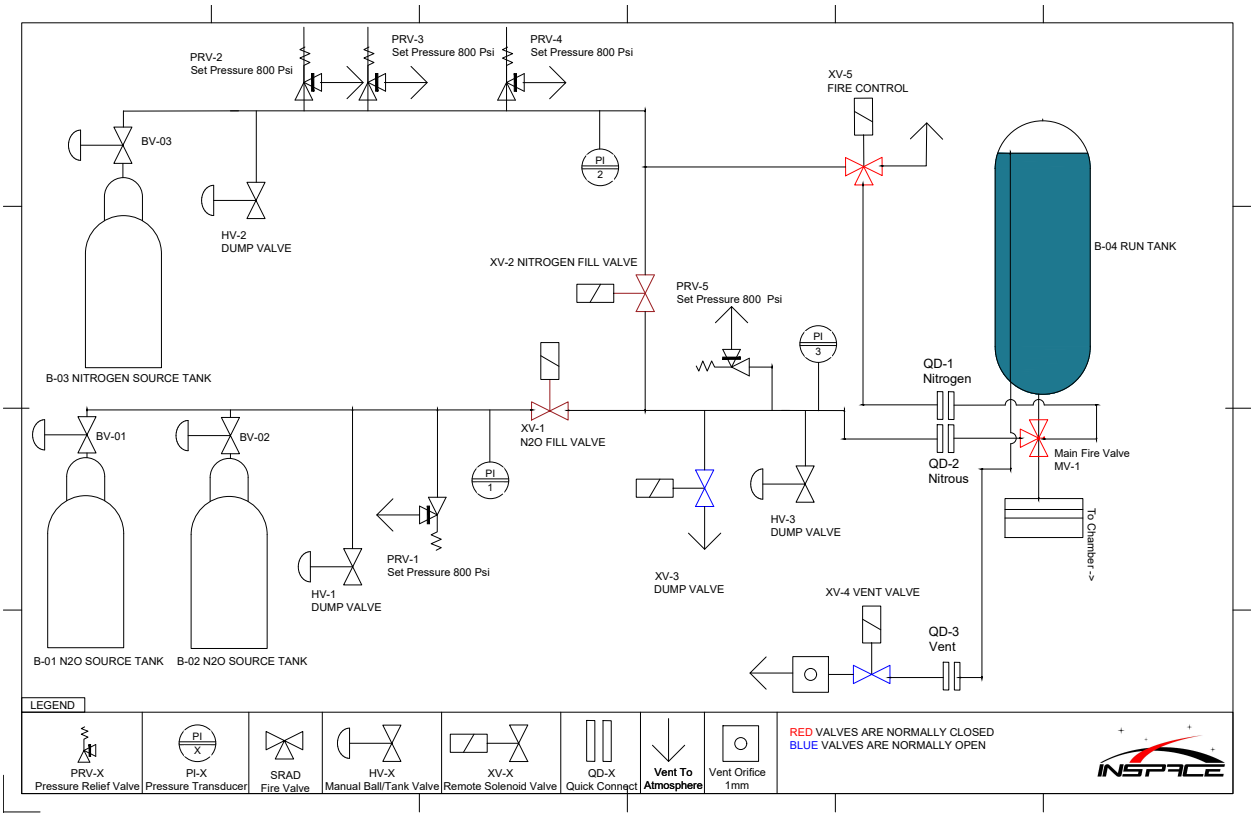

Figure 41 Fill and Run System P&ID

The fill system consists of three primary sections: Nitrogen fill (top left), Nitrous fill (bottom left), and fill/run (right). The Nitrogen fill system includes all components left of the Nitrogen fill valve, XV-2. Nitrogen is used for leak testing the oxidizer systems, pre-pressurizing the run tank before Nitrous fill, and actuating the main fill and fire pneumatic valve. The Nitrogen source tank is connected to a regulator to allow for Nitrogen pressure selection, this is selected as ≈ 100 PSI less than the Nitrous pressure for pre-pressurization. A manual dump valve, three pressure relief valves, a pressure transducer, and manual pressure gauge are also present on the Nitrogen fill segment. This section is made of 1/4" 304 stainless steel tubing with AN fittings for connections. The Nitrogen fill system also includes a pneumatic control solenoid, XV-5, to control the SRAD main valve. The Nitrous Oxide fill system consists of all components left of the Nitrous fill valve, XV-1. This includes two upside down Nitrous Oxide source tanks. Similar to the Nitrogen fill section there is also a hand valve, one pressure relief valve, a pressure transducer, and a manual pressure gauge. The fill and run system are a single volume until until the main valve is actuated, this is because the main valve is a three way valve (discussed in detail in the following section). This section also consists of a pressure relief valve, a remote dump valve, a hand valve, and a pressure transducer. It also includes the main valve and run tank. Since the run and fill system are a single volume until the engine is fired no pressure relief valve or pressure transducer are present on the run system. The fill section uses 3/8" 304 Stainless steel tubing and 3/8" stainless steel tubing for the GSE and 3/8" nylon line to connect to the rocket.

All components used in the fill system were chosen or designed to have a greater than 2x safety at factor at the selected MEOP. Table 18 below lists all of the components on the fill system and their purpose. Table 19 lists the working pressure ratings and smallest orifice for all the major components on the fill and run system.

Table 18 Oxidizer System Component Summary

Component Name	Purpose	Other Info
XV-1	Nitrous Fill Control Valve	Normally Closed Solenoid
XV-2	Nitrogen Fill Control Valve	Normally Closed Solenoid
XV-3	Dump Valve	Servo Actuated Ball Valve
XV-4	Vent Valve	Normally Open Solenoid
XV-5	Fire Control Valve	Pilot Valve for MV-1
PI-1	Pressure Transducer	0-1000 psi pressure transducer
PI-2	Pressure Transducer	0-1000 psi pressure transducer
PI-3	Pressure Transducer	0-1000 psi pressure transducer
PRV-1	N_2O Fill System Relief Valve	800 psi setpoint
PRV-2	N_2 Fill System Relief Valve	800 psi setpoint
PRV-3	N_2 Fill System Relief Valve	800 psi setpoint
PRV-4	N_2 Fill System Relief Valve	800 psi setpoint
PRV-5	Run Tank Relief Valve	800 psi setpoint
MV-1	Fire and Fill Valve	3-Way SRAD Pneumatic Valve
HV-1	Manual N_2O Fill System Dump Valve	Ball Valve
HV-2	Manual N_2 Fill System Dump Valve	Ball Valve
HV-3	Manual Run System Dump Valve	Ball Valve
B-01	N_2O Source Tank	K Bottle
B-02	N_2O Source Tank	K Bottle
B-03	N_2 Source Tank	K Bottle
B-04	Run Tank	SRAD Pressure Vessel

Table 19 Oxidizer System Component Working Pressure and Orifice Summary

	Working Pressure Rating (psi)	Smallest Orifice (in)
1/4" stainless tubing	3600	0.19
3/8" stainless tubing	2900	0.305
MV-100 Valves	3000	0.1
MV-74 Valves	3000	0.1
Fire Valve	1500	0.87
SS-63 series ball valve	2500	0.5
Oxidizer Tank	1800	N/A
Pressure Relief Valve	6000	0.19

The oxidizer systems were designed such to never allow the run tank to be pressurized with no way of depressurizing it. The primary abort system is XV-3, a 1/2" Swagelok servo actuated ball valve, this valve is ground side and connected to the rocket via 3/8" tubing at all times until the point at which the main valve is actuated. When the main valve is actuated the the tank is open to the atmosphere via the combustion chamber. A backup 1/2" Swagelok ball valve is present and connected to a long rope to allow for remote manual dumping in case of failed electronic actuation. As a final option the vent valve can be used to slowly vent the run tank. If power to the valves is lost from the gse or fill system both fill valves are normally closed to stop filling and the vent valve normally the open to vent the tank. If communication is lost with the valve control system the dump valve, XV-3, will automatically open after 5 minutes.

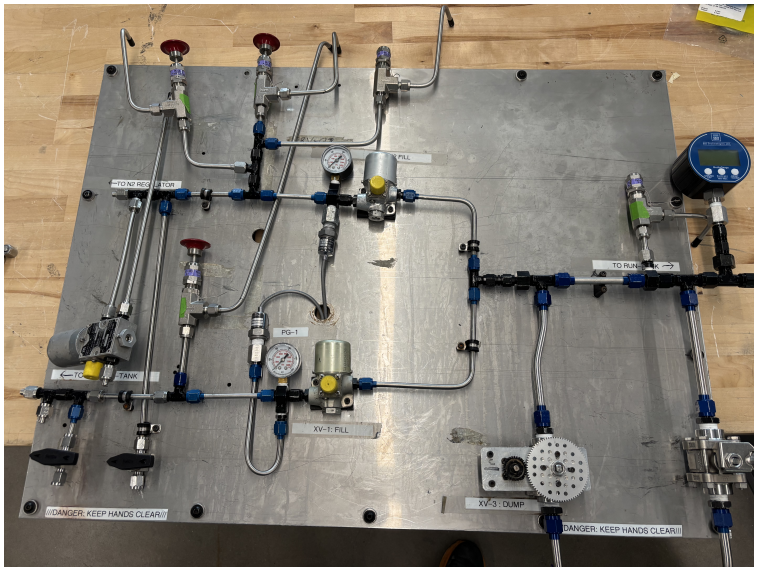

Figure 42 Fill System for SB-3

7.2.2 Main Valve

Iced Cappogee utilizes a SRAD 3 way pneumatic valve to facilitate run tank filling, dumping, and firing.



Figure 43 Main Valve for SB-3

In the valves normal, depressurized, position it allows flow from the fill line to the run tank as shown in Fig. 44. A spring is present in the valve to return to this position when no pneumatic pressure is present. When the valve receives pneumatic pressure from XV-5 it allows flow from the run tank to the combustion chamber; sealing off the fill/dump line. The open position is shown below in Fig. 45.

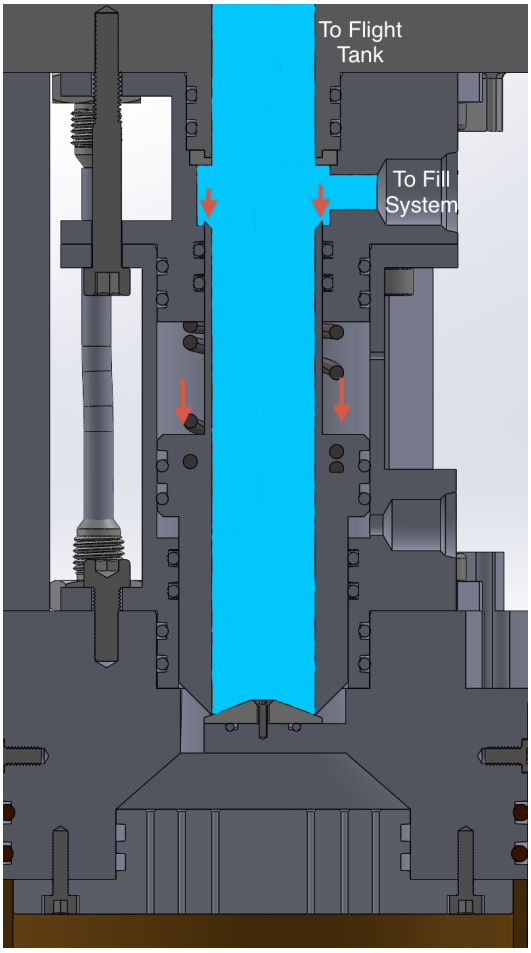

Figure 44 Main Valve Normal Position

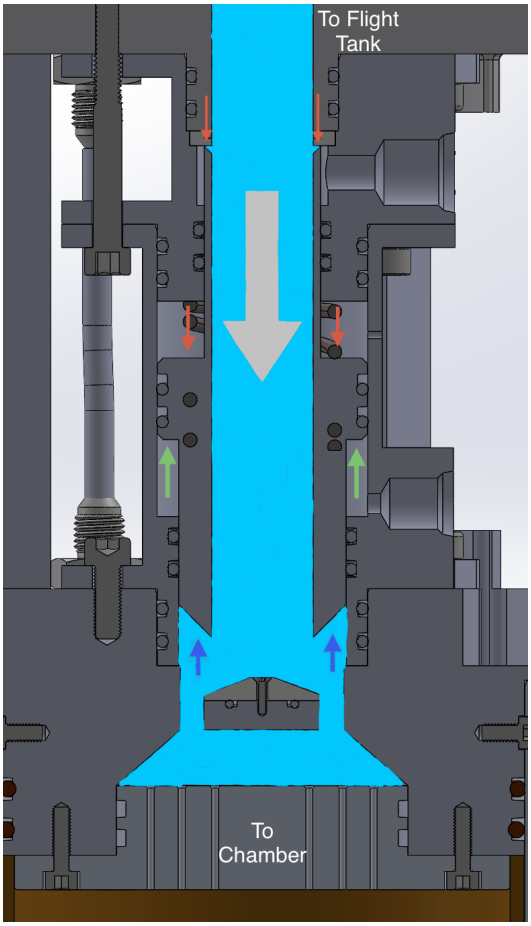

Figure 45 Main Valve Pressurized Position

Due to the nature of the 3 way valve the ground side dump valves, pressure transducer, and relief valve are connected to the run tank at all times until the engine is fired. This allows for reduced on rocket hardware.

Once the main valve receives pneumatic pressure from the fill system and opens it will stay open even when the pneumatic pressure is vented due to the pre-injector pressure. This is required as the pneumatic pressure will be vented when the tear away umbilical system is used. The pneumatic control valve, XV-5, is a three way solenoid valve that connects the pneumatic cavity to the atmosphere when it is unpowered and connects the Nitrogen fill line when powered. The valve requires a minimum Nitrogen pneumatic pressure of 160 PSI to actuate with a full run tank, it is stated in the flight procedures to never proceed to launch with less than 400 PSI of Nitrogen pressure available.

The valve body is machined out of Aluminium 6061-T6 and is fastened using stainless steel M6 bolts. All structural failure modes of the valve were designed to have a greater than 2 times safety factor. The valve body is sealed with dual radial Buna-N o-rings at all connection points. These o-rings are replaced after each use with Nitrous Oxide. All o-rings are lubricated with Krytox due to Nitrous compatibility. The lower seal which stops Nitrous from entering the combustion chamber during fill and hold is machined from PTFE. This seal has a tested lifetime of greater than 30 high pressure actuation and will be replaced when it is sufficiently worn. The upper seal is made of fiberglass filled PTFE (RPTFE) and has a tested life cycle of about 5 high pressure actuations, this seal is replaced before every test. The upper seal was altered after

initial valve testing and the material changed from PTFE to RPTFE due to seal lifetime issues.

7.2.3 Passive Umbilical System

To allow for the fill/dump and pneumatic control of SB-3 is Iced Cappogee a passive umbilical system in employed. Nylon lines are connected to push-to-connect (PTC) fittings on the rocket that are torn away as the rocket leaves the rail. The nylon lines are rigidly attached to the launch tower to avoid the posiblity of the rocket leaving the rail before the the nylon lines are ripped from the PTC fittings. The tear away system was tested as shown below in Fig. 46 to confirm that the nylon lines will break at the PTC fittings at a feasible force. Both lines broke where expected with the 1/4" line used for pneumatic pressure breaking at 350 N and the 3/8" line breaking at 650 N; this is a high estimate since dynamic forces present in launch were not taken into account.



Figure 46 Tear Away Testing

7.2.4 Vent System

The SB-3 engine uses a vent system which is static during flight and active during fill and hold. A PTC with an 1.1 mm inline vent orifice is connected to the bottom of the ox tank. A dip tube is run 95 percent up the ox tank. A long dip tube was chosen over a vent port on the top of the tank since the parachute sits directly on top of the ox tank. The PTC fitting is then connected to a 1/8" nylon line and to a normally open solenoid valve. This nylon line will be fixed similarly to the tear away umbilical system and tear away when the rocket leaves the rail. This setup allows for the ability to hold and allow the run tank to come up to temperature after fill; increasing performance.

7.3 Combustion Chamber

7.3.1 Structures

The combustion chamber is constructed from Aluminum 6061-T6 and is 29-5/16" long, providing the volume to contain all internal chamber components. It has an inner diameter of 4.5 in, an outer diameter of 4.75 in, and a wall thickness of 0.125 in. Structural analysis at the Maximum Expected Operating Pressure (MEOP) indicates adequate margin, with safety factors against yielding of 5.62 for longitudinal stress and 3.37 for

hoop stress, and corresponding safety factors against ultimate failure of 6.32 and 3.79, respectively. The structural robustness of the design is further supported by successful hydrostatic testing of the present chamber and by two previous static fires performed using a chamber that is structurally identical to the current design.

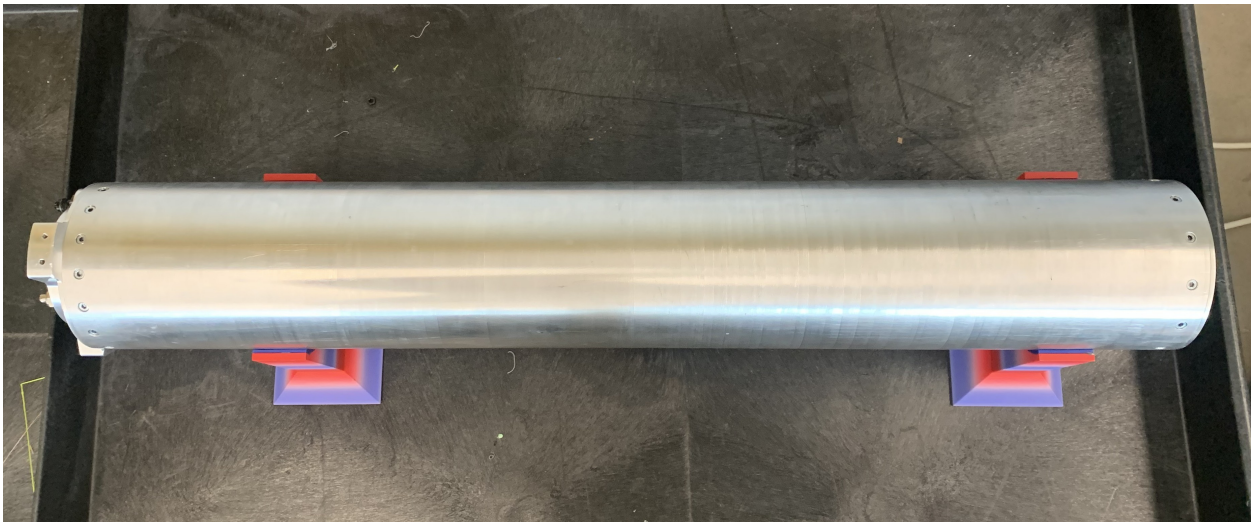

Figure 47 Thrust Chamber Casing

The combustion chamber assembly uses two radial bolt circles. The forward enclosure is secured with 16 M4 socket head fasteners, while the aft enclosure that retains the nozzle is secured with 12 M4 socket head fasteners. Both bolt patterns use an edge distance of 0.475 in, corresponding to an edge-distance-to-bolt-diameter ratio of 1.61.

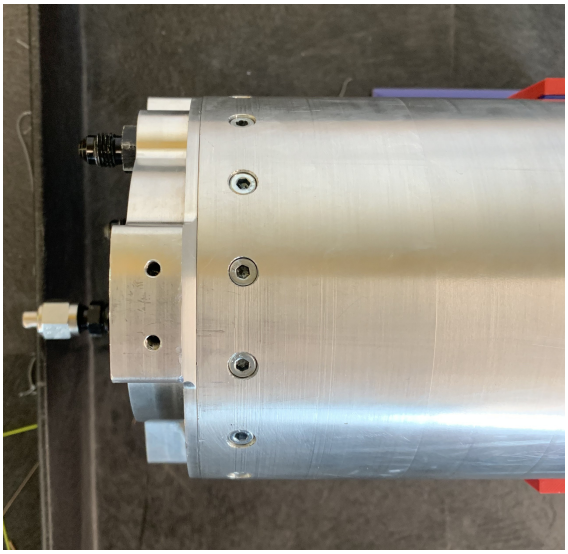

Figure 48 Injector Bolt Circle

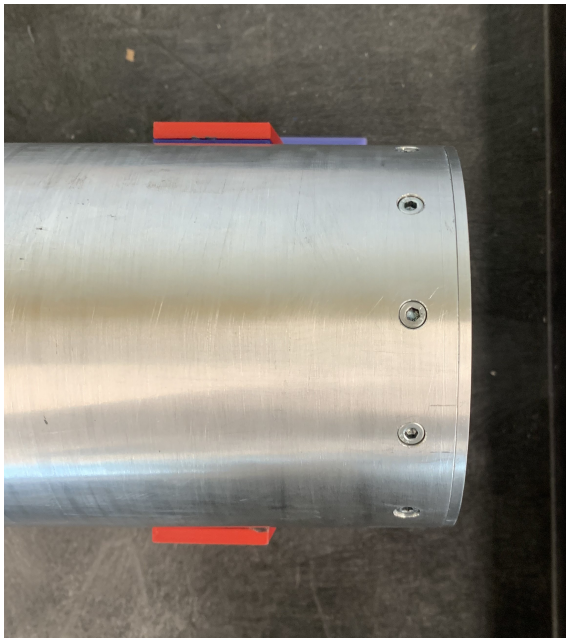

Figure 49 Nozzle Bolt Circle

Both bolt circles use counterbored, recessed bolt heads, with the aft enclosure using only 12 M4 fasteners, it

is the limiting bolted joint and therefore the primary failure location in the event of over-pressurization. For both bolt circles, the governing failure mode is bearing stress. The aft bolt circle has an ultimate safety factor of 2.30, while the forward bolt circle has an ultimate safety factor of 3.07. Prior to static firing, the combustion chamber was successfully hydrostatically pressurized to 900 ± 50 psi, which is approximately 1.5 times the maximum expected operating pressure (MEOP), and held at pressure for two minutes before depressurization.

7.3.2 Injector Design

The thrust chamber's injector design features a bulkhead and a removable plate. The plate is removable to allow for different injector geometries to be tested.

7.3.3 Bulkhead

The injector bulkhead used in static fires and for flight contains 2 pressure transducers; a -4 O-Ring Boss (ORB) fitting used to measure the chamber pressure, and a second -3 ORB fitting to measure the pressure drop across the fire valve from the oxidizer tank to the injector plate. Additionally there is 6 M6 mounting holes in pairs of two for stringer attachments that will be used for trust transfer from the combustion chamber to the load cells. The bulkhead also contains a -4 ORB fitting for the vent line which used to run into the chamber. This port was plugged in our latest static fire, and in flight all ports will be plugged as we have no in flight pressure sensors.

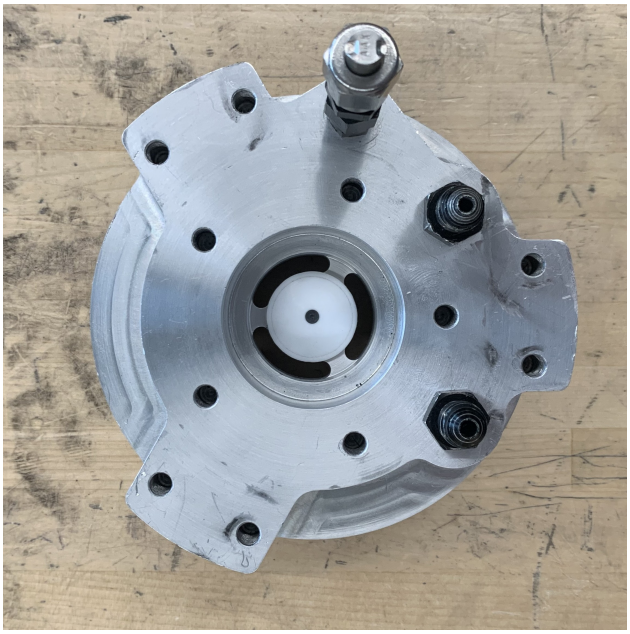

Figure 50 Top of Injector Bulkhead

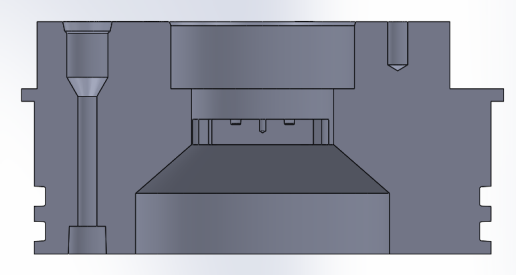

Figure 51 Injector Bulkhead Vent Line Port

The injector bulkhead has two O-ring seals to keep combustion gases within the chamber. The O-rings are -244 high temperature silicone. These O-rings are backup to a seal created by the liner and red Room Temperature Vulcanizing (RTV) silicone. The injector bulkhead when integrated with the injector plate creates a step where it slots into the liner, which can be seen in the visible O-ring grooves below.

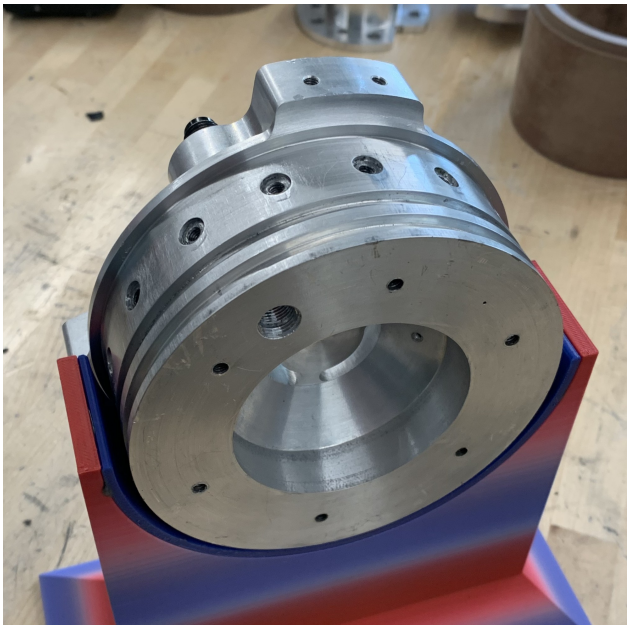

Figure 52 Injector Bulkhead

The injector bulkhead is attached to the casing using 16 grade 12.9 M4 alloy steel fasteners. The bolts are deliberately recessed into the bulkhead to put the heads of the bolts in shear, making the joint stronger. Half Cat Rocketry's Pressure Vessel Design Guide was used to calculate the strength of the bolt circle [7]. The safety factors relative to the MEOP of various failure modes are given below. Further information behind the analytical methods used to determine the strength of the combustion chamber see

7.3.4 Retaining Ring

The nozzle rests on a 6061-T6 aluminum ring, which is radially bolted into the chamber casing using 12 grade 12.9 M4 fasteners.

Table 20 Injector Bolt Circle Factors of Safety

Failure Mode	Yield	Ultimate
Bolt Shear	6.00	7.81
Casing Bearing Failure	2.59	3.07
Bulkhead Bearing Failure	4.33	5.13
Bolt Tear-Out	4.32	4.87
Casing Tensile Failure	7.74	8.70



Figure 53 Retaining Ring

The nozzle retention joint is attached to the casing using 12 counterbored fasteners, while the bolt shanks and head carry the shear load. Because this joint uses fewer fasteners than the forward enclosure, it is intentionally the weaker of the two bolted closures, making the aft bolt circle the primary failure location in the event of over-pressurization. Half Cat Rocketry's Pressure Vessel Design Guide was also used to calculate the strength of the bolt circle. The governing failure mode for this joint is bearing stress, with an ultimate safety factor of 2.30 relative to the chamber MEOP. The safety factors for the relevant nozzle bolt circle failure modes are given below. See appendix C for more detailed calculations and explanations.

7.3.5 Injector

SB-3 utilizes a 94 hole shower head injector with a 15 length to diameter (L/D) ratio. The shower head pattern was chosen due to ease of manufacturing while having demonstrated sufficient atomization for our uses in our prior testing. 94 1.51 mm holes were chosen to provide the required oxidizer mass flow into the combustion chamber. The primary change on this injector compared to the injector used on SB-1 was the increased L/D ratio, this change allowed for increased atomization and increased engine efficiency due to two phase flow being occuring across the injector. Cold flow testing was conducted to determine the discharge coefficient of the two phase injector as well as analyze the spray. The determined discharge coefficient from a 60 hole injector was used to determine that 94 holes provided the O/F ratio desired.

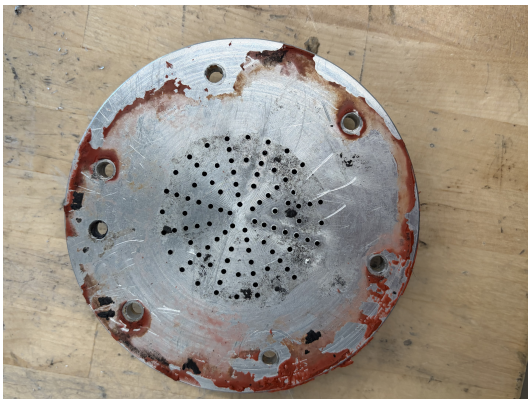

Figure 54 94 Hole Injector Plate



Figure 55 Injector Spray During Cold Flow

7.3.6 Thermal Protection

The thermal protection of the combustion chamber is a four-piece assembly machined from CE-grade phenolic stock that spans the full internal length of the chamber. The primary thermal protection element is a custom linen phenolic liner. This main liner is 18-3/8 in long and 1/8 in thick, protecting the pre-combustion chamber and fuel grain region. Downstream of this section, the post-combustion chamber is lined using two additional phenolic components, each 3 in long and 3/8 in thick.
The main liner houses the solid fuel grain, which is spin-cast directly into the liner. It also provides space at the forward end of the grain for installation of the igniter puck and pre-combustion. The liner is slotted into the injector bulkhead and sealed at that interface with red RTV silicone.



Figure 56 Combustion Chamber Fuel Liner Cross Section

Downstream of the fuel grain, the post-combustion chamber liners enclose the mixing plate between them. These liners incorporate shoulder features that create overlapping joints, eliminating a direct path for hot gases to escape through the liner interfaces. A thin layer of red RTV silicone is applied to the mating faces of these joints to seal any remaining gaps between the adjoining liner sections.

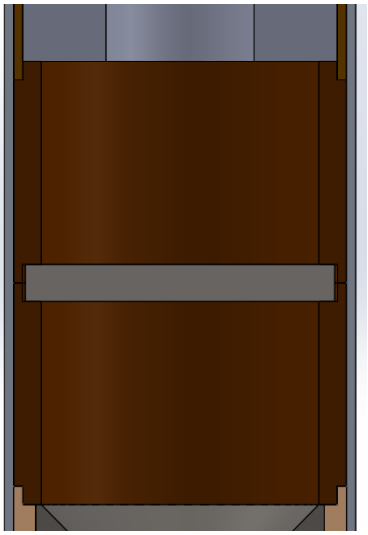

Figure 57 Post Combustion Chamber Spacers

The phenolic thermal protection components described above, with the exception of the nozzle carrier, are the same designs used in previous years' static fires and have provided successful qualitative evidence of the ablative performance of the material. During a previous static fire, failure of the mixing plate led to aft-end damage involving the retaining ring and graphite nozzle, and reduced support at the nozzle bearing surface was considered a possible contributing factor in that failure sequence.



Figure 58 Recovered Retaining Ring



Figure 59 Recovered Graphite Nozzle

New to this year's design is a phenolic nozzle carrier intended to thermally isolate the retaining ring and surrounding aluminum hardware from the heat of the combustion chamber. This change was introduced to reduce thermal loading on the aft retention hardware and to minimize any resulting thermal stress or deformation that could reduce the effective contact area supporting the graphite nozzle. In the current design, the phenolic carrier provides a thermally isolating interface between the hot graphite nozzle and the aluminum retention hardware while also helping maintain better support of the retaining ring and nozzle interface. This phenolic component includes two male glands for two -244 O-rings that seal against the combustion chamber casing. In addition, the interface between the nozzle and the phenolic carrier is coated

with red RTV silicone to improve sealing.

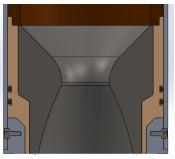

Figure 60 Nozzle Assembly Cross-Section



Figure 61 Phenolic Carrier

7.3.7 Nozzle

The combustion chamber uses a graphite bell nozzle positioned at the aft end of the motor assembly. Graphite was selected because it retains useful strength at elevated temperature and can tolerate the short-duration thermal environment associated with the exhaust flow. The nozzle is machined from a superfine isomolded graphite rod, with a throat diameter of 1.37 in and an exit diameter of 2.75 in, yielding an expansion ratio of 4.03. The nozzle contour provides the transition through which the combustion products accelerate and expand before leaving the chamber.

The bell contour replaces the simpler conical geometry used in an earlier design. In a conical nozzle, the exhaust follows the straight divergent wall and therefore leaves the exit with both axial and radial velocity components. Only the axial component contributes fully to useful thrust, so a larger exit-flow angle produces a greater divergence loss. The bell contour, featuring an 80% bell profile, initially permits rapid expansion and then gradually turns the flow toward the motor axis near the exit. This reduces the equivalent exit-flow half-angle and increases the proportion of exhaust momentum directed axially, offering a theoretical performance improvement over a simple conical nozzle for a given expansion ratio. The contoured design can provide expansion behaviour comparable to a longer conical nozzle while using a shorter divergent section. This improves packaging within the aft chamber assembly and may reduce the mass associated with an unnecessarily long nozzle. The transition must nevertheless remain smooth because abrupt changes in wall slope can disturb the boundary layer and reduce the intended performance benefit. The nozzle was sized using isentropic flow relations and verified in Hybrid Rocket Analysis Program (HRAP) [**?**]. Final contour definition and verification remain part of the reviewed propulsion analysis rather than the general design description.



Figure 62 Graphite Nozzle

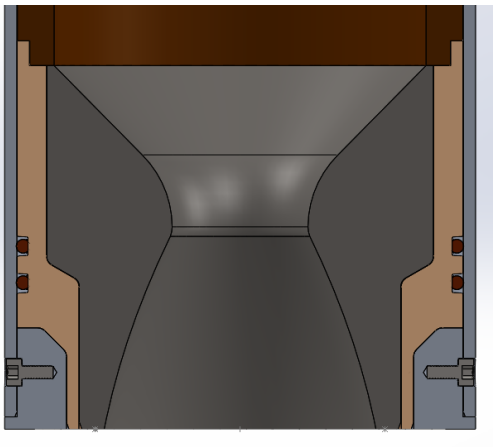

Figure 63 Nozzle Assembly Cross-Section

7.3.8 Fuel

Iced Cappogee is propelled by a spincasted Paraffin Wax-based liquifying fuel grain. The grain measures 16 inches long with an outer diameter of 4.25 inches and an inner diameter of 2.4 inches and is characterized by a circular port geometry. The fuel contains additional additives which decrease regression rate and increases overall fuel performance. The overall fuel mixture and effects of each material are as below:

Table 21 Fuel Grain Material Summary

Material Name	%w/w	Material Effect
Paraffin Wax	84	Fuel base. Liquifying nature provides high regression rate, stable combustion and flame holding
Ethylene-Vinyl Acetate	12	Reduces regression rate while increasing strength of fuel grain
Carbon Black	4	Stablizes liquid melt layer by preventing deep penetration of thermal radiation into the grain

The design choice to include the above additives and their respective amounts comes as a solution to a problem the team had earlier in the design cycle. Early simulations of the motor through HRAP and CHRMS (Carleton Hybrid Rocket Motor Simulator) determined a fuel burnout diameter greater than the outer diameter of the fuel grain, signifying that the regression rate of a previous iteration of fuel (Paraffin-based with Vybar, A-C6A, Carbon Black) was too high, and a new fuel mixture was needed. EVA (Ethylene-Vinyl Acetate) was chosen as the main additive for the new Paraffin-based fuel mixture, due to its interaction with the liquid fuel layer of the fuel grain as well as its high mechanical properties. The addition of EVA increases the overall viscosity of this liquid layer therefore increasing the amount of shear force needed to produce fuel droplet entrainment. This then causes an overall reduction of the entrainment mechanism, reducing overall fuel regression rate while strengthening the fuel grain.



Figure 64 Mixing Plate w/ Ceramic Coating

7.3.9 Mixing Plate

Situated in between the fuel liner and the post combustion chamber, SB-3 contains a mixing plate. Manufactured out of stainless steel, the plate's circular ring shape with a cross in the center generates strategic chamber turbulence while making sure the total cross sectional area of the gaps are at least 2x larger than the cross sectional area of the nozzle. This design choice of sizing the plate to the nozzle allows for the minimization and prevention of undesirable choking and shockwaves.

The plate utilizes its mass and shape to divert, squeeze and expand the hot gases which travel through it. The strategic turbulence generated in that area of the combustion chamber helps mix the gases of the oxidizer and unburned parts the fuel together, allowing unburned fuel to fully combust improving overall engine efficiency. Last years mixer suffered a rapid unscheduled disassembly shortly into the burn. This was noted to decrease the efficiency of the engine as it lead to more "chugging" and instabilities. Thus a new strategy was needed to ensure it's survival for the entire burn.

The solution to increase the plate longevity was introducing two ceramic coatings to protect the plate: ITC 213 and ITC 100 HT. ITC 100 HT, a refractory coating rated to 5000°F, provides the meat of thermal protection, while ITC 213 provides the oxidation, erosion and fatigue protection at high temperatures as well as a proper binding surface for the ITC 100 HT ceramic coating.

Unfortunately due to the small batch size of three static fires, the efficiency increase that the plate provides was unable to be characterized, though static mixing devices such as our mixing plate can provide anywhere from 5% to upwards of a 40% bincrease in efficiency. The figure below showcases the plate after it's been coated with both coatings.

7.3.10 Ignitor

The ignitor used in SB-3 is a 70% Potassium Nitrate and 30% Epoxy Resin composition. The ignitor is positioned on top of the fuel grain in the combustion chamber to transfer heat to the fuel grain. A 1.2 ohm nichrome coil is embedded in the puck and is powered via a 12 V car battery. The resistance in the coil was

chosen to provide sufficient nichrome temperature to ignite the ignitor quickly without melting the nichrome. A puck mass of 150 grams was chosen this has been demonstrated provided sufficient heat and flame for long enough to ignite the engine.



Figure 65 Ignitor Puck

The ignitor was tested to determine the ignition time, this was determined to be 3.5 seconds from power to smoke. More information on testing can be found in the ignitor testing section, section 7.4.4. The ignitor with this ignition method was used at Launch Canada last year as well as 4 static fires successfully. No ejection of burning ignitor was observed during the static fire with this composition.

7.4 Propulsion Testing

7.4.1 Hydrostatic Tests

Throughout the year each different SRAD vessel designed to hold pressure was been tested prior to use. The three components that were tested are the main fire valve, oxidizer tank, and the combustion chamber. The setup for each test remained consistent for each component, the vessel was filled with water before pumping more water into the vessel with a hand pump to increase pressure. The tests were conducted outside in a fenced yard with the component placed behind poly carbonate shields, the set up can be seen in below in Fig. 66

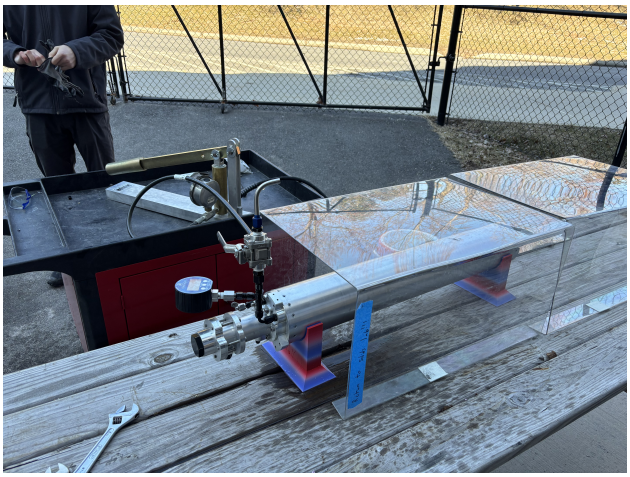

Figure 66 Hydrostatic Test Setup

Both the main fire valve as well as the oxidizer tank were tested at 1350 psi for 60 minutes to ensure the components are able to maintain integrity during the full duration of pressurization. The chamber was tested at a pressure 975 psi for a duration of 2 minutes, for the chamber this gets done before and after each firing of the engine to ensure the chamber can be reused safely.

7.4.2 Cold Flows

The team has performed a total of 5 successful cold flow tests on this year's flight system. The tests occurred at Carleton University over the course of the year. Carbon Dioxide was used to simulate Nitrous Oxide for these tests. Throughout these tests, the team learnt numerous lessons that helped evolve and improve the system. One such improvement was the the upper valve seal, which the valve original cut through upon firing but with some deburring and changing the seal's material, no longer is an issue. The cold flows helped in the experimental determining of the valve and injector's CD and overall performance as the tests occurred at a wide range of pressure. The cold flows have also allowed the team useful practice of their operations and procedures to allow for a smooth transition into static fires.
A wet dress rehearsal of a static fire with the chamber was completed before static firing, this allowed for the cold thrust to be determined of the system. The average cold thrust of the engine is 375 N with a peak of 450 N. Thus in the event of an ignition failure the rocket would leave the rail.

7.4.3 Valve Actuation

The SRAD fire valve has been subjected to numerous valve acutation tests. These tests have been performed at both working pressure and 990 psi under a variety of weather conditions. The valve has performed nominally in temperatures ranging from $-20\,^{\circ}\text{C}$ to $30\,^{\circ}\text{C}$. Throughout the testing process for the main fire valve, the only time the valve has had issues is when either the nitrogen pressure is to low to pneumatically actuate the valve, or the cable that relays power to the solenoid valve that controls pneumatic pressure has had bad solder joints. In order to remedy the low nitrogen pressure, a step was added into the procedures to verify the nitrogen pressure is above 400 psi before loading oxidizer to ensure there will be ample pressure to actuate the valve. The issue with the valve cable was addressed by checking the voltage across the cable terminals when plugged into the control box to find bad cables before use.

7.4.4 Igniter Tests

The composition for this year's ignitor was initial tested using small scale pucks hooked up to the control box. Once the team was satisfied with the injection of the composition, full size pucks were created and tested. The average ignition time is 3.5 seconds. During all three static fires, the ignitor did not fail to ignite in any of the three tests, increasing the team's confidence in a good ignition.

7.4.5 Static Fires

Leading up to Launch Canada, CU InSpace has performed two failed static fires and one moderately successful static fire of this year's engine. All three tests occurred at Morrison's Quarry, just north of Chelsea, QC. During the first static fire it was quite windy which lead to the vibration of the solder joint on the connector for the valve cable causing it damage it's connection, despite working during multiple valve checks, it was unable to open up the pneumatic line to actuate the fire valve. This coupled with our chamber vent nylon line breaking earlier than anticipated caused off nominal performance of the engine. Numerous lessons were learnt from this first test, first of which was to implement more stringent and rigorous cable inspections, especially when solder joints are involved. Secondly, the early breaking of the nylon vent line in the chamber raised concerns among the team and thus a new vent path was created as mentioned above in the Vent System. The second static performed by the team on this year's engine ended with a hole burnt in the chamber as seen in the figure below.
Upon inspection of the chamber post fire and the video of the static fire, the failure point was decided to be a lack of thermal protection around the edges of the injector place. There was a gap in the injector plate from the previous chamber vent line that was no longer present. This gap was not sufficiently protected with red RTV and heat was able to be conducted from the injector plate, to the injector bulkhead, allowing hot gasses to bypass the phenolic barrier and melt the casing resulting in the failure. Furthermore the team believes that the issues was magnified by having a very lean burn which caused the chamber to be much hotter than expected. In order to remedy this issues, a new injector plate was machined without the cut out for the no longer needed chamber vent, coupled with a more liberal application of RTV for the next static fire and flight. To help the burn become more fuel rich than before, the fuel recipe was changed to have less EVA and thus increases the regression rate.
The third static fire was successful and the team was able to get a full length burn of the engine. There was an issue with the electronics however and the team was only able to get the first couple of seconds of data before the a sensor wire shorted the systems and tripped the breaker in the control box causing power to the sensors to be lost. The measured performance from this static fire was be examined in above in the Motor Performance section above. Overall each static fire has provided valuable lessons for improvements of the engine, as well as improvement the operations and procedures related to firing the engine which has helped the team prepare for flight.

7.4.6 Procedures

Testing procedures have been linked below.
Hydro-static Test Procedure
Ignitor Test Procedure
Cold Flow Procedures
Static Fire Procedures Launch Procedures

8. Recovery

8.1 Overview of Recovery

CR26H - Iced Capogee will use a skirt reefing recovery system, with the goal of achieving CU InSpace's third successful reefing-based recovery. Skirt reefing involves passing a reefing line (i.e., a Kevlar string) around the skirt of the parachute in order to restrict the diameter of the parachute and thus simulates a drogue configuration. At a predetermined height, the reefing line is cut, allowing the full inflation of the parachute (i.e., dis-reefing), thus mirroring a main configuration. Therefore, skirt reefing combines the effects of both a drogue and main into a single parachute, allowing both weight and space savings for Iced Capogee.
The Iced Capogee recovery system will utilize wireless communication between Raspberry Pi Pico W's to perform dis-reefing of a toroidal parachute at 1500 feet. Iced Capogee's recovery system will be packed into the forward body tube, with re-designed reefing components fitted onto the parachute and mounted securely to the bulkhead. Deployment will be facilitated by two SRAD black powder charge cannons for redundancy.

8.2 SRAD Wireless Reefing System

The skirt reefing system developed and successfully flown by CU InSpace uses a wireless Raspberry Pi Pico connection and altimeters to trigger dis-reefing. Dis-reefing of the parachute is accomplished through actuation of line cutters, which sever the reefing line. These electronics are stored within receiving boxes (RB) along the outside of the parachute's skirt on opposite ends as shown in Fig. 67. The line cutters can be initiated by either the Raspberry Pi Pico charge or the altimeter's main charge for redundancy. The wireless line cutter initiation occurs at 1500 ft, where the RB Pico receives a signal from a second Pico located in the Transmitting Garage Door (TGD) situated on the bulkhead. The TGD Pico is connected to a second EasyMini on the deployment avionics stack to detect altitude. The second RB's redundant EasyMini sends a charge to the line cutter at 1400 ft, ensuring dis-reefing of the chute and allowing post-flight analysis to indicate which system performed nominally.

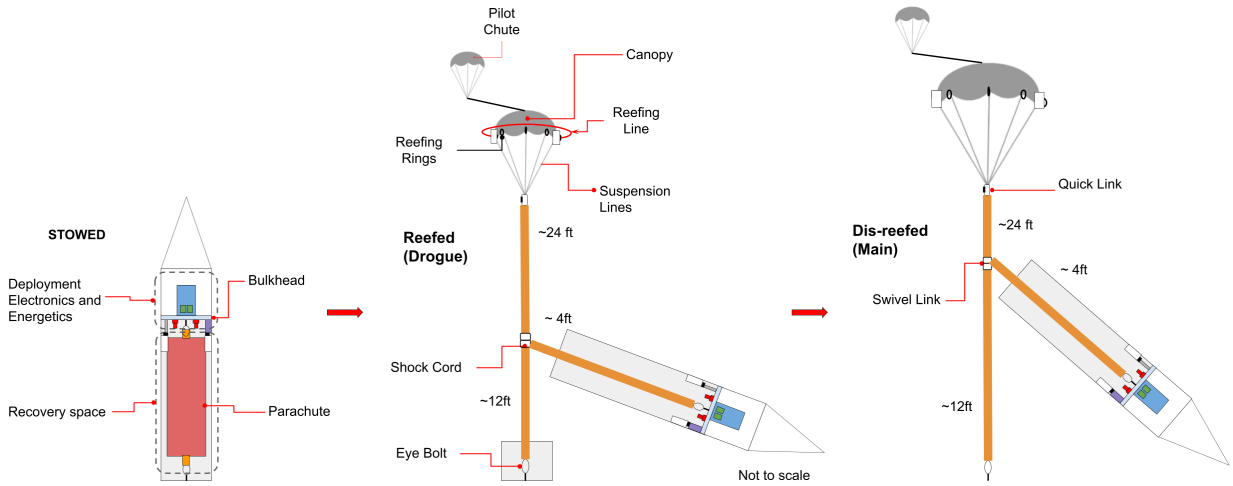

Figure 67 CR26H Recovery Diagram

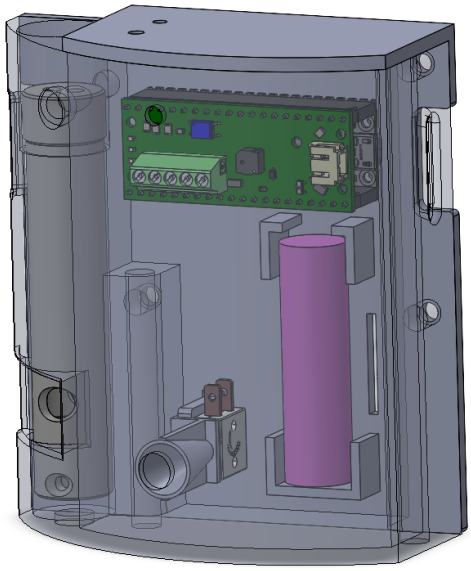

(a) SRAD PCB-Raspberry Pi Pico W Assembly

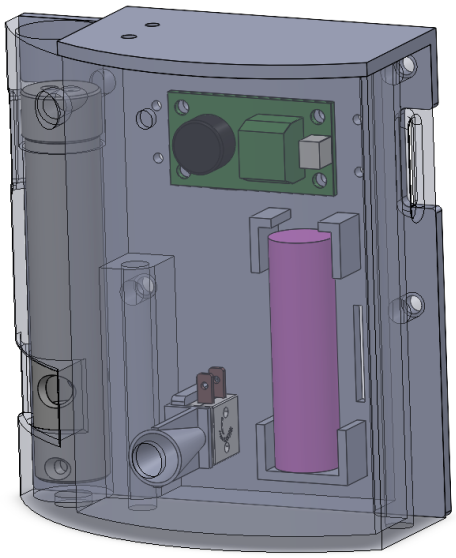

(b) COTS Altimeter Assembly

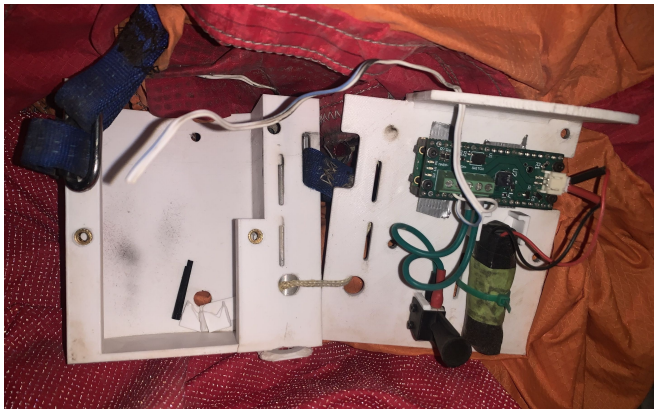

(c) Physical receiving box example

Figure 68 Receiving Box CAD Assembly

Receiving Box The first box (Fig. 68a) contains an SRAD Pico PCB, screw switch, battery, and COTS Mako line cutter. Note that all batteries contained in the recovery system are cylindrical, 14500, Li-ion batteries with a capacity of 1500 mA h. The second RB EasyMini Altimeter (Fig. 68b contains an SRAD Pico PCB, as well as a screw switch, COTS Mako line cutter, and battery. Each box will be mounted on vertical rods which are directly attached to the bulk head. The receiving boxes are held above the bulkhead by spacers on the rods, separating the parachute-attached components from the bulkhead-attached components as shown in Figure 69. This choice has been made to provide a more secure hold of the boxes for the arming process in addition to saving space by replacing the parachute bay design used last year.
The receiving boxes have undergone line cutter tests to ensure the structural integrity of the prints and have withstood charges, as seen in Fig. 70 below,

Transmitting Garage Door The TGD Pico is connected to a second EasyMini on the deployment avionics stack to detect altitude. The battery for the TGD is also located on the avionics stack, to reduce space taken

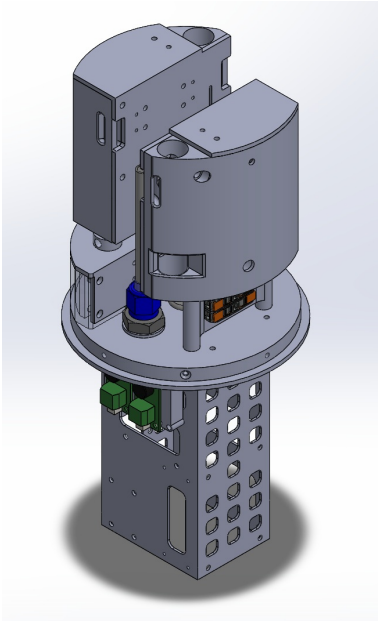

Figure 69 Recovery Section Full Assembly



Figure 70 Receiving box line cutter test

up by the recovery assembly. The second RB's redundant EasyMini sends a charge to the line cutter at 1400 ft, ensuring dis-reefing of the chute and allowing post-flight analysis to indicate which system performed nominally.

Wireless Reefing Avionics The recovery reefing electronics - PCB-Raspberry Pi Pico W assembly - integral to the wireless reefing system, was successfully tested at Launch Canada 2024 and IREC 2026. Improvements made to the PCB-Raspberry Pi Pico W assembly design include: 1) Increasing the buzzer electronic component sound pressure level specification from 65 dB to 78 dB at a frequency of 4 kHz, 2) introducing a terminal block with five positions and 180 degree in-line cable mounting, and 3) implementing male and female headers for ease of assembly and testing.

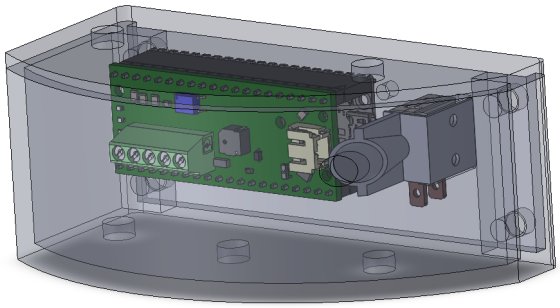

Figure 71 TGD 3D CAD Assembly

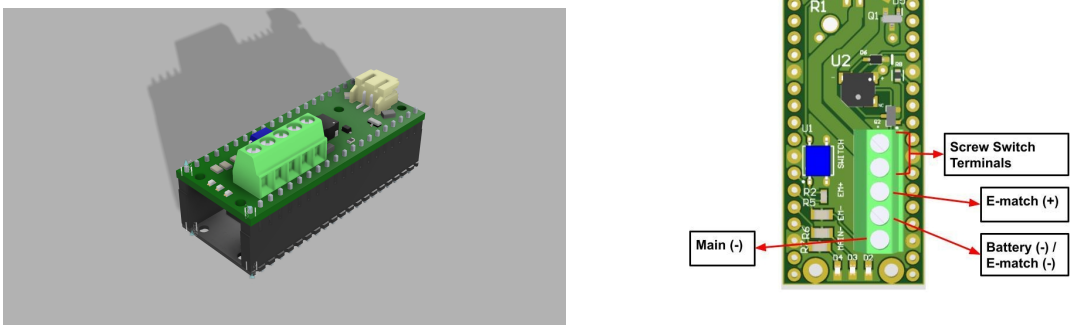

(a) 3D full assembly **(b) PCB 2D schematic**

Figure 72 Recovery reefing electronics assembly

The PCB-Raspberry Pi Pico W (recovery reefing electronics) assembly is a critical component of the recovery wireless reefing system. The Raspberry Pi Pico W allows for wireless communication between the deployment avionics and the skirt reefing avionics of the parachute. The reefing PCB permits for 1) a charge to be received from the deployment avionics altimeter, and 2) the required voltage to deploy the line cutter E-match located within the receiving box. The Raspberry Pi Pico W programming logic required to achieve these functions are outlined in Fig. 73.

The recovery reefing electronic assembly receiving a charge from the deployment avionics altimeter, is achieved through the connection between the avionics deployment altimeter's Main (-) and Battery (-) terminals, and the PCB terminals. The PCB Main (-) terminal is directly connected to GPIO28 of the Raspberry Pi Pico W. The transmitting Raspberry Pi Pico W is programmed to constantly monitor the GPIO28 voltage levels where, 1) a LOW pin charge indicates a charge has been sent; and 2) a HIGH pin charge indicates no charge has been sent. If a LOW pin charge is detected at GPIO28, the transmitting PCB-Raspberry Pi Pico W assembly communicates this through its Wi-Fi connection to the receiving Pico in the RB as observed in Fig. 73.

The recovery reefing electronic assembly deploying a charge is achieved through the PCB's P-channel MOSFET which allows an amplified voltage at the PCB E-match terminals. The receiving Raspberry Pi Pico W is programmed to monitor its GPIO10 voltage levels where, 1) a LOW pin charge indicates no charge has been communicated; and 2) a HIGH pin charge indicates a charge has been communicated. The latter

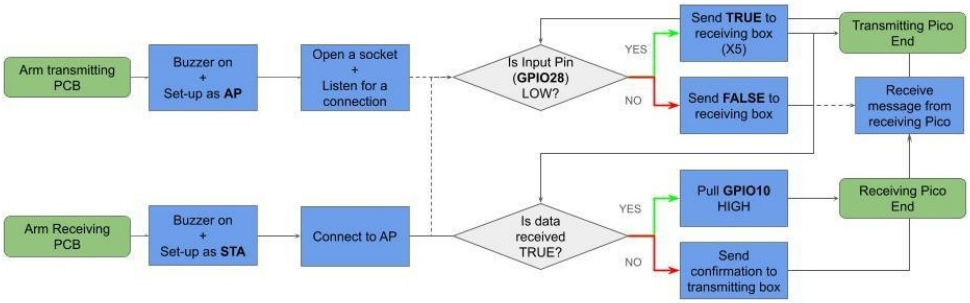

Figure 73 Recovery Wireless Reefing Logic

triggers the e-match allowing the line cutter to sever the reefing line.
Recovery reefing avionics range testing was conducted to confirm the strength of the connection between the receiving and transmitting Raspberry Pi Pico W's. These tests were carried out at locations with minimal interference. The distance between the Pico's were increased incrementally to observe the limits of the connection, with the goal of surpassing the main riser distance as outlined in Table 25. Range testing results demonstrated a solid connection for approximately 100 ft, surpassing distance requirements, with the ability to reconnect in the event of interference.

8.3 Deployment

Replacing the COTS CO2 Raptors flown on previous rockets, CR26H's deployment system will feature two SRAD black powder charge cannons, each containing 1.75g of black powder. The charges consist of a xx long 3/8" flared tube, capped at the bottom end with an epoxy filled -6AN to ORB fitting that threads directly into the bulkhead.The lower 1/3 of the tube is packed with cellulose insulation (commonly known as "dog barf") wadding, followed by black powder, and then more insulation in the remaining length of tube. The e-match is placed in the black powder segment such that the head is in contact with the top of the black powder to promote complete combustion. The charge is capped with a small amount of hot glue, to holding the e-match in place and create a light seal on the charge.

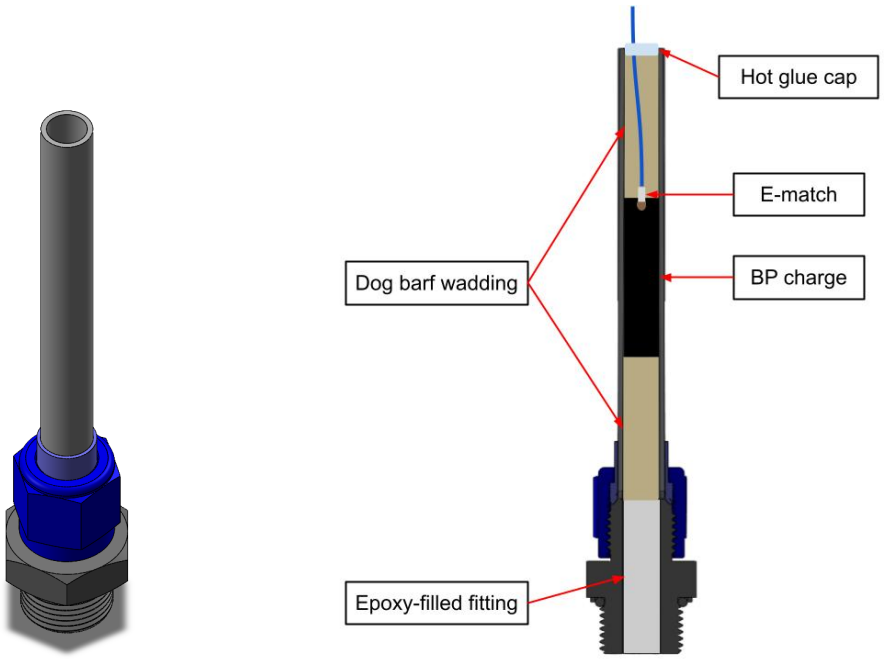

(a) BP charge cannon **(b) BP charge packing**

Figure 74 BP Charge Visualization

To protect the parachute from the charges, a chute protector blanket was cut and sewn out of 200 gsm Aramid 3A fabric. Due to the concentrated output of the charge cannons, the blanket is three layers thick. A slot was cut out of the center of the blanket to allow the webbing to pass through, and a knot was tied in the webbing approximately 1 ft from the eye bolt to prevent the chute protector from passing too far up the line and potentially suffocating the parachute.

8.4 Parachute Design

This year's parachute was designed with size in mind to mitigate the issues experienced with oversized parachutes in at Launch Canada 2025. As such, a toroidal chute was selected for its high drag coefficient, allowing the parachute to reach the required descent speeds while having a small packing volume. The toroidal chute not only has suspension lines along the skirt, but additional lines at the vent, which are brought together on a quick link. A carefully sized length of shock cord runs between the vent quick link and the skirt suspension line quick link to give the parachute its annular appearance and drag characteristics.
The rocket's burnout mass and desired descent velocities under reefed and disreefed configuration were used to size the parachute, along with the parameters found in the table below.

Parameter	Value	Units
Drag Coefficient	1.8	
Opening Force Coefficient	1.30	
Canopy Fill Constant	8	
Desired Descent Velocity (Reefed)	25.6	m/s
Desired Descent Velocity (Disreefed*)	7.8	m/s
Rocket Mass	29	kg
Deployment Altitude (Reefed)	9144	m
Deployment Altitude (Disreefed*)	457.2	m
Ground Altitude (ASL)	295	m
Reefing Line Force Percentage	7.5	%

Table 22 Parachute Parameters

MATLAB scripts were used to calculate the parachute's size and shock forces. The results are tabulated below.

Parameter	Value	Units
Reefed area	0.167	m^2
Reefed diameter	0.461	m
Reefing line length	1.45	m
Reefed CD	10.08	
Disreefed area	4.171	m^2
Disreefed diameter	2.3	m
Landing speed	7.82	m/s
Reefed opening shock force	3096.18	N
Disreefing shock force	682.63	N
Reefing line shock force	51.2	N

Table 23 Parachute Characteristics

With the major dimensions of the parachute, a stencil was generated in order to cut each gore, as seen in Fig. 75a below. Note that the overall gore shape varies from the traditional conical shape to allow the vent to be pulled in, forming the desired annular shape. A visualization of the 3D toroidal parachute shape is shown in Fig. 75b.

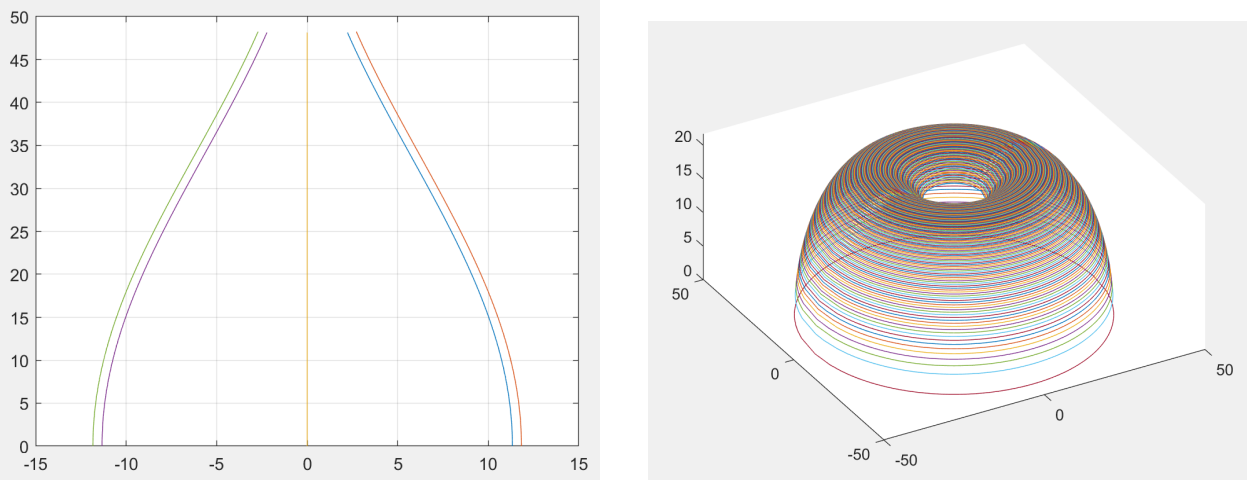

(a) Parachute Stencil **(b) Parachute 3D Mockup**

Figure 75 Toroidal Parachute Visualization

Term	Description	Value (m)
h_1	Primary canopy gore height	2.23
D_v	Vent hole diameter	0.32
N	Number of gores	12

Table 24 Parachute Geometric Dimensions

Once manufactured, the parachute inflation was verified by towing the parachute while running. The profile displayed in Fig. 76 below shows the vent being pulled in, generating the desired toroidal shape.



Figure 76 Toroidal chute inflated side profile

8.5 Rigging

The rigging of this year's recovery system has been summarized in the following table. Note that shock cord lengths are proportional to the rocket length. To further reduce the packing space required in the body tube, 5/8" tubular nylon was used instead of 1" tubular nylon.

Table 25 Recovery System Parameters

	Deployment Type	Reefing
	Deployment Method	BP Charge Cannon (Forward Section Deploy)
Parachute	Total Number	1
	Reefed Diameter	1.89 ft
	Dis-reefed Diameter	7.87 ft
	Material	Ripstop Nylon
Suspension Lines	Total Number	12
	Length	11.5 ft
	Diameter	1/8 in
	Material	550 paracord
	Strength	550 lb
Shock Cords	Total Number	3
	Length	Main riser: 36ft, Nosecone riser: 4.85 ft Vent-Skirt line: 10ft
	Diameter	5/8 in
	Material	Tubular Nylon
	Strength	2300 lb

9. Avionics

The avionics system for CR26H of various SRAD and COTS flight computers. Telemetry is transmitted from many of these devices over radio and logged to an on board storage for some of the devices. The telemetry systems within this section do not control energetics, as the recovery subteam have their own avionics which control energetics. The completely assembled Avionics stack comprised of all flight computers and batteries can be seen in Fig. 77.



Figure 77 Assembled Avionics Stack Flown at Launch Canada 2025

A singular stack housing all COTS and SRAD electronics allows for integration of the multiple systems before the final assembly as well as a singular mass estimate with limited variables. The complete wiring diagram can be seen below in Fig. 78.

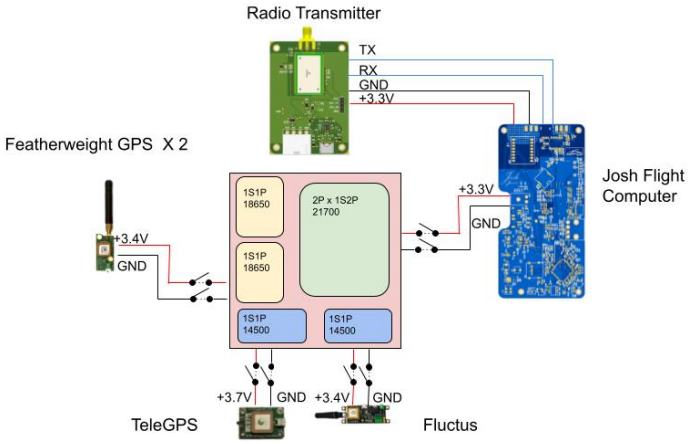

Figure 78 Avionics Stack Wiring Diagram

9.1 SRAD Telemetry

9.1.1 SRAD Telemetry

This years telemetry system shares the same hardware as flown previously at Launch Canada with software improvements. The flight computer is based on a STM32H743 Microcontroller Unit (MCU) which collects various flight data from onboard sensors listed in Table 26. Onboard the flight computer is a micro SD card slot, rated for a shock resistance of up to 50 G. This is used for the main flight data recording, used in addition to live telemetry transmission as a secondary method of collecting data. The last hardware feature on the flight computer is an Electrically Erasable Programmable Read-Only Memory (EEPROM), storing critical flight state information as well as the radio configuration. The flight computer connects externally to a radio board, containing a RN2483 Long Range radio (LoRa)radio transceiver.
The SRAD flight computer has flown and operated successfully three times, including twice at Launch Canada 2025, as well as once at IREC 2026. It was able to log data throughout the flight, as well as transmit data from apogee from rockets targeting thirty thousand feet. The battery life has also been tested through these flights, remaining on for over twelve hours. Global Positioning System (GPS) data was also received over radio, with coordinates matching COTS solutions. Range testing and battery life testing has also occurred, with ranges of at least 9 kilometres and battery life exceeding 10 hours.

Table 26 SRAD Flight Computer Sensors

Sensor	Type	Data	Collection Frequency
MS5607	Barometric pressure sensor	Temperature and Pressure	25Hz
LIS2MDL	Magnetometer	3-axis Magnetic Field	100Hz
LSM6DSO32	6-axis IMU	Angular Velocity and Linear Acceleration	100Hz
L86-M33	GPS	Position, Altitude and Velocity	10Hz

Using data collected from the sensors, the rocket's position, altitude, orientation, speed, and acceleration can be displayed in real time using sensor fusion algorithms.

9.1.2 Power

The flight computer has two battery connections that use JST connectors. The battery connections are precrimped 22 American Wire Gauge (AWG) JST leads soldered to 0.15mm pure nickel strips which were then spot welded to the battery. All connections underwent tug tests before being wrapped to prevent short circuits. Additionally, the flight computer can provide charging through a 5v USB-C connection which can be connected externally from the rocket using a magnetic dongle. This allows the flight computer to be recharged without disassembling the rocket.
The batteries for the SRAD flight computer were chosen based upon the power budget as seen in Table 27. All component current draw values were taken from manufacturer published data where available or best estimates where manufacturer data was not available, where an typical current draw was not provided the max current draw was used. These typical power consumptions where then used with the battery capacity and efficiency factors of 0.9 for the dual battery setup and 0.85 for the voltage regulator to get the expected battery life of greater then 48 h. Additionally, the current draw of the full system was previously tested to be very similar to the current draw predicted by the analysis below. Additionally, this flight computer houses a 3V 20mAh Lithium Ion (Li-on) coin cell battery to provide backup power to the L86-M33 GPS in case of power failure. This allows for appropriate redundancy in the case of emergency such that the GPS will retain the current time and last known position, substantially decreasing the time it requires to regain an accurate GPS position fix after power has been regained.

Table 27 Josh Flight Computer Power Budget

Component	I_{typ}(mA)	I_{max}(mA)	P_{typ}(mW)
MS5607	1	1.4 [8]	3.3
LIS2MDL	0.2	0.2 [9]	0.66
LSM6DSO32	0.55	0.55 [10]	1.815
L86-M33	22	26 [11]	72.6
RN2483	33	44 [12]	108.9
STM32H743VIT6	154	260 [13]	508.2
SD Card	50	200	165
Total	260.75	426.15	860.5

Table 28 Josh Flight Computer Battery Calculations

Parameter	Value
Battery Capacity (mA h	20 000
Battery Voltage (V)	3.63
Battery Power (W h	72 600
Efficiency Factor (%)	76.5%
Power Draw (mW	860.5
Battery Life (h)	64.5

9.1.3 Telemetry Software

The software has remained similar to last year. It remains in C, and still utilizes the NuttX Real Time Operating System (RTOS). This was chosen as it was efficient, easy to develop for, and reliable. The software contains three main threads, each one accomplishing a different task. **??**ig:josh-software shows the software architecture (reword). One feature of NuttX is the Micro-Object Request Broker (uORB) system, which is a publish-subscribe pattern that allows for easier collection of sensor data. This simplifies the software, as the separate threads can have access to the latest data from each sensor, without having to use lower level interfaces to collect data.

The main goal of each thread is rather simple, with the most complex being the downsampling thread. This thread aims to balance the amount of data transmitted over the radio from each sensor, such that each packet contains an equal amount of each sensor. It accomplishes this by averaging sensors that have a higher rate, into an equal amount of data as lower frequency sensors. The radio thread then uses this balanced data to transmit over radio. The logging thread is the simplest thread, as it directly pulls sensor data and writes it to the SD card.

Another part of this system is the state detection, which uses sensor data to determine the state that the rocket is in. Sensor data is filtered using a median filter or a moving average filter, to increase accuracy. States functions as a simple finite state machine, going from idle, ascent, apogee, descent and landed. The transition between states are determined by certain conditions, such as going from idle to ascent if the acceleration or altitude rises to a certain level. This system remains the same as last year, which was able to accurately determine the state of the rocket throughout flight. However, one change this year was to start logging and transmitting data immediately, rather than waiting for the state detection to detect liftoff to log data.

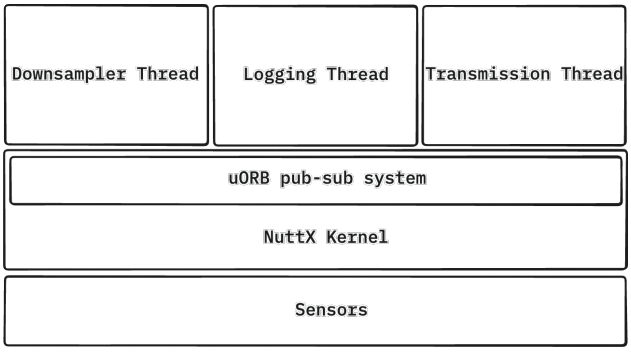

Figure 79 Flight Computer Software Architecture

9.1.4 Ground Station

The ground station's main purpose is to receive and display information from the SRAD telemetry system. Overall, the setup has only been minorly changed from last year. There are two main parts, with a backend and a frontend. The backend connects to a radio, and decodes packets, and then connects to the frontend via web sockets. The frontend runs with a server client setup, with the server connecting to the backend to receive packets and show it to clients which are connected over the network. This allows for multiple clients to connect to one server, which all share information from one radio. The frontend also includes a live map, which displays the current GPS and altitude information on the main page. Cesium ion is used to provide the satellite imagery. Figure 80 below shows the full user interface.

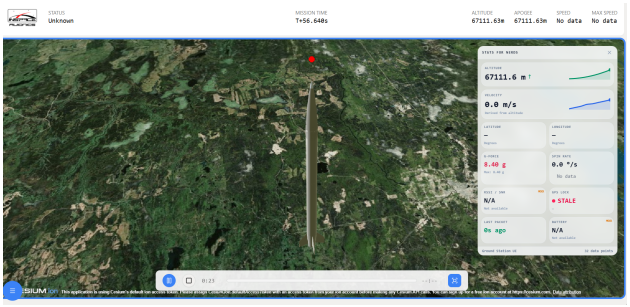

Figure 80 Ground Station Frontend

9.2 COTS Tracking

For redundancy there are multiple COTS GPS trackers being flown on CR26H. These trackers are detailed in the following paragraphs.

Primary COTS Tracker The primary COTS tracker for CR26 will be a Featherweight Altimeters Featherweight GPS. This featherweight GPS will be powered by a cylindrical 18650 Li-Ion cell with an capacity of 3000 mA h. This battery are expected to give the tracker a battery life of approximately 30 h although this battery life will be validated prior to competition. The team has successfully flown Featherweight GPS units on similar altitude flights in the past with no range issues, as well as performed multiple range tests which have validated that these tracker can work at ranges exceeding that expected to be required by CR26H.

Secondary COTS Tracker As a secondary tracker a a TeleGPS from Altus Metrum will be flown in CR26H as a redundant tracker. This tracker is being flown to validate its reliability as a secondary tracker to allow the team to no longer rely on a singular tracker model for redundancy. This tracker will be powered by a cylindrical 14500 Li-Ion cell with an capacity of 1500 mA h. This battery are expected to give the tracker a battery life of approximately 48 h.

Evaluation COTS Flight Computer Additionally, CR26H will fly a Silicdyne Fluctus COTS flight computer for the purposes of evaluating the performance and reliability of the flight computer before using it as a primary GPS tracker and flight computer. An additional benefit of flying this flight computer is the detailed data it will provide which can later be compared to the data generated by the SRAD flight computer discussed below. This flight computer will be powered by a cylindrical 14500 Li-Ion cell with an capacity of 1500 mA h. This battery are expected to give the tracker a battery life of approximately 12 h.

9.3 Power

The SRAD flight computer and COTS GPS trackers are powered by individual cylindricalLi-on battery packs, listed in Table 29, with varying capacities chosen to accommodate their respective system's run-times. The power choice for many of these systems are described in more depth in their respective sections, however the battery choices and expected operating durations are summarized below.

Table 29 SRAD and COTS Battery Pack Specifications

System	Arrangement	Size	Capacity (mAh)	Expected Runtime (Hours)
Josh	2P X 1S2P	21700	20 000	48
Featherweight	1S1P	18650	3000	120
TeleGPS	1S1P	14500	1500	48
Fluctus	1S1P	14500	1500	14

9.4 Enclosure Design

The SRAD and COTS system are securely housed on the avionics enclosure as shown in Fig. 77. The enclosure was improved upon previous proven enclosure designs flown at Launch Canada 2025 and IREC 2026. The material is aluminum 50-52 adonized blue and is 60mm x 80mm x 150mm in size. On the surface, the enclosure mounts the Josh flight computer, the featherweight GPS, fluctus flight computer, and TeleGPS modules on corresponding sides. Additionally, the enclosure mounts the SRAD radio transceiver and provides a secure Universal Asynchronous Reciever/Transmitter (UART) connection to Josh using 4-pin molex connectors. The enclosure was designed such that adequate space was given to the battery packs, as specified in Table 29, as well as spaces for connections to be threaded through the walls of the enclosure. The battery packs are oriented such that the wires providing power to the systems are the necessary length, while providing enough slack to assemble the system without tearing under pressure.
The enclosure is mounted securely on a dedicated bulkhead for avionics and recovery which is secured in the nosecone of the rocket. The placing of the avionics enclosure was chosen such that the length of COTS GPS antennas would not impede with the ogive shape of the nosecone.

9.5 Arming

All telemetry and deployment systems have independent vibration-resistant screw switches (Fig. 81) which ensure that the high vibration and G-loads experienced during flight does not disable any electronics. All systems are powered by independent packs of cylindrical Li-Ion batteries of carrying sizes depending on the current draw of the system.

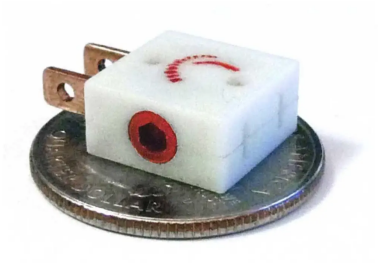

Figure 81 Exemplar Screw Switch

10. GSE

10.1 Launch Tower

10.1.1 Tower

The main supporting structure of the launch tower are 10’ antenna tower sections acquired by the team a number of years ago. This modular system allows for varying launch rail heights from 16’ to 40’. This year and last year the rail is set at 26’, meaning there are two 10’ sections and a 6’ section of extrusion. The launch rail is comprised of 1.5" aluminum extrusion supported by a 1.5" U-channel. The U-channel is secured to the antenna tower section using carriage bolts inter spaced evenly along the length of the tower sections. The U-channel and extrusion are pictured next to each other in Fig. 82.



Figure 82 Aluminium U-channel (left), and Aluminium Extrusion (Right)

The three pieces of aluminum extrusion seen in Fig. 83 will allow a launch vehicle to have a simple and standard sliding track system. The aluminum U-channel holds the extrusion in place and adds strength to the 10’ sections of extrusion by having its own joints off set from the extrusions. The main tower sections themselves are made from steel tubing and are bolted together to create the full 26’ tower. Lastly is the bolt plates which are simply .25" steel plates with bolts and nuts (some are specific nuts made for extrusion), these are positioned to overlap the connections between pieces of aluminum extrusion and aluminum channel.

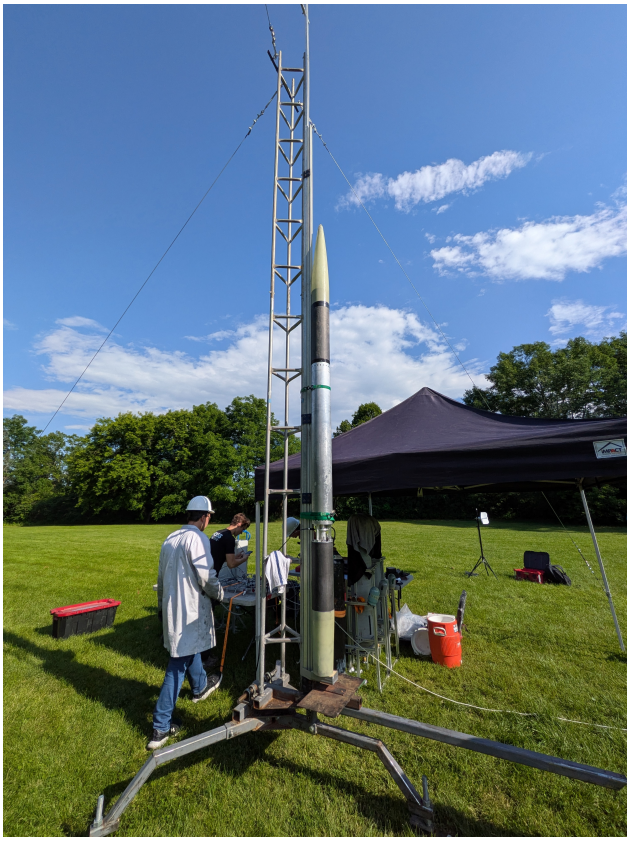

Figure 83 Side View of Tower Section

10.1.2 Base

The base of the launch tower system is compromised of three "legs" each around 3 feet in length, made from square steel tubing. At the end of each leg we have a down turn in the tubing to lift the whole base off the ground. This extra height allows us to level the tower more efficiently on uneven terrain. At the end of each leg is a 1.5" hole to secure a helical ground anchor (pictured in Fig. 84. Each leg assembly is slotted and bolted into a larger piece of square tubing in the centre of the tower base. The centre assembly is made of the three pieces of square tubing and two truncated triangular plates of .25" steel. Connected to the central base of the tower is a riser bar made from square steel tubing. Bolted to the riser bar is four thrust bearings that support the full range of motion of the tower. The tower uses a rack and pin system to allow for launch angles between 81 and 90 degrees. See Fig. 85 for a the completed base.



Figure 84 PE 36 helical Ground Anchors



Figure 85 Tower Base

The tower is lifted using 6 or more people, one on each of the three guy lines, two below the tower and one to place the pin when it has reached the desired launch angle. All people under and around the tower are required to wear hard hats and work gloves, to avoid injury. The raising process can be seen below in Fig. 86.



Figure 86 Tower Raising Process

10.1.3 Loads

The tower uses two guy lines mounted 20' up the tower sections. These guy lines are built to withstand winds up to 35 kts with at least a 2 times safety factor. With a total lateral load of 2 kN in the direction of the wind. The guy lines are made of 1/4" braided steel cable, connected to aluminum turnbuckles to allow the tensioning of the lines. Each line is connected to the same ground anchors which each have a pull out force of 4 kN. The tower is held in position by a 1/4 steel pin that maintains the angle when the tower is in it's raised position. The tower was used last year to fly a significantly larger and heavier rocket, demonstrating it's structural stability. The tower has also been set up a number of times on our own sites in many different wind conditions and has showed no signs of structural instability.

10.2 Hybrid Engine Control

This year the avionics and propulsion sub-teams worked in close coordination this year to improve the SRAD hybrid engine control system previously used for the team's first hybrid rocket, CR25H. The majority of the work was focused on improving the data collection and ease of setup of the system used last year.
The SRAD electrical systems used to control the fill system is composed of four key logical subsystems arranged into two physical systems.

- Mission Control Center (MCC) Systems
  - The Valve Control Console (VCC)
  - A telemetry monitoring UI
- Pad Control Center (PCC) Systems
  - The Valve Control Board (VCB)
  - The Telemetry Control Center (TCC)

All the communication between the different components of the system is done over a Local Area Network (LAN).
At a high level, the system performs as a client-server architecture. The Valve Control Board (VCB) acts as a server, which generates a publicly readable telemetry stream with the current valve states and processes requests to actuate the fill system solenoids and actuators. The telemetry stream can have an unlimited number of subscribers within the network bandwidth limitations, allowing multiple personnel to monitor the system in real-time from PEDs. The control connection, however, allows only a single operator to control the hybrid rocket systems.

10.2.1 Mission Control Center

The Mission Control Center (MCC) acts as the centralized control hub and UI for the entire hybrid control system. In addition to the components listed below the MCC also contains a Wireless Fidelity (Wi-Fi) Access Point (AP), Ethernet switch, and wireless Ethernet bridge discussed in more depth in Section 10.3

Valve Control Console The VCC acts as the primary control mechanism for the hybrid system. It consists of a switch panel that controls each actuator. Switch actuations are read by an MCU and transmitted over the network to the Pad Control Center (PCC) using Transport Control Protocol (TCP).
In order to maintain one source of truth, the VCC maintains absolutely no information about the current state of the pad control system. It does not track which valves are currently open or the current arming state. This ensures that an unintentional failure in either system (such as a brief power loss) does not cause a mismatch in state which will lead to control issues.
The VCC is solely responsible for translating switch actuations into commands sent over the network to the VCC. The VCC validates all of these commands against the current arming level and responds with either a success or failure to the MCC.
The VCC constantly attempts to connect to the VCB with a TCP connection. Only one VCC instance can be connected to the VCB at a time to prevent multiple control points. The TCP connection is used to enforce a stable connection that requires each side to acknowledge every command, preventing unknown loss of commands.



Figure 87 The VCC Switch Box Alongside User PEDs Running the Telemetry Monitoring UI

Hybrid Engine UI The Hybrid Engine UI acts as a telemetry sink and is used to consume the multicast telemetry stream sent over the network from the PCC. This UI both logs this data (as a back up to the logging

described in Section 10.2.2) and visually displays it to the system operators.
The hybrid engine user interface can be seen in Figure 88. It displays the most recently received value for each of the sensors in the sensor array, the state of all actuators in the system, and time series graphs of all of the telemetry data whose range of displayed values can be configured dynamically. The user interface is also capable of opening a second window which displays the Process & Instrumentation Diagram (P&ID) for the hybrid launch system (Figure 89. This window displays readings from various sensors within their position as represented by the P&ID).

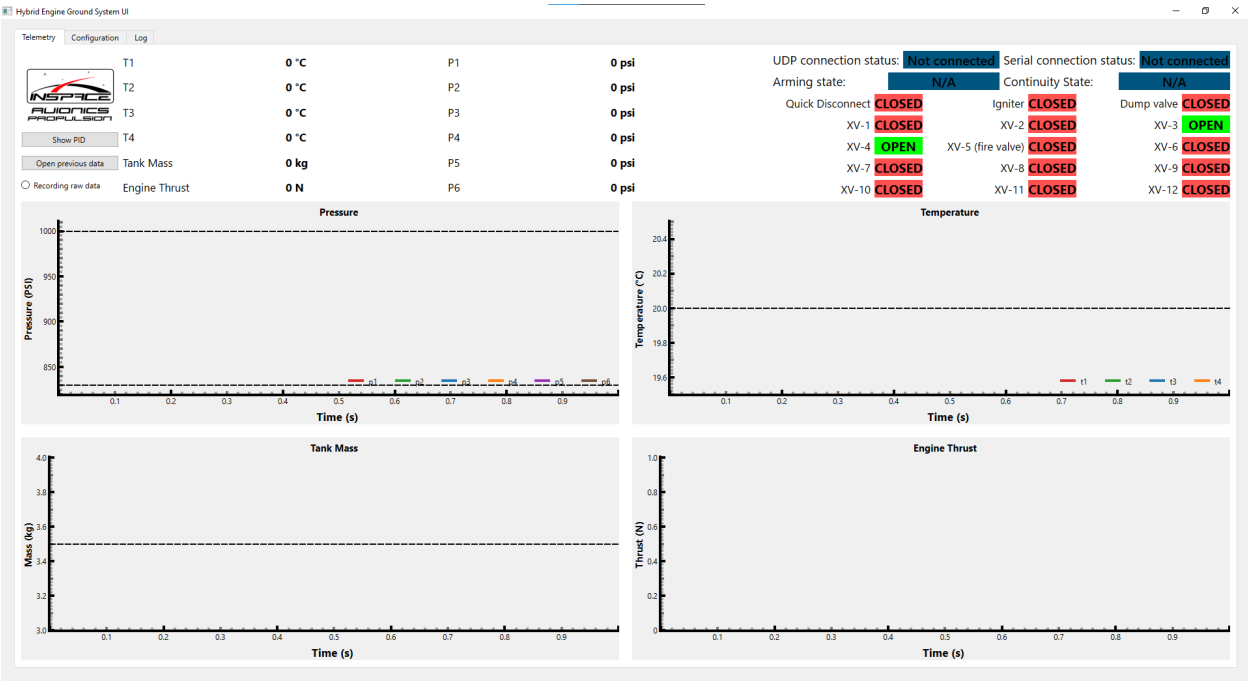

Figure 88 The Hybrid Engine User Interface when Idle

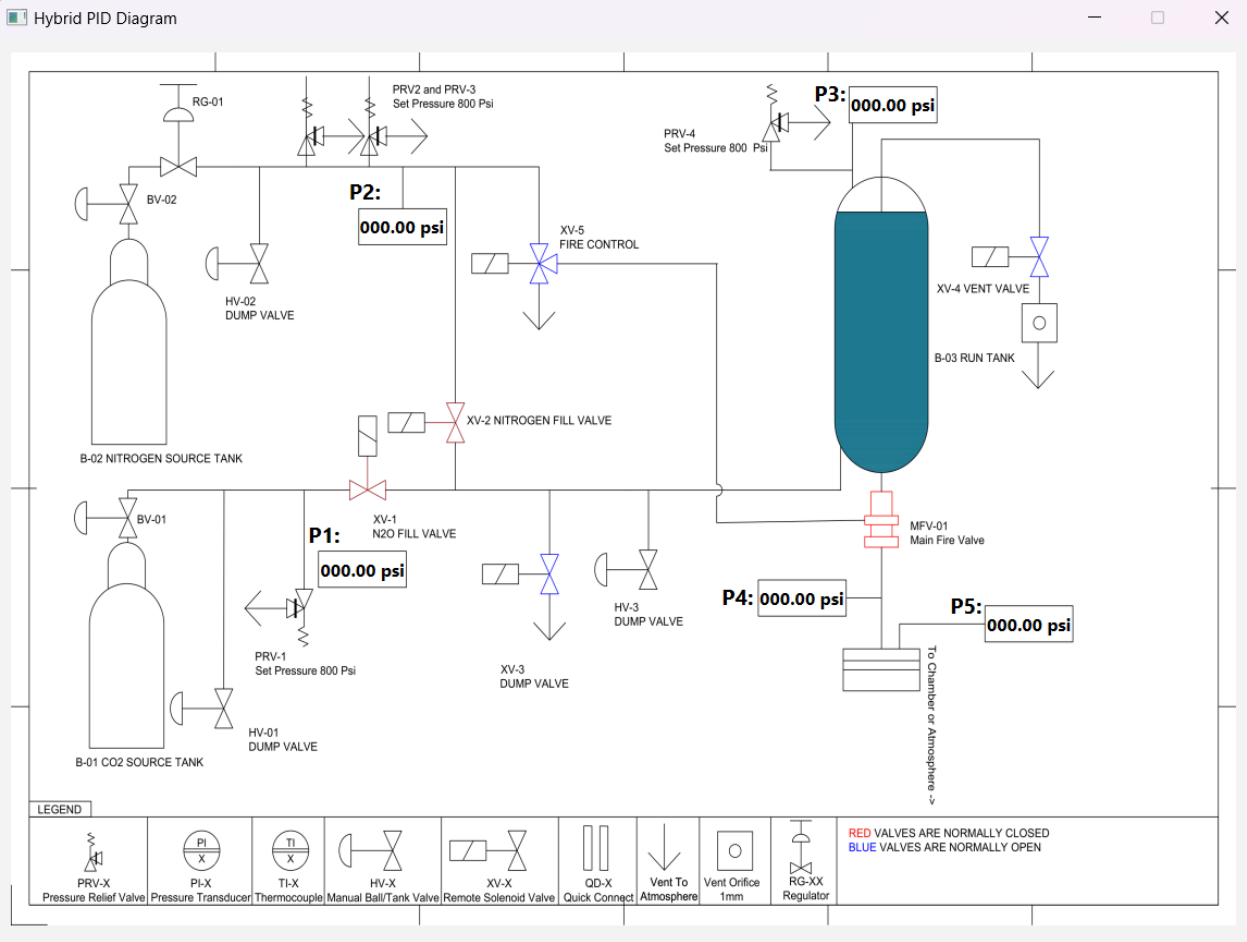

Figure 89 The Hybrid Engine UI P&ID Display [NOTE: This Image is using the P&ID from last year's system but has since been updated]

Since the telemetry sinks are set up to subscribe to a multicast address from the Telemetry Control Center (TCC) & VCB, there is no limit to the number of telemetry sinks that can be connected to the system (at least within the capabilities of the LAN). Additional telemetry sinks do not cause any extra burden to the PCC since the User Datagram Protocol (UDP) multicast protocol does not require any connections to be explicitly established or acknowledged. This allows for every team member to view the live state of the control system from their own device.

10.2.2 Pad Control Center

The PCC is the main hub of all the different aspects of the hybrid control system. It is electrically connected to multiple subsystems which are in turn connected to all of the actuators and sensors in the system. It maintains a network connection to the MCC from which it is instructed to actuate the system, saves all telemetry data locally, and provides a constant stream of the current valve states and telemetry data over a UDP multicast address for any telemetry sink (such as the Hybrid Engine UI) to listen to. The main subsystems which comprise the PCC are the VCB, TCC, networking subsystem, and the power subsystem. Each of these subsystems is explained in more depth below.

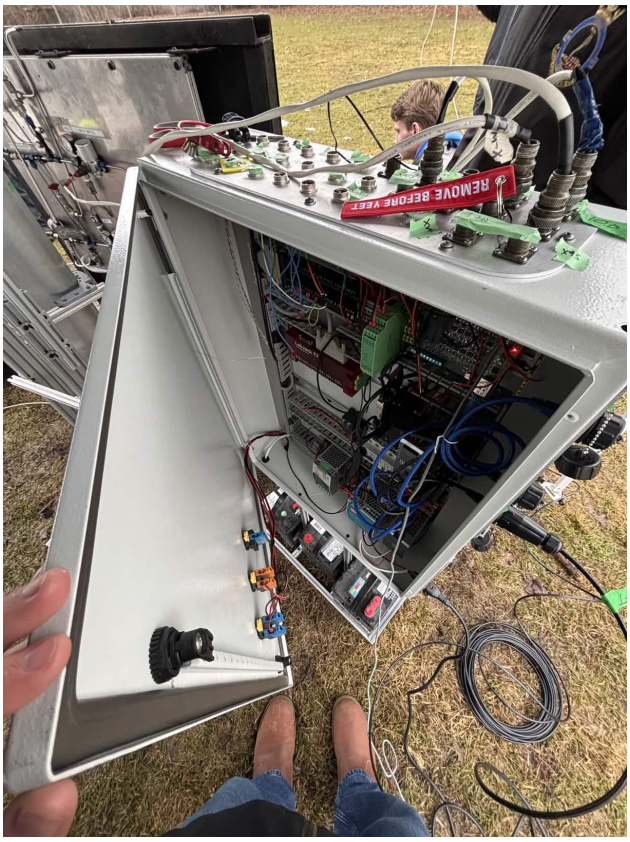

Figure 90 The Pad Control Box with its Lid Open During Testing.

Valve Control Board The primary actuators in the system are solenoid valves. There is also one high current relay used to control the ignitor and two servo motor actuators: one for the servo actuated ball valve used as a dump valve, and one currently unused but available for potential future upgrades.
The solenoid valves are actuated through the use of Metal-Oxide-Semiconductor Field-Effect Transistors (MOSFETs) and the main 24V rail inside the PCC. The MOSFETs are protected using large fly-back diodes for the magnetic field collapse of the solenoid valves. When turned on, 24V is supplied to the solenoid through the MOSFETs, and when turned off the connection with the solenoid is broken.
The MOSFETs themselves are actuated with a switching circuit that is connected to the PCC MCU. The MCU will send a high (3.3V) signal to close the circuit and turn on the solenoid, and a low (0V) signal to open the circuit and turn off the solenoid.
The servo motors are actuated more simply, with a direct connection from the MCU to the servo motor control inputs. They are driven with a 3.3V PWM signal, which is only used to move the servo motor between a pre-selected "on" and "off" position. The servo motor is powered with a voltage supplied from an 3S Lithium Polymer (Li-Po) battery separate from the main power supply system in the pad control box.
The VCB software is written on top of the Apache NuttX embedded RTOS. Using a RTOS allows InSpace to make guarantees about the response time and robustness of the system. NuttX provides several features that make the design of the VCB robust.
Another feature that is leveraged by the VCB box is panic notifier call-chains. On NuttX, if a program behaves unexpectedly or there is a critical error in the system, the RTOS kernel will "panic". This is a crash. When this happens, a "panic handler" is called. Panic handlers are short routines to perform some task at the time of the crash. NuttX allows these routines to be registered through a panic handler interface. [14] On the VCB, there are two routines that get registered when the MCU boots up: one which turns off power to all of

the solenoid valves, and another which opens the dump valve. This feature means that if the system crashes unexpectedly, it is guaranteed to enter a safe, de-pressurized state. This is the automatic-abort routine discussed in Section 10.2.2.
The panic notifier feature is further leveraged by the deliberate use of assertion statements throughout the VCB software. Assertion statements are logical statements which must evaluate to true, otherwise they trigger a panic. The VCB software is filled with assertion statements in locations where the program should not reach, or on statements that cannot fail. For instance, during operation the control handling thread should never exit. An assertion statement is used to guarantee that, or cause a panic which will safe the system. These assertion statements allow the VCB software to guarantee a safe system state on any logical failure or unexpected behaviour in the program.
NuttX implements a TCP networking stack which allows the use of TCP keepalive for monitoring connection status. TCP keepalive allows the PCC software to guarantee that if the control connection disconnects for longer than 5 minutes, the system will be de-pressurized by powering off all valves and opening the dump valve as discussed in Section 10.2.2.

Telemetry Control Center The Telemetry Control Center (TCC) is composed of a Raspberry Pi 5 connected to a LabJack T7 Data Acquisition (DAQ) device [15]. This system is used to collect, process, and log data from the multiple sensors monitoring the hybrid engine and oxidizer systems at approximately 8000 Hz. The high data rates collected are faster then is feasible to send over the limited network bandwidth. To minimize this problem the data is downsampled to approximately 30 Hz before being sent over the network to any telemetry sinks.
The sensor array that this system is capable of monitoring is listed below:
- Pressure transducers (6)
- Thermocouples (2)
- Tank Mass Load Cell (1)
- Thrust Load Cell Array (1)

Due to the high data rates recorded human readable file formats introduce too much overhead and would reduce the rate the data can be sampled at. To work around this the TCC record the data to an Apache Avro file [16]. This is a binary file format which takes up substantially less disk space to store and can be written substantially quicker then human readable file formats, such as csv.
The pressure transducers used in this system are MSP300 pressure transducers from TE Connectivity [17]. The specific models used contain a built in amplifier to provide an output signal 1-5V which is then read by the Labjack's built in Analog to Digital Converter (ADC). These pressure transducers are supplied from the 24V rail discussed in Section 10.2.2.
The TCC is capable of reading two K-type thermocouples to measure temperature of various aspects of the system. One of these thermocouples is used to measure the temperature inside the combustion chamber near the ignitor to determine when the ignitor has lit while the second is reserved for measuring air temperatures near the oxidizer tank when required for testing. These thermocouples are amplifier by a dual channel K-type thermocouple amplifier from Brightwin Electronics capable of converting an input temperature from 0 °C to 1300 °C to an output of 0 V to 10 V [18]. This amplifier is supplied from the main 24 V rail discussed in Section 10.2.2
The tank mass load cell is a 108BA bar type load cell from Tacuna Systems with a capacity of 50 kg and a sensitivity of 3.0 mV/V [19]. This load cell signal is amplified to an output of 0 V to 5 V using an EMBSGB200 amplifier from Tacuna Systems [20]. This amplifier is mounted next to the load cell and powered from the 24 V rail discussed in Section 10.2.2.
The engine thrust is measured by an array of three 101NH S-type load cells from Tacuna Systems with individual capacities of 1 klb and sensitivities of 3.0 mV/V [21]. These load cells are then combined into an array of three load cells by using an ANYLOAD J04EA-16 load cell summing junction to give an array with a total capacity of 1 klb [22]. This summing junction allows for the individual adjustment of the excitation

voltage to each load cell to ensure that each load cell responds equally giving reliable outputs no matter the angle the force is applied at. This load cell is then amplifier by an EMBSG200 amplifier from Tacuna Systems to give an output voltage of 0 V to 5 V [20]. This amplfiier is located in an separate enclosure on the test stand beside the thrust load cell array and powered by the main 24 V rail discussed in Section 10.2.2. All sensors are measured through unique channels on the labjack and are assigned an identification number. This allows the telemetry data to differentiate which parts of the system the readings correspond to (pressure readings across the system may be very different). The telemetry visualization UI can use these identification numbers to associate measurements to different portions of the live P&ID graph.

Arming Progression The arming states of the system are as follows, listed from lowest to highest privilege:
1) `DISARMED`
2) `ARMED_SHUNTED`
3) `ARMED_PAD`
4) `ARMED_VALVES`
5) `ARMED_IGNITION`
6) `ARMED_LAUNCH`

The `DISARMED` level is achieved simply by powering on the PCC. In this level all valves except the dump valve are physically disconnected from their power source ensuring that no failure of the control circuitry can cause any valves to actuate. Note that this status is not shown on the UI and instead is combined with `ARMED_PAD` which only differs from this level in the number of failures required to actuate any valves.
The `ARMED_SHUNTED` level is achieved by turning and removing the arming key from the PCC, connecting the valve control circuitry to the power source. In this arming level the ignitor leads are disconnected from the ignitor circuitry and shunted, preventing any accidental activation of the ignitor. In this arming state the vent valve and dumb valve can be opened, all other commands will be rejected by the VCB
The `ARMED_PAD` level is achieved by using the same key removed from the PCC to progress from `DISARMED` to `ARMED_PAD` in the arming switch for the ignition circuitry connecting the ignitor to the ignition circuitry and removing the shunt between the ignitor leads.
The `ARMED_VALVES` level is achieved by turning the valve arming key in the MCC switch panel. The key used to arm the valves is the same key that is used to arm the valve control & ignition circuitry at the PCC, ensuring that the pad team has safely left the pad and returned to the base station before arming the valves. In this state, any of the valves (with the exception of the fire valve) on the system can be actuated.
The `ARMED_IGNITION` level is achieved by turning the ignition arming switch to the armed position on the MCC. This is a safegaurd to prevent any accidental actuation of the ignition actuators. This arming level grants access to the ignitor actuator.
The `ARMED_LAUNCH` level is achieved only after actuating the ignition circuitry, which results in the igniter puck being lit. This arming level grants access to the fire valve, allowing the operator to open it and cause a launch.
The arming sequence must proceed in the order listed above. If any actuation commands are sent for actuators that are not permitted at the current arming level, the commands will be denied and nothing actuated. This ensures that the arming sequence is obeyed for safe operation. At any point in the arming sequence, it is possible to safe to a lower arming state. For instance, if the system is currently in the `ARMED_DISCONNECTED` state, it is possible to safe back to the `ARMED_PAD` state by turning the valve arming key back to the disarmed position.

Ignition Circuitry The ignition of the igniter puck is accomplished through the use of a ni-chrome coil embedded inside the igniter pucks. As mandated by the Design, Test, and Evaluation Guide (DTEG) there are multiple actions required to ignite this igniter, both software implemented and hardware implemented. The physical ignition circuitry consists of an ignition relay driven by the pad control center, and a dedicated 12 V deep cycle car battery. In addition to this relay and battery there is also an key switch controlled relay in

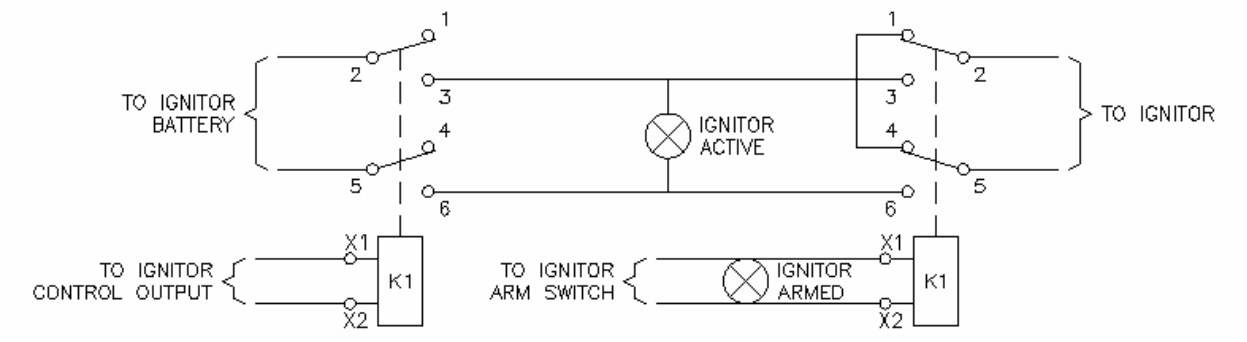

Figure 91 igniter Control Circuitry

series used to arm the ignition. This relay fully disconnects power from the igniter circuitry and shunts the ignitor leads together. Power is only supplied to the igniter circuitry when the arming key is *armed*, indicating that the pad personnel have left the site. This same arming key is what is used to arm the valve control circuity on the PCC (from which it can not be removed until the PCC valve control circuitry is armed) and later used to arm the valve control circuitry from the mission control side. There are also indicator lights on the exterior of the PCC and ignitor control box which will illuminate if the system is armed or if the ignitor circuitry is active allowing personnel to verify at a glance that the ignitor circuitry is not powered and if the circuitry is armed.
On the mission control center side there are three distinct actions required before ignition command will be sent to the pad control center. First the key used to arm the igniter at the PCC must be inserted and turned in a key-switch at the MCC to arm all hazardous commands, when these commands are armed the key is physically retained in its switch at the MCC. Then to arm for ignition a switch must be closed. Only after both these actions have been performed will the MCC box respond to the ignition button and forward this command to the PCC.

Automatic Failsafes The connection between the MCC and the PCC MCUs is established using TCP. Alongside requiring each packet to be acknowledged, this protocol allows for detection of severed connections.
This is implemented using the "keepalive" method. Periodically, the PCC sends a single `ACK` packet to the MCC. The MCC will respond with its own `ACK` if the connection is nominal and both systems are behaving as expected. However, if the connection is interrupted, the PCC will not receive an acknowledgement back. The current system is set up such that the PCC probes the MCC with an `ACK` packet every 5 seconds. It will do so without receiving a response from the MCC up to 3 times, and then decide that the connection has been interrupted. Once the PCC has detected an interruption in the connection, it will open its network interface to accept a new connection. The MCC also sends its own `ACK` probes via the "keepalive" method, and if an interrupted connection is detected it will attempt to re-connect to the PCC. This means that after 15 seconds of communication interruption, both systems will attempt to re-connect to each other.
Once these 15s second have passed and the PCC re-opens its network interface to accept the MCC's re-connection attempt, a 5 minute timer is started on the PCC. At the end of this timer, the PCC will cut power to all solenoid valves and open the the dump valve. This prevents a scenario in which the connection cannot be re-established in 5 minutes and the fill system becomes completely uncontrollable with no abort mechanism. If the connection interruption is fixed with the 5 minute timer, the MCC will re-connect to the PCC and operations can continue as normal. The duration of 5 minutes is completely configurable, and can be reduced or lengthened prior to the mission. In addition, if power were lost to the PCC all solenoid valves will return to their default states, including the vent valve which will open and slowly vent the pressure from the system.

In addition to the automatic abort of the system when a broken connection is detected, the PCC accounts for unexpected failures as well. The PCC control logic is implemented on top of the Apache NuttX embedded RTOS. This RTOS supports what is called a "kernel panic", which is an event which occurs when an unrecoverable fault is detected. This can happen due to a failed logical assertion or an unexpected system crash because of something like an out-of-bounds memory access.
When a kernel panic occurs, the panic handler is called. This handler is a function that performs some very basic level of indicating the failure. Typically, this involves flashing a red LED on the board until the board is reset. In this control system, the panic handler has been modified to cut power to all solenoid valves. This means that in the event of a logical error or program crash, the system will be vented to prevent it from becoming unstable during a loss of control or system integrity. The control program running on the PCC has additional "assertion" statements which will trigger a kernel panic if any unexpected behaviour is encountered (for instance, inability to lock a mutex, a thread unexpectedly dying, etc.).

Power The PCC is powered from two different power sources with automatic failover between them. The primary power source is a 120 VAC to 24 VDC power supply and the secondary source is a 24 VDC Uninteruptable Power Supply (UPS) which is powered by two 12 V car batteries in series. This UPS automatically takes over with no power interruption if the AC to DC power supply were to fail for any reason. All the primary components of the PCC are then powered by this 24 V rail with each individual component protected by a circuit breaker ensuring that no single component can cause the entire power system to fail. All current carrying wiring is sized in accordance with Federal Aviation Administration (FAA) Advisory Circular (AC) 43.13-1B [23].

10.3 Networking

The primary method of communication in the hybrid control system is a LAN network and a wireless network bridge to allow communication between the pad and mission control site without needing to run a cable between the two sites. The network architecture is shown in Figure 92 and discussed in more detail below.
This LAN is leveraged to send two primary kinds of data. The first way this is leveraged is the consumable telemetry stream. Telemetry is generated by the TCC, discussed in more depth in Section 10.2.2. The telemetry stream from the TCC is implemented using UDP multicast. This has several major advantages. The first advantage is that UDP is a connection-less protocol, which means it does not incur any additional overhead for acknowledging receipt of packets or re-transmitting dropped packets.
This is suitable for a LAN based telemetry system, where packets are unlikely to be dropped. If a packet is dropped, it will be milliseconds before another is sent containing new telemetry information. There is no point to requesting re-transmission of outdated telemetry information, since this will incur more delay than simply waiting for the latest packet. The second major advantage is in multicast addressing: the UDP packets need to only be sent once by the PCC to the multicast address, but an unlimited number of subscribers (at least, up to the network bandwidth and LAN capabilities of the router) are able to receive the telemetry data at no additional overhead to the PCC. This allows the hybrid engine UI to run on multiple devices connected to the wireless router at the mission control side, and have all of them monitor the system in real-time.
The second area using the LAN is the use of TCP for the connection between the VCC and the PCC. This connection is used for the VCC to send control commands to the PCC for actuating valves and arming sub-systems. Unlike UDP, TCP is a connection-based protocol which is used for networked systems that require reliability. It requires all packets to be acknowledged in a three-way handshake (both the sender and receiver acknowledge messages), and also provides re-transmission of dropped packets. This is very important for the control connection, where command packets are much less frequently sent (compared to telemetry packets) and where it is not acceptable to drop packets (it would not be safe to "drop" a command to open a valve). TCP, being connection-based, also provides the ability to detect connection loss between the sender and receiver. If the PCC detects a loss of communication with the VCC, a 5 minute timer is started that automatically saves the system by opening the dump valve if the connection is not re-established.

Typically, TCP will only detect the connection break if a message is not acknowledged. This means that a message must be sent as a precursor to detecting a broken connection, which is not acceptable for the control connection where commands are infrequently sent. For instance, the operator may be monitoring the fill process and not actively sending commands. To resolve this problem and guarantee that both sides of the connection are able to detect a disconnect within 15 seconds, TCP "keepalive" was used to monitor the connection. This protocol extension sends "ACK" probes at a set interval on the connection automatically. If the probes are not acknowledged within the time limit, the TCP connection is considered disconnected. The current implementation sends 1 probe at 5 second intervals for a total of 3 probes which allows detection of a disconnect within 15 seconds.
The VCC acts a control client, which sends out control commands for the pad server discussed above to validate and process.
The telemetry monitoring UI is a sink for the VCB & TCC telemetry streams generated as described above. In the current system, there are two ways this data is consumed. One is via the UI itself, which displays the status of all actuators and the pressure, temperature and mass readings of the system components. The other type of sink simply logs all the data from the telemetry stream to a file for review later.
There are two types of messages that can be exchanged within the control system, control messages sent over TCP from the VCC to the VCB and telemetry packets sent from the VCB & TCC to PEDs running the Hybrid Engine UI. For more details on these packet types see [24]. The physical network architecture of the system is discussed in more depth below.

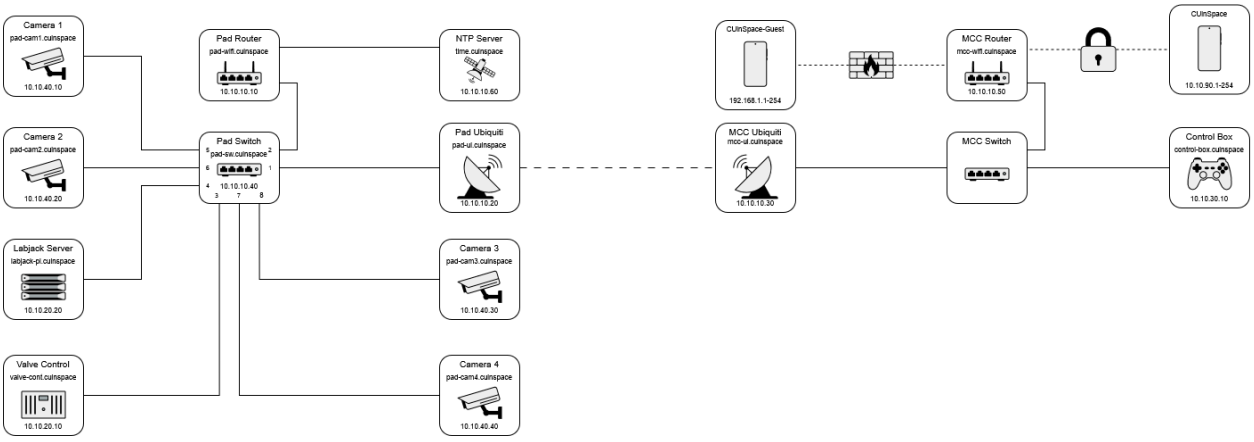

Figure 92 Network Topology of the Electrical Control Systems

Network Bridge To bridge the network between the PCC & MCC a pair of Ubiqui LiteBeam M5 wireless network bridges are used [25]. This pair uses a 5 GHz wireless link to achieve speeds of up to 100 Mbps at a distance of up to 15 km. These bridges are mounted on tripods at both the MCC & pad to ensure they can retain line of sight even if there is low level brush and debris between the pad & MCC.

PCC Networking The PCC contains the bulk of the networking equipment. Built into the PCC is a Teltonika Networks RUT140 router used for a Dynamic Host Configuration Protocol (DHCP) server and to handle the UDP multicast telemetry traffic [26]. In addition there is a Teltonika Networks TSW202 Power Over Ethernet (POE) switch to provide ethernet ports for all the different components of the PCC and provide POE to cameras used to remotely monitor the pad and hybrid engine [27].

MCC Networking The networking at the MCC is relatively simple compared to the networking at the PCC. The MCC networking only consists of a router used as an ethernet switch an Wi-Fi AP to provide enough

ethernet ports for all the required devices to connect to as well as a Wi-Fi network for personnel to connect PEDs to for monitoring the UI and camera feeds.

11. Range Safety

11.1 Hazard Analysis

Table 30 Potential Hazards

Hazard	Causes	Risk of Mishap and Rationale	Mitigation Strategy	Risk After Mitigation	Severity	Risk Score
Outbreak of illness within the team	Transmission through material transfer. Infection during manufacturing	Low: All team members doing manufacturing follow standard cleanliness practices.	Mandatory PPE during all periods of manufacturing contact to reduce the risk of cuts and bleeding.	Very Low	Medium	Low
Injury of team members during SRAD part development	Improper use of tools. Not using PPE	Very low: All team members are aware of the manufacturing procedure and should have proper training on tools/equipment	Define dangerous goods and equipment to all personnel before manufacturing begins. Use proper PPE. Do a dry run of any dangerous procedures to define areas/steps that may have increased risk	Very Low	High	Medium Low
Launch vehicle falls from launch rail or elevated position and comes in contact with personnel, causing injury	Improperly installed launch lugs. Launch rail lifting is done too quickly or with incorrect personnel position	Low: Launch rail attachments are installed onto aluminum load bearing bulkheads designed to withstand the weight of the rocket	All mechanical components such as rail attachment and launch rail installation are checked by experienced members prior to installation on launch rail. Rail attachments are directly connected to main structural members to assure rigidity	Low	High	Medium Low
High temperature electrical failure while personnel are working on the system, causing injury	Shorted Electrical Components	Low: Battery and power will be disconnected from the system while personnel are working. Potential injuries are minimal	All safety switches will be safed and power disconnected while electronics modifications are being done. Static bracelets will be worn when applicable. Personnel will wear personal protective equipment while working with the avionics	Very Low	High	Medium Low
Rocket weathercocks off launch rail during boost and comes into contact with personnel at high speed	High winds at launch. Improper launch rail or lug alignment	Low: Launch rail alignment will be checked prior to launch. Wind speed will be verified acceptable before launch.	Launch rail will be between be at 84 +/1 degrees prior to launch. Wind speeds will not exceed Tripoli guidelines prior to launch. Personnel will be a safe distance and behind cover	Low	Very High	Medium High
Premature activation of recovery system during assembly of the rocket while personnel are working on it, causing injury	Improperly installed CO2 Cartridges. Ejection system is prematurely armed	Low: Recovery system is only fully armed on the launch rail within the launch range	Electronic systems are designed and tested to avoid such events. Armed at the launch site only by experienced executives involved in the system.	Very Low	Very High	Medium
Ignition of unexploded charges during recovery of the rocket, causing injury	Spontaneous ignition of propellant during recovery	Low: Avionics has redundant backups, charges proven through multiple ejection tests.	All electrical connections are to be checked prior to launch. Recovery personnel have proper training to check for unexploded charges. Pyrotechnic devices are to be securely installed and checked by experienced members, assuring wires are not stressed	Very Low	Very High	Medium
Personnel dehydration or injury during rocket recovery	Improper PPE/Equipment taken during recovery procedure	Low: Personnel should be well informed of the weather and environment, ensuring adequate measures taken in PPE and supplies	Ensure all personnel in recovery of the rocket is well dressed and equipped. Equipment includes PPE, adequate equipment and water.	Low	Medium	Medium Low

Table 30 Potential Hazards

Hazard	Causes	Risk of Mishap and Rationale	Mitigation Strategy	Risk After Mitigation	Severity	Risk Score
Premature Ignition of ignitor during motor loading	Power is applied to the ignition system prematurely. Ignitor is improperly grounded/shorted	Low: Personnel responsible should be well versed in installation of ignitor. Ignition capability is only accessed through a keyed mechanism.	Ignitor system checked at the pad prior to installation. System only armed once personnel is well clear of the pad at a predetermined safe distance set by the competition	Low:	Very High	Medium High
Recovery system fails to properly deploy, rocket and/or payload comes in contact with personnel.	Improper parachute packing and installation. Nose cone fails to deploy. Parachute caught on deployment. Drogue parachute fails to pull main	Medium: Recovery system ejection testing is performed in a static environment without the presence of conditions in flight.	Parachutes should be packed and installed by recovery executives. Clean and smooth inner surfaces of rocket in path of recovery system deployment. Electronic systems are checked, tested, and armed at the launch site by senior avionics or recovery executives	Low	Very High	Medium High
Rocket does not ignite when the command is given, ignites when personnel approaches.	Faulty ignitor. Wiring fault. Failure in electronics	Low: Engine and engine ignitor systems are proven commercial solutions	Igniters are ensured to be securely installed mechanically and electrically. Initial installation of ignitor performed by experienced members	Low	High	Medium
Rocket suffers a CATO after ignition, causes injury.	Personnel are too close. Improper motor assembly. Damage to motor during assembly	Very low: All team members and other personnel are at well understood safe distances set by competition. Failure mode of the combustion chamber is to eject the nozzle before chamber walls fail due to overpressure.	Personnel are to comply with safe viewing distance requirements set by the competition. Motor assembly is to be performed by experienced propulsion subteam members.	Very Low	Very High	Medium

11.2 Hybrid Development Hazard Matrix and Risk Assessment

Table 31 Potential Hybrid Development Hazards

Hazard	Causes	Risk of Mishap and Rationale	Mitigation Strategy	Risk After Mitigation	Severity	Risk Score
Damage to hearing of members	Loss of power in the electrical system causes normally open valves to discharge high-pressure gas	Medium: control box relays have burnt out in previous tests, and while the issue has been fixed before the test the possibility still exists	Medium: control box relays have burnt out in previous tests, and while the issue has been fixed before the test the possibility still exists.	Very Low	High	Medium Low
Personnel hit by flying debris from component bursting	Failure of nitrogen tank regulator causes overpressure of system	Low: the system has 2 Normally open solenoid vent valves that can be opened if pressure is seen to be rising above operating pressure, as well as a mechanical relief valve that will open before the burst pressure of any component is reached	All Personnel will be over 80m from the test stand when at operating pressure(1000 psi), which is the standoff distance for hazardous fragments calculated by-DoD 6055-09-M for the TNT equivalent energy of the system at operating pressure. All components have a safety factor of at least 2x operating pressure as well as redundant venting methods.	Very Low	Very High	Medium
Uninvolved personnel entering the standoff zone	Bystanders may wander into the test standoff distance while the system is pressurized	Low: if bystanders are seen inside the standoff radius the test will be paused and the system will be depressurized	Two members will patrol the standoff radius to notify any passers-by to stay clear of the test stand while pressurized.	Very Low	Medium	Low

Table 31 Potential Hybrid Development Hazards

Hazard	Causes	Risk of Mishap and Rationale	Mitigation Strategy	Risk After Mitigation	Severity	Risk Score
Harm to a member by cold temperatures in plumbing post-cold flow	After the cold flow, the carbon dioxide flowing out of the tank may have cooled the plumbing to a point where it could give frostbite from touching	Medium-low- temperature on the system will be monitored by a temperature sensor so any members approaching the test stand will be notified of any low temperatures present	In case the temperature sensor is inaccurate or not representative of the entire system, members approaching the stand after cold flow will make use of insulated gloves to protect their hands from any cold temperatures that may exist on the plumbing.	Very Low	Medium	Low
Harm to personnel due to improper Personal Protective Equipment	Personnel are injured or harmed due to improper PPE. That is, a risk as outlined above, resulting in bodily damage to personnel.	Low: ALL personnel will be required to wear the appropriate PPE before they are allowed near the test site.	To prevent hearing damage: Earmuffs MUST be worn within the minimum safety distance of 80m. Around the perimeter of which, ear plugs MUST be worn. To prevent damage to skin, feet, or limbs: Long sleeves, long pants, and closed-toe shoes MUST be worn. That is, NO loose articles of clothing are allowed and any loose hair MUST be tied back. To prevent facial damage: Face shields and safety glasses MUST be worn within the minimum safety distance of 80m. Around the perimeter, safety glasses MUST be worn. To prevent damage to hands: Insulated gloves MUST be worn when within the minimum safety distance as well as while handling any pressurized vessel.	Very Low	High	Medium Low

12. Risks and Mitigation Strategies

CU InSpace faces a number of risks to the successful operation of its CR26H launch vehicle. Some of these risks are analyzed in sections 12 and 13. The risks in these sections have been ranked according to severity. Our severity index is as follows:

- 1 - Minor Inconvenience, delay under 1 week
- 2 - Moderate delay, 1-2 week delay
- 3 - Considerable delay, 3-4 week delay
- 4 - Severe Delay, 1-2 month delay
- 5 - Vehicle can not launch

Programmatic Risks

The programmatic risks presented in Table 32 are some of the risks that could disrupt CU Inspace's ability to launch at the Launch Canada challenge.

Table 32 CR25H Programmatic Risk Matrix

Pre-Mitigation					Post-Mitigation			
Program Risk	Description	Probability of Occurrence	Severity of Risk	Risk Level	Mitigating Action	Probability	Severity	Risk Level
Launch vehicle unmanufactured due to lack of suitable workspace	The lack of student workspaces on campus may cause delays or shortfalls in manufacturing	10.00%	5	0.5	1) Risk accepted, Carleton's composites manufacturing facility is open for limited hours each day and team can not control anything with regards to this leading to delays in repair of critical composite components	10.00%	5	0.5
Missing components at competition	Inadequate checklists and packing procedures may result in a forgotten component	10.00%	1	0.1	1) Pre-shipping checklists of all components to be completed and signed off by team executives 2) Check lists to be completed upon arrival to allow for shipping of missing components should they not be packed	5.00%	1	0.05
University does not permit travel of design teams to competitions	Carleton University does not insure team or permit team to leave for competition	25.00%	5	1.25	1) Risk accepted, team can not control the university's travel policy	25.00%	5	1.25
Team experiences budget cuts	Carleton University's funding stream for design teams does not fund critical components for launch vehicle	100.00%	4	1.75	1) Risk accepted, team can not control the university's club operation and funding policy	100.00%	4	1.75
Insufficient team member numbers at critical period	Team membership may drop off at a critical point in manufacturing, leading to a strain in the vehicle's development	15.00%	2	0.3	1) Team to continue outreach to assure member levels do not drop below the threshold for operation	10.00%	2	0.2

13. Technical Risks

The technical risks presented in Table 33 are some of the risks that could disrupt CU InSpace's ability to successfully bring a launch vehicle to the Launch Canada challenge.

Table 33 CR25H Technical Risk Matrix

Pre-Mitigation					Post-Mitigation			
Technical Risk	Description	Probability of Occurrence	Severity of Risk	Risk Level	Mitigating Action	Probability	Severity	Risk Level
Inability to satisfactorily manufacture composites	Composite components are difficult to manufacture consistently outside of carefully controlled environments. The composites lab has limited hours which are not sufficient for the duration of some manufacturing processes	50.00%	4	2	1) COTS Alternatives Available for Critical Components 2) Composites testing is performed as early as possible	25.00%	4	1
Inability to locate recovery test grounds	Recovery testing is critical before flight; the reefing system is complex and requires enough time to inflate and then activate the reefing system. This is complex to test.	80.00%	3	2.4	1) Independently verify each component 2) Continue to discuss the use of wind tunnel facilities with Carleton. Wind tunnel is a location to bring parachutes to steady state before charge deployment	35.00%	3	1.05
Unexpected component failure at critical period	Flight components may be damaged in the weeks leading up to departure for competition	25.00%	5	1.25	1) Perform testing as early as possible without using intended flight hardware 2) If not possible to use test articles in lieu of flight hardware, test at conditions component will experience and shield components from conditions outside expected flight envelopes (ie. assure unshielded wires are not brought close to electronics, as this is not a flight condition to test)	25.00%	3	0.75
Sensitive components damaged in transport	Transportation of the launch vehicle and payload components is a significant risk due to many uncontrollable factors (other road vehicles, road conditions, environmental conditions)	10.00%	5	0.5	1) Components to be placed in protective containers during transport to prevent uncontrolled movement and potential damage 2) Containers storing flight-critical components should be water-tight 3) Components to be inspected before departure and upon arrival for damage 4) Bringing duplicates or COTS alternatives to critical high risk components (ie. additional fins, COTS altimeters, etc.)	5.00%	5	0.25
Manufacturing bottlenecks	The school has a single machine shop used by all Carleton Capstone teams and design teams, this leads to high lead times, especially when students are not permitted to enter the machine shop to perform their own machining	30.00%	3	0.9	1) Assure school machine shop has months of lead time in schedule to produce components 2) Source COTS replacement components for high-lead time components as contingency 3) Be in contact with external machine shops to produce components	25.00%	3	0.75
Electronics failure due to adverse launch site conditions	Flight vehicle avionics must be robust to withstand the hot and dry conditions in New Mexico and the potential wet conditions at Launch Canada	25.00%	5	1.25	1) Shield electronics against water ingress and assure components are rated for high heat environment in launch vehicle 2) Have backups for flight-critical components (ie. batteries, altimeters, etc.)	10.00%	5	0.5

Pre-Mitigation					Post-Mitigation			
Program Risk	Description	Probability of Occurrence	Severity of Risk	Risk Level	Mitigating Action	Probability	Severity	Risk Level
Unexpected initial structural testing results	Initial structural testing may yield unexpected results when compared to simulations, these may require redesign of specific load bearing components for the rocket to be able to fly; this is combined with the potential bottlenecks from the school's machining resources	50.00%	2	1	1) Assure designed components have been analyzed in finite element analysis software and meet a predetermined safety factor 2) Communicate designs with team mentors prior to manufacturing 3) Produce test articles prior to flight hardware to avoid breaking flight hardware	50.00%	1	0.5
Flight component damage during testing	Many flight components are not currently planned to have separate test articles due to needing to construct a second airframe. Thus, the flight component may become damaged prior to competition, requiring remanufacturing and potential redesign	25.00%	5	1.25	1) Assure designed components have been analyzed in finite element analysis software and meet a predetermined safety factor 2) Communicate designs with team mentors prior to manufacturing 3) Produce test articles prior to flight hardware to avoid breaking flight hardware	25.00%	1	0.25
Unacceptable vehicle manufacturing tolerances during assembly	Should the vehicle's airframe not meet the bending tolerance requirements, it may be prevented from launching at competition as the flight characteristics may be unexpected	10.00%	4	0.4	1) Assure tolerances are checked with previous team leads 2) Compare tolerances with previous nominal toleranced parts 3) Communicate designs with team mentors prior to manufacturing	5.00%	4	0.2
Vehicle mass outside of predicted mass budget	The rocket may be heavier or lighter than predicted using the mass budget, causing issues with meeting altitude and stability requirements	25.00%	1	0.25	1) Regularly update mass budget with measured values 2) Hold sub-teams to mass limitations to assure they do not exceed them	12.50%	1	0.125
Vehicle stability caliper outside of predicted window	Should the vehicle's stability caliper change prior to launch, the vehicle may not be permitted to launch	25.00%	5	1.25	1) Regularly update aerodynamic simulations as per the mass budget to assure fin sizing does not change 2) Perform computational fluid dynamics simulations to verify centre of pressure position 3) Perform physical testing to verify centre of gravity position prior to departure for launch	12.50%	5	0.625

References

[1] Milligan, T. V., "Basics of Dynamic Flight Analysis Part 1 - Moment of Inertia," 2007.

[2] Milligan, T. V., "Basics of Dynamic Flight Analysis Part 2 - The Corrective Moment Coefficient," 2007.

[3] Milligan, T. V., "Basics of Dynamic Flight Analysis Part 3 - The Damping Moment Coefficient," 2007.

[4] Jr., H. L. G., "The Effect of a Fin Trailing-Edge Wedge on the Roll History of a Nike Apache," Tech. rep., Goddard Space Flight Center, 1966.

[5] StabilityOR, *Accurately Modeling Stability in OpenRocket*, n.d.

[6] Milligan, T. V., "Basics of Dynamic Flight Analysis Part 5 - The Damping Ratio," 2007.

[7] *How to Design Pressure Vessels, Propellant Tanks, and Rocket Motor Casings*, Half Cat Rocketry Technical Resources, 1st ed., ????

[8] *MS5607-02BA03 Barometric Pressure Sensor*, TE Connectivity, 03 2024. URL https://www.te.com/commerce/DocumentDelivery/DDEController?Action=srchrtrv&DocNm=MS5607-02BA03&DocType=Data%20Sheet&DocLang=English&DocFormat=pdf&PartCntxt=MS560702BA03-50.

[9] *LIS2MDL Digital Output Magnetic Sensor*, ST Microelectronics, 11 2018. URL https://www.st.com/resource/en/datasheet/lis2mdl.pdf.

[10] *LSM6DSO32 iNEMO intertial module*, ST Microelectronics, 03 2020. URL https://www.st.com/resource/en/datasheet/lsm6dso32.pdf.

[11] *L86 Hardware Design*, Quectel, 09 2014.

[12] *RN2483 specification sheet*, Microchip, n.d. URL https://ww1.microchip.com/downloads/en/DeviceDoc/RN2483-Data-Sheet-DS50002346E.pdf.

[13] *STM32H743/753*, ST Microelectronics, 2024. URL https://www.st.com/en/microcontrollers-microprocessors/stm32h743-753.html.

[14] Apache NuttX, "Notifier Chain," , 2025. URL https://nuttx.apache.org/docs/12.9.0/reference/os/notifier.html.

[15] *Labjack T-Series Datasheet*, Labjack, n.d. URL https://support.labjack.com/docs/t-series-datasheet.

[16] Apache Avro, "Apache Avro," , ???? URL https://avro.apache.org/.

[17] *MSP300 Pressure Transducer*, TE Connectivity, 09 2024. URL https://www.te.com/commerce/DocumentDelivery/DDEController?Action=srchrtrv&DocNm=MSP300&DocType=Data%20Sheet&DocLang=English&DocFormat=pdf&PartCntxt=CAT-PTT0016.

[18] *Isolated K Type Thermocouple Signal Conditioner Dual Input Dual Output*, Brightwin Electronics, n.d. URL www.brightwinelectronics.com/product/isolated-k-type-thermocouple-signal-conditioner-dual-input-output.

[19] *108BA*, ANYLOAD, n.d. URL https://www.anyload.com/wp-content/uploads/2014/03/ANYLOAD-108BA-load-cell-transducer.pdf.

[20] *Embedded Strain Gauge and Load Cell Signal Conditioner/Amplifier*, Tacuna Systems, v2.41 ed., 08 2025. URL https://tacunasystems.com/wp-content/uploads/EMBSGB200_2_4.pdf.

[21] *101NH*, ANYLOAD, n.d. URL https://www.anyload.com/wp-content/uploads/2014/03/ANYLOAD-101NH-load-cell-transducer.pdf.

[22] *J04EA-16; J04SA-16*, ANYLOAD, n.d. URL https://www.anyload.com/wp-content/uploads/2024/11/J04EA-16-J04SA-16-junction-box.pdf.

[23] *Acceptable Methods, Techniques, and Practices—Aircraft Inspection and Repair*, ch 1 ed update ed., 09 2001.

[24] Golin, M., "Hybrid Control System Packet Format," Tech. rep., CU InSpace, 06 2025.

[25] *LiteBeam; 5 GHz, airMAX® Technology Solutions*, Ubiquiti, n.d. URL https://dl.ubnt.com/datasheets/LiteBeam/LiteBeam_DS.pdf.

[26] *RUT140*, Teltonika Networks, v1.01 ed., 06 2025. URL https://assets.rs-online.com/image/upload/v1762427243/Datasheets/d5943c41f25305e4aa9fd969583e25c2.pdf.

[27] *TSW202*, Teltonika Networks, 1st ed., 02 2026. URL https://www.teltonika-networks.com/products/ethernet-switches/tsw202.

[28] *gibco User Guide: Primary Rat Cortex and Hippocampus Neurons*, gibco, ???? URL https://assets.thermofisher.com/TFS-Assets/LSG/manuals/MAN0001574-PrimaryRatCortex-HippocampusNeurons-UG.pdf.

[29] *OpenMEA: Open-Source Microelectrode Array Platform for Bioelectronic Interfacing*, bioRxiv, 11 2022. https://doi.org/https://doi.org/10.1101/2022.11.11.516234, URL https://www.biorxiv.org/content/10.1101/2022.11.11.516234v1.full.

A. Payload

A.1 Overview of Payload

The Payload sub-team constructs a scientific payload to compete in the Payload Competition at Launch Canada. This payload follows a 3U CubeSat form factor (10 cm × 10 cm × 30 cm). This year, the team is developing a payload to house cultured neurons, which will be observed under a microscope. The payload will also contain a Micro Electrode Array (MEA) to study the neurons' electrophysiology before, during, and after rocket flight.

A.2 Rat Cortex Neurons

The experiment will use primary rat cortex neurons sourced from Fisher Scientific, which will be cultured directly on the MEA. These cells are highly sensitive to environmental conditions, necessitating a life support system. The neurons will be cultured at Carleton University and given time to develop a healthy neural network and adhere to the MEA before departure for Launch Canada. The culturing procedure is based on a guide provided by Fisher Scientific, with modifications for use on an MEA [28].

Safety data sheets indicate that the dye used in the experiment is the only potentially hazardous substance, as it may cause skin and eye irritation. Therefore, whenever the dye is not in a sealed container, it will be handled using nitrile gloves and lab safety goggles. Although not strictly required, the same precautions will be applied when handling the neurons and other reagents. To prevent contamination, the neurons will only be exposed to air under a laminar flow hood, which directs filtered air onto the neurons to prevent particulates from causing harm.

A.3 Life Support System

The life support system is responsible for maintaining the strict environmental conditions required for neuron survival. Cultured neurons require a temperature of 36–37.5°C, approximately 5% CO2 content, and at least 65% humidity. Additionally, minimizing vibrations is essential for improving microscope imaging and preventing the neurons from detaching from the MEA.

Temperature control is achieved using a thermoelectric heat pump that can heat or cool based on sensor feedback. Humidity will be adjusted manually by spraying water mist before sealing the life support compartment. CO2 will be introduced into the sealed compartment using a CO2 injector. The compartment is thermally insulated and equipped with shock absorbers, while the microscope is isolated from the compartment walls using rubber vibration dampers to further reduce vibrations.

A.4 Micro Electrode Array

The MEA is a device used to measure neuronal action potentials and stimulate neurons with electrical pulses. The design is based on the OpenMEA open-source MEA [29]. To reduce cost and complexity, the OpenMEA design has been modified to use 16 channels/electrodes instead of 64. By using an MEA, it is possible to assess both the viability and electrical activity of the neurons. The user interface of the OpenMEA software can be seen below in Figure

A.5 Fluorescent Microscopy

Inside the life support compartment, the microscope observes neuron viability using fluorescence from an applied dye. The experiment will use Calcein Blue, which fluoresces blue when cells are alive. This dye has an excitation wavelength in the ultraviolet range, requiring an LED that emits in that spectrum.

The microscope uses a Raspberry Pi to capture images and store them on an SD card. A dichroic mirror is used to separate excitation and emission light; it reflects ultraviolet light from the LED onto the dyed neurons while allowing the emitted blue light to pass through to the camera. A diagram of the fluorescent microscope

can be seen below in Figure 93.

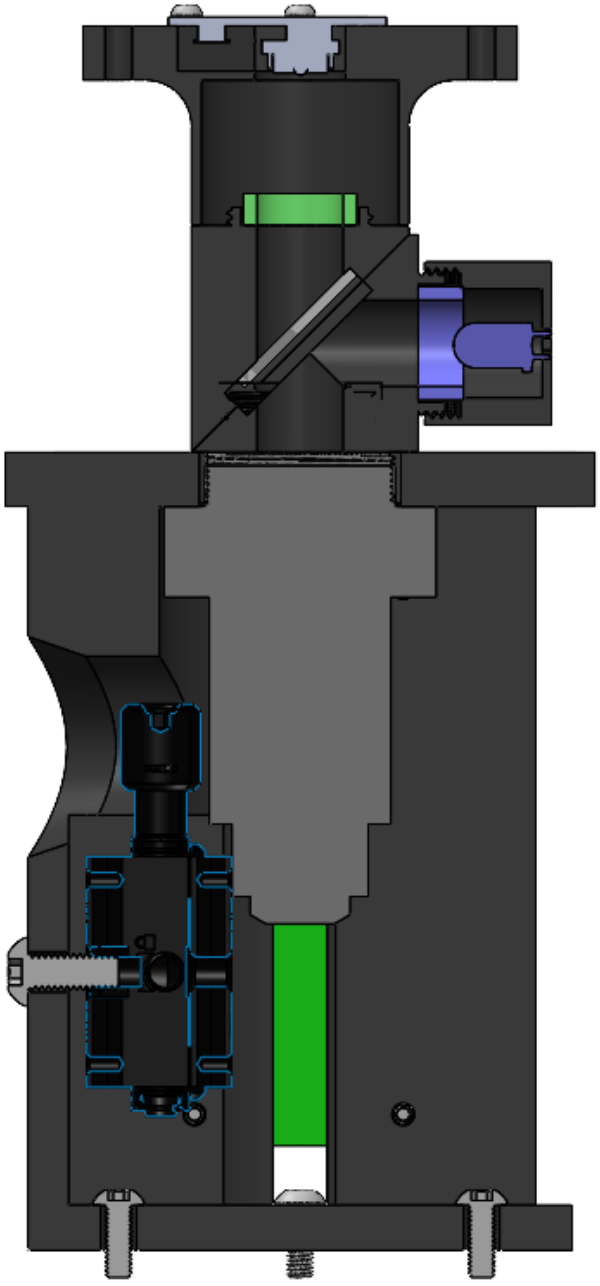

Figure 93 SRAD Fluorescent Microscope Block Diagram

B. Detailed Design Trade Studies and Calculations

C. Thrust Chamber Structural Calculations

C.1 Safety Factors

The tables below show the factors of safety for the thrust chamber's mechanical design, relative to the MEOP. Explanations for each of the calculations are included in the next section.

Table 34 Chamber Casing Factors of Safety

Failure Mode	Yield	Ultimate
Hoop Stress Failure	3.37	3.79
Longitudinal Stress Failure	5.06	5.69

Table 35 Injector Bolt Circle Factors of Safety

Failure Mode	Yield	Ultimate
Bolt Shear	6.00	7.81
Casing Bearing Failure	2.59	3.07
Bulkhead Bearing Failure	4.33	5.13
Bolt Tear-Out	4.33	4.87
Casing Tensile Failure	5.06	5.69

Table 36 Nozzle Bolt Circle Factors of Safety

Failure Mode	Yield	Ultimate
Bolt Shear	4.50	5.86
Casing Bearing Failure	1.95	2.31
Bulkhead Bearing Failure	3.25	3.85
Bolt Tear-Out	3.24	3.65
Casing Tensile Failure	5.62	6.32

C.2 Calculation Inputs

The material properties for aluminum 6061-T6 were obtained from the Metallic Materials Properties Development and Standardization (MMPDS) as well as Matweb. The mechanical properties of the fasteners used in the chamber are from the vendor's website, as well as online thread charts.

Table 37 Aluminum 6061-T6 Material Properties

Parameter	Value	Unit
Tensile Strength (Yield)	40,000	psi
Tensile Strength (Ultimate)	45,000	psi
Bearing Strength (Yield)	54,000	psi
Bearing Strength (Ultimate)	64,000	psi
Shear Strength (Ultimate)	30,000	psi

The bearing strength values for the chamber were taken assuming a pin edge distance to diameter ratio of 1.5, which is more conservative and appropriate for the chamber's bolted joint geometry.

Table 38 M4 Fastener Mechanical Properties

Parameter	Value	Unit
Tensile Strength (Ultimate)	170,000	psi
Minor Diameter	3.002	mm
Major Diameter	3.838	mm
Head Diameter	7	mm
Head Height	4	mm
Hex Drive Size	3	mm

The major and minor diameters of the fasteners are taken as their minimum possible values, to be conservative.

Table 39 Chamber Casing Geometry

Parameter	Value	Unit
Inner Diameter	4.5	in
Wall Thickness	1/8	in

Table 40 Injector Bolt Circle Geometry

Parameter	Value	Unit
Number of Bolts	16	N/A
Bolt Head Protrusion	2.75	mm
Casing Clearance Hole Diameter	7.1	mm
Thread Engagement	8	mm

Note that bolt head protrusion refers to the distance the bolt head extends past the bulkhead and into the casing. It is the depth of the counter bores in the bulkhead subtracted from the height of the bolt head.

Table 41 Nozzle Bolt Circle Geometry

Parameter	Value	Unit
Number of Bolts	16	N/A
Casing Clearance Hole Diameter	4.1	mm
Thread Engagement	7	mm

C.3 Recessed Bolt Head Calculations

The design and analysis of the thrust chamber structure closely followed the methods outlined in Half Cat Rocketry's "How to Design Pressure Vessels, Propellant Tanks, and Rocket Motor Casings" [**?**]. However, the injector bolt circle with the recessed bolt heads adds some nuance to the calculations. These nuanced calculations are explained below, all other calculations were done in accordance with Half Cat Rocketry's guide.

C.3.1 Bolt Shear

In the typical case of determining the shear stress in the radial bolts, the following formula is used:

$$\sigma_{boltshear} = (\tfrac{\pi}{4} D_{i,casing}^2 \times MEOP)/(N \times \tfrac{\pi}{4} d_{bolt,minor}^2)$$

Where $D_{i,casing}$ is the casing inner diameter, $d_{bolt,minor}$ is the fastener minor diameter, and N is the number of bolts used in the bolt circle. However, in the case of the bolt head being in shear, the cross sectional area of the bolt head must be considered. As a result, the formula becomes

$$\sigma_{boltshear} = (\tfrac{\pi}{4} D_{i,casing}^2 \times MEOP)/(N \times A_{bolt,shear})$$

where

$$A_{bolt,shear} = \tfrac{\pi}{4} d_{bolt,head}^2 - \tfrac{\sqrt{3}}{2} W_{drive}^2$$

Note that $d_{bolt,head}$ is the fastener's head diameter and W_{drive} is the width of the fasteners hex drive size.

C.3.2 Casing Bearing Stress and Bolt Tear-Out

For both the casing bearing stress and bolt tear-out calculations, the modifications to the formulas are very simple. The thickness of the casing is simply replaced with the bolt head protrusion, or the height of the bolt head that is within the casing wall. Note that when the bolt heads are recessed, the tear-out failure mode becomes less likely, as an extra shear plane is added in line with the top of the bolt head. This however is neglected in the calculations to be more conservative.

C.3.3 Bulkhead Bearing Stress

The bearing stress on the injector bulkhead was calculated to verify the geometry of the bulkhead's counter bored bolt holes. Calculating bearing stress is not outlined in the Half Cat Rocketry design guide as in most cases, bearing stress generated in the bulkhead/retainer from the bolts will be far less than that developed in the casing. Despite this, the use case of recessed bolts is not clearly addressed in the design guide, so the calculation was done to confirm the bulkhead bearing stress would not be an issue.
The calculation is done using the following formula:

$$\sigma_{bearing,bulkhead} = (\tfrac{\pi}{4} D_{i,casing}^2 \times MEOP)/(N \times A_{bolt,bearing})$$

where

$$A_{bolt,bearing} = L_{counterbore} \times d_{bolt,head} + \tfrac{1}{2} L_{thread} \times d_{bolt,major}$$

$L_{counterbore}$ is the depth of the counter bore in the bulkhead, L_{thread} is the engaged thread length in the bulkhead, and $d_{bolt,major}$ is the major diameter of the bolt threads. The above calculation assumes the bearing area of the bulkhead is combined between the head and shank of the bolt. However, only half of the bolt's shank is considered to yield a more conservative estimate.